IN VITRO AND IN VIVO EFFECTS OF α7 NICOTINIC ACETYLCHOLINE RECEPTOR GENE DELIVERY ON NEUROPROTECTIVE PATHWAYS

By

YAN REN

A DISSERTATION PRESENTED TO THE GRADUATE SCHOOL
OF THE UNIVERSITY OF FLORIDA IN PARTIAL FULFILLMENT
OF THE REQUIREMENTS FOR THE DEGREE OF
DOCTOR OF PHILOSOPHY

UNIVERSITY OF FLORIDA

2011

To my parents, Bao’er Ren and Qiaozhen Pu, and my grandmother, Fenlan Ge

ACKNOWLEDGMENTS

The research described in this dissertation is made possible through the help and support from the faculty, staff and fellow students at the University of Florida. First of all, I would like to express my sincere appreciation to my mentors, Dr. Sihong Song and Dr. Jeffrey A. Hughes, for their invaluable guidance and support throughout my graduate education. I would also like to thank Dr. Edwin M. Meyer for his care along every step of my graduate study. Not only has he mentored me in developing research skills, Dr. Meyer also took the patience to read my presentations and manuscripts and made great effort to help improve my English speaking and writing. I am also grateful to Dr. Michael A. King, for his generosity in sharing ideas and experience. He is always there when I need advice and has been my constant source of neuroscience knowledge.

I also thank all my committee members for their helpful comments and suggestions. Dr. Hartmut Derendorf has an amazing knowledge of pharmacometrics, and has inspired my interest in this area with his brilliant teaching skills. Dr. Veronika Butterweck is always very kind and willing to help. Dr. Marta L. Wayne used to be my director in Genetics and Genomics Graduate Program. She provided me the opportunity to pursue my Ph.D degree at University of Florida; her thoughtfulness and consideration have accompanied me through all these years.

This project could not have been completed without the help and encouragement of many other people. Dr. Aaron C. Hirko, my current labmate, consistently helps me with my experiments and I enjoyed every passionate discussion with him. Dr. Ke Ren, my previous labmate and dear “sister”, have made my first year enjoyable both in lab and in personal life. Dr. Roger L. Papke, professor in Department of Pharmacology and Therapeutics, inspired me a lot with his talent and pursuit in science. He is also my

supplier of experimental drug. Mike Matheny, working next door to us, is an excellent lab manager and generously lends me anything that I cannot find in our lab. I would also like to thank all the staff and fellow graduate students in the Department of Pharmaceutics as well as the Genetics and Genomics Program for their friendship and support.

Last but not least, I thank my parents, for the loneliness they endured and the love they constantly offered during my study oversea. I am grateful to my husband for his listening and encouragement through good times and bad times. I would also like to thank all my friends, in the United States and back in China, for making my ordinary life extraordinary.

TABLE OF CONTENTS

page

LIST OF TABLES

Table page

LIST OF FIGURES

LIST OF ABBREVIATIONS

AAV	Adeno associate virus
Aβ	β amyloid
ACh	Acetylcholine
AChE	Acetylcholinesterase
AD	Alzheimer disease
APP	Amyloid precursor protein
Bcl-2	B -cell lymphoma
BDNF	Brain derived neurotrophic factor
BH	Bcl-2 homology
CaMKII	Calcium / calmodulin-dependent protein kinase II
cAMP	Cyclic adenosine monophosphate
CBA	Chicken β-actin
ChAT	Choline acetyltransferase
CMV	Cytomegalovirus
CNS	Central nervous system
CREB	cAMP response element-binding protein
DMXB	3-(2, 4)-Dimethoxybenzylidine anabaseine
ER	Endoplasmic reticulum
ERK	Extracellular signal regulated kinase
FDA	Food and Drug Administration
GDP	Gross domestic product
JAK2	Janus kinase 2
JNK	c-jun-N-terminal kinase
KRH	Krebs Ringer buffer

MAPK	mitogen-activated protein kinases
MLA	Methyllycacotinine
MRI	Magnetic resonance imaging
nAChR	Nicotinic acetylcholine receptor
NBM	Nucleus basalis of meynert
NGF	Nerve growth factor
NT-3	Neurotrophin-3
PBS	Phosphate buffered saline
PC12	Rat phaeochromocytoma cells
PET	Positron emission tomography
PKC	protein kinase C
PI3K	Phosphoinositide 3-kinase
STAT3	Signal transducer and activator of transcription protein 3
TrkA	Tyrosine kinase receptor type 1

Abstract of Dissertation Presented to the Graduate School
of the University of Florida in Partial Fulfillment of the
Requirements for the Degree of Doctor of Philosophy

IN VITRO AND IN VIVO EFFECTS OF α7 NICOTINIC ACETYLCHOLINE RECEPTOR GENE DELIVERY ON NEUROPROTECTIVE PROCESSES

By

Yan Ren

May 2011

Chair: Sihong Song, Ph.D
Major: Genetics and Genomics

Basal forebrain cholinergic neurons are essential for normal memory-related behaviors but are dysfunctional at early stage of Alzheimer's disease. Brain α7 nicotinic acetylcholine receptors abundantly expressed on these neurons. While not essential for their survival, they nonetheless regulate neurotransmitter release, modulate neuroplasticity and protect them against a wide variety of insults involving trophic factor deprivation, apoptosis, and phenotypic silencing. Many data have indicated that α7 agonist can either prevent neuron death or restore their cholinergic phenotype, and improve memory related performance. However few studies have attempted to restore the loss of these receptors through gene delivery approaches.

In this study, we investigated the effects of α7 receptor gene delivery on pathways associated with cell survival. Rat PC12 cells transfected using an optimized gene delivery system to overexpress α7 receptor showed more ERK2 and AKT activity and less caspase 3/7 activity in a dose dependent manner after treatment with the α7 partial agonist, 4OH-GTS-21. These effects could be blocked by the α7 receptor selective antagonist MLA, indicating that elevated α7 receptor expression improves the efficacy and potency of agonist treatment for PC12 cells. Elevated α7 expression also increased

TrkA phosphorylation as well as enhanced NGF induced neuron-like differentiation in the same cells, suggesting its involvement in regulating NGF-TrkA signaling pathway. AAV8-α7 gene delivery into mouse septum promoted TrkA expression in this brain region and improved performance in Morris water maze tasks. Since the activation of TrkA receptors, which are also diminished in AD patient brains, positively modulates neuron survival and cholinergic functions, these results suggest potential dual protection for cholinergic neurons after α7 gene delivery.

Together, α7 overexpression potently activated survival signaling pathways when combined with selective agonist and enhanced neurotrophin related functions. α7 gene therapy, which can restore the function of these receptors and TrkA receptors, may provide a new approach for treating AD patients.

CHAPTER 1
INTRODUCTION

Alzheimer Disease

Alzheimer disease (AD) is currently the most common neurodegenerative disorder characterized by widespread cognitive impairments including memory, language and behavioral abilities. It was named after German psychiatrist Alois Alzheimer who first documented a relationship between progressive cognition decline and neurological lesions at autopsy in early 19th century (Alzheimer, 1907). Postmortem examination found pathological changes in the patient's brain regions involved in memory and emotional behaviors such as cortex, hippocampus, basal forebrain and amygdala. The changes included reduced volume as the result of synapse degeneration and neuron death, extracellular senile plaque containing aggregated amyloid β (Aβ) peptide, and intracellular neurofibrillary tangles formed by microtubule-associated protein tau that exhibit hyper-phosphorylation (Reviewed by Mattson, 2004). Studies using magnetic resonance imaging (MRI) and positron emission tomography (PET) have confirmed brain shrinkage at certain region, as well as showed glucose metabolism reduction in cortex, comparing to aged controls (Wenk, 2003). People who suffer from Alzheimer disease will progressively lose their normal cognitive function and eventually be completely dependent on caregivers. According to the 2010 World Alzheimer Report, there are 35.6 million people living with Alzheimer's disease and other dementias worldwide. The number is estimated to increase to 65.7 million by 2030 and 115.4 million by 2050. In the past year, the costs associated with AD amounted to more than 1% of the world's gross domestic product (GDP). Intensive efforts have been devoted to

find promising therapeutic approaches for AD, yet its pathogenesis has not been fully elucidated. To data, several hypotheses have been proposed and studied in depth.

Cholinergic Hypothesis

The cholinergic hypothesis was initially presented in 1970s, which suggested that dysfunction of cholinergic neurotransmitter system in certain brain regions contributes to the cognitive decline (Bartus *et al*., 1982; Coyle *et al*., 1983). The cholinergic system is one of the most important nervous pathways. Acetylcholine (ACh) is the neurotransmitter that is synthesized, stored and released by cholinergic neurons. Reductions in the activity of the cholinergic enzymes choline acetyl transferase (ChAT) were identified as being most severe in the cortex and hippocampus (Davies, 1979) in AD patients' brain compared to age-matched controls, along with descending ACh synthesis and release (Bowen *et al*., 1981). A loss of cholinergic forebrain neurons of the nucleus basalis of meynert (NBM) was then shown to be the first evidence of neurotransmitter-specific neuronal loss in AD (Whitehouse *et al*., 1982). Since NBM projects the majority of cholinergic input to hippocampus and cortex (Mesulam and Van Hoesen, 1976; Wenk *et al*., 1980), it suggested that selective loss of cholinergic neurons in basal forebrain resulted in reduced cholinergic input in these two regions reflecting decreased ChAT activity. Disrupting cholinergic function by using antagonists (anti-muscarnic or anti-nicotinic receptors) or fimbria-fonix lesion (which damages the cholinergic input to cortex or hippocampus from the basal forebrain) revealed similar memory deficits in animals and young humans as those in AD animal models / patients (Terry and Buccafusco, 2003). In contrast, appropriately enhancing cholinergic activity by providing anti-acetylcholinesterase (AChE) inhibitor or receptor agonists reduced memory impairments in aged subjects. Based on the cholinergic hypothesis, four

among the five Food and Drug Administration (FDA) recognized drugs for AD are AChE inhibitors (Table 1-1): tacrine, donepezil, rivastigmine and galantamine. They have provided convincing therapeutic effects balanced with an acceptable burden of side effects. Memantine is a glutamate receptor antagonist, which reduces the excitotoxicity induced by glutamate receptor over activation in AD (Molinuevo *et al*., 2005). All of these currently available medications, however, can only help control symptoms of the disease. Studies focusing on halting or preventing the disease process are pursued.

Table 1-1: FDA approved drugs for treating Alzheimer disease.

Brand Name	Generic Name	Year Approved	AD Stage	Mechanism
Namenda®	memantine	2003	moderate to severe	Glutamate receptor antagonist
Razadyne, Reminyl®	galantamine	2001	early	AChE inhibitor / Nicotinic receptor agonist
Exelon®	rivastigmine	2000	early	AChE inhibitor
Aricept®	donepezil	1996	early	AChE inhibitor
*Cognex®	tacrine	1993	early	AChE inhibitor

*Cognex is the first approved drug for AD and is rarely prescribed now as for its severe side effect.

Neuronal Nicotinic Acetylcholine Receptor

In the cholinergic system, one of the key components that execute and modulate the acetylcholine message are the neuronal nicotinic acetylcholine receptors (nAChRs), which were intensively studied during 1980s and 1990s. nAChRs belong to the superfamily of ligand-gated ion channels including the glycine, GABA-A and serotonin receptors (Sargent, 1993; Karlin and Akabas, 1995). They are membrane proteins composed of five subunits which are distinguished in subunits carrying the principal component of the acetylcholine binding site (named α2–α9) and the subunits carrying

the complementary component of the acetylcholine binding site (named non α or β2–β4) (Cooper *et al*., 1991). In central nervous system (CNS), two major classes of nAChRs have been characterized: α4β2 heteromeric receptors and α7 homomeric receptors (Figure 1-1). They act both as receptors via ligand binding and as "effectors" via opening of the central cationic ion channel. The cholinergic innervations acting via nAChRs regulates processes such as transmitter release, cell excitability and neuronal integration, which are crucial for network operations and a number of cognitive functions (Gotti and Clementi, 2004).

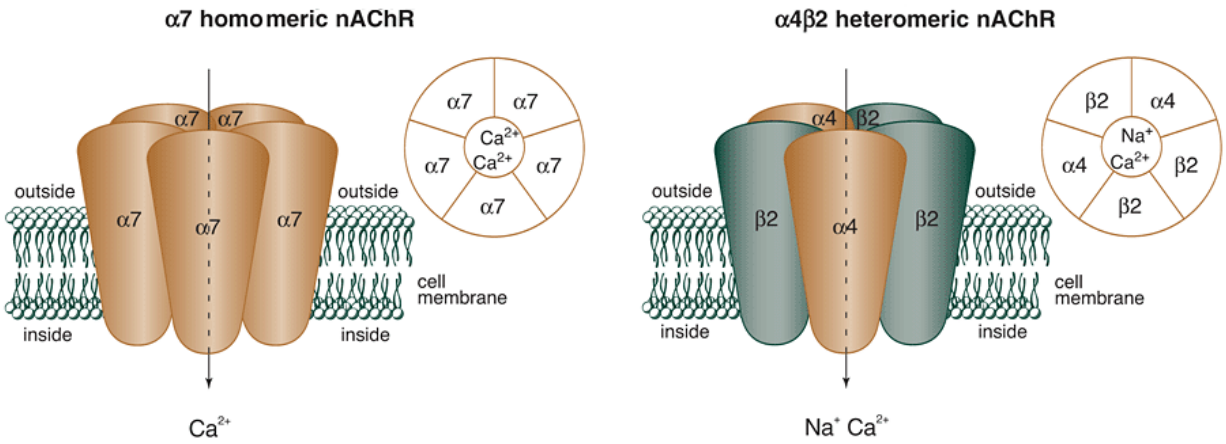

Figure 1-1: Structure of α7 and α4β2 nAChRs. Picture is obtained and modified from National Institute on Alcohol Abuse and Alcoholism (NIAAA) Graphics Gallery.

Investigation into the involvement of nAChRs in AD is based on several reasons. One is that as component of the cholinergic system which is affected in AD, the loss of nicotinic receptors occurs at early stages of histopathological changes, probably preceding neuron loss (Perry *et al*., 1995). Another reason is that the potential neuroprotective and cognitive enhancing effects of nicotine appeared to be nAChR mediated (Holladay *et al*., 1997). Also, elucidating nAChR functions and changes in AD helps to focus new therapeutic approaches to counteract the abnormalities. In

particular, the homomeric α7 receptors acquired particular attention because they exhibited special role in memory enhancing and neuroprotective actions as discussed below.

α7 nAChRs in Alzheimer Disease

Identification

Historically, α7 subtypes of nAChRs were distinguished from α4β2 nAChRs by its high affinity to α-bungarotoxin (Kd 0.65~1.7 nM) and relatively low affinity to nicotine (Clarke *et al* 1985, Marks *et al*., 1986, Schoepfer *et al.,* 1990). α-bungarotoxin is a peptide isolated from a species of East Asian snake (Bungarus multicinctus), and has been recognized for its high affinity to muscle-type nicotinic receptors (Changeux *et al*., 1970). These results were supported by the observation that α-bungarotoxin but not nicotine binding sites were absent in α7 knockout mice (Orr-Urtreger *et al*., 1997). α7 genes of different species were then cloned and proven to encode homomeric functional nicotinic channels, in which the β subunit is not needed (Couturier *et al*., 1990; Seguela *et al*., 1993).

Localization

α-bungarotoxin binding sites are found in many brain regions and are especially concentrated in hippocampus, cerebral cortex, hypothalamus (Domingues del Toro *et al*., 1994; Bina *et al*., 1995), where they locate presynaptically to facilitate the release of transmitters such as glutamate, GABA or dopamine (ALkondon *et al*., 1996; MacDermott *et al*., 1999), as well as exist postsynaptically to mediate fast synaptic responses (Jones *et al*., 1999, Broide and Leslie, 1999). Hippocampal and septal α7 receptor density is decreased at early stages of AD (Perry *et al*. 1995). Normal aging may be associated with reductions in α7 subunit mRNA as well as protein expression

(Court *et al*. 2001), while in AD α7 protein loss (Engidawork *et al*. 2001; Perry *et al*. 2001) is observed without significant mRNA level change (Wevers *et al*. 2000) or even increased α7 mRNA levels (Hellstrom-Lindahl *et al*. 1999), possibly in a compensatory manner.

Function

The α7 nAChRs have an unusually high permeability to calcium compared to other subtypes (Fucile *et al*., 2003) and exhibit exceptionally rapid desensitization following exposure to agonists (Couturier *et al*., 1990; Castro and Albuquerque, 1993). Ca^{2+} influx can facilitate transmitter release when presynaptic a7 receptors are activated, depolarize postsynaptic cells and act as a second messenger to initiate many cell processes, including those promoting neuronal survival (Messi *et al*., 1997; Role and Berg, 1996). The particularly rapid receptor desensitization could be beneficial in terms of preventing the excitotoxicity of an excessive Ca^{2+} influx.

These emerging evidences suggested roles for α7 subtype nAChR in maintaining the cholinergic synaptic function, regulating neuronal plasticity and modulating septohippocampal cholinergic phenotype. Along with their special pharmacological behaviors, these functions of α7 nAChRs illuminate useful therapeutic target for Alzheimer disease.

α7 nAChRs Mediated Neuroprotection

Effects on *in Vitro* and *in Vivo* Models

Activation of α7 nAChRs triggers neuroprotective effects have. *In vitro* studies showed α7 nAChR activation protected cells in models of neuronal apoptosis, at least in part: trophic factor and serum deprivation in rat phaeochromocytoma (PC12) cells (Li *et al*., 1999b), glutamate-induced excitotoxicity in primary rat brain neuronal cultures

(Shimohama *et al*., 1998), Aβ amyloid exposure in neurons and cell lines (Meyer *et al*., 1998a; Marrero *et al*., 2004), and ethanol toxicity in primary neuronal cultures and PC12 cells (Li *et al*., 1999a and 2002). *In vivo*, activation of α7 nAChR promoted survival of neurons from trophic factor deprivation (Messi *et al*., 1997), ischemic damage (Shimohama *et al*., 1998), oxygen/glucose deprivation (Rosa *et al*., 2006; Egea *et al*., 2007) and fimbria-fornix Lesions lesions which damage the septohippocampal connection (Meyer *et al*., 1998b; Ren *et al*., 2007a).

α7 nAChRs and Cellular Signaling Pathways

One mechanism underlying α7 nicotinic receptor mediated neuroprotection involves several intracellular processes triggered by receptor activation. Phosphorylation of calcium/calmodulin-dependent protein kinase II (CaMKII), protein kinase C (PKC), mitogen-activated protein kinases (MAPK), phosphoinositide 3-kinase (PI3K) / AKT and Janus kinase 2 (JAK2) have been found in response to α7 nAChRs activation. These kinases transduce signals by further activating cyclic adenosine monophosphate (cAMP) response element-binding protein (CREB) and signal transducer and activator of transcription protein 3 (STAT3), which regulate new gene synthesis (Figure 1-2). Mitochondria membrane stabilization, reduced release of mitochondria cytochrome oxidase and increased B-cell lymphoma 2 (Bcl-2) protein expression are also found to be involved in these protective effects (Kihara *et al*., 2001; Dajas-Bailador *et al*., 2002a; Li *et al*., 2002; Ren *et al*., 2005; Marrero and Bencherif, 2009).

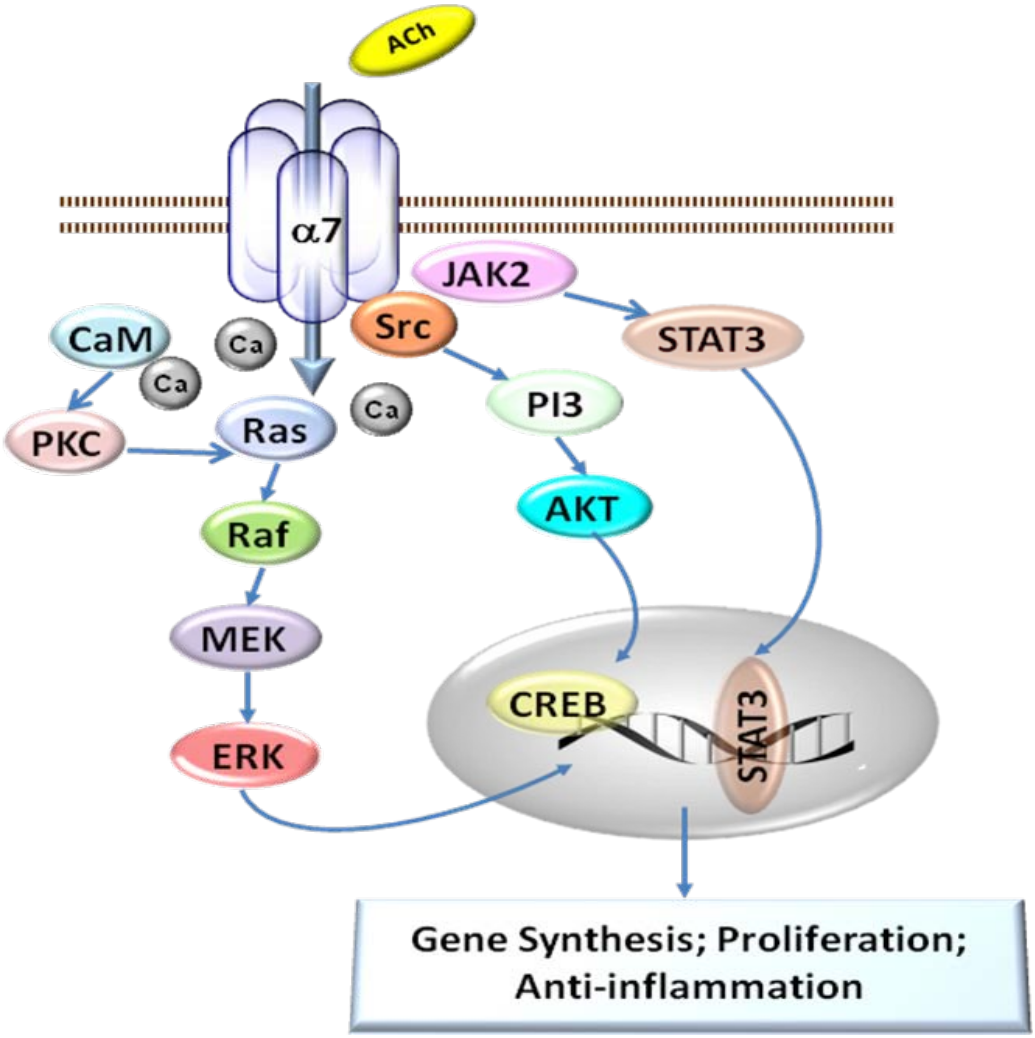

Figure 1-2: Cellular signaling pathways involved in α7 nAChRs mediated neuroprotection.

α7 nAChRs and TrkA

Another possible neuroprotective mechanism may relate to high affinity nerve growth factor (NGF) receptor tyrosine kinase receptor type 1 (TrkA) signaling. Loss of trophic factor support is an apparent underlying reason for the loss of cholinergic function in basal forebrain during AD progression (Fischer *et al*., 1987; Salehi *et al*., 2004; Cuello *et al*., 2007). Basal forebrain (e.g., NBM and septum) cholinergic neurons express TrkA receptors which are transported to the synaptic terminals in hippocampus, where NGF is synthesized and released from intrinsic neurons. After binding

extracellular NGF, membrane-spanning TrkA is endocytosed and transported retrogradely to cell bodies in basal forebrain. This trophic complex modulates cholinergic neuron morphology and function by enhancing sprouting, ACh synthesis, cholinergic neuronal firing and transmitter release. In AD brain, NGF levels are normal or even elevated in hippocampus and neocortex, but are reduced in the basal forebrain (Scott *et al*., 1995), suggesting reduced retrograde transport of this peptide to basal forebrain via TrkA receptors (Cooper *et al*., 2001), due to a combination of lower TrkA levels (Kerwin *et al*., 1992) and altered TrkA isoform expression (Dubus *et al*., 2000). It has been found that α7 nAChRs agonists increased NGF as well as TrkA levels in multiple brain regions (Garrido *et al*., 2003; Martinez-Rodriguez *et al*., 2003; Jonnala *et al*., 2002; French *et al*., 1999); while the α7 selective antagonist methyllycacotinine (MLA) blocks TrkA elevation (Jonnala *et al*., 2002). The anti-apoptotic effect of nicotine in spinal cord neurons was blocked with TrkA inhibition (Garrido *et al*., 2003). These studies with nicotinic agonists and antagonists suggested α7 activation induced TrkA and NGF up-regulation, which protects the neurons in complement to direct α7 effects.

α7 nAChRs and β Amyloid

In recent years, a significant body of evidence suggested the role of α7 nAChRs in the processing and clearance of Aβ peptide, another rational target for treating AD. Aβ represents the key molecule of the “amyloid hypothesis”, which states that the aggregation of Aβ in memory related brain regions is toxic to the neurons in either soluble or insoluble forms and contributes to the progress of cognitive decline (Hardy and Selko, 2002). Aβ competitively binds to α7 receptors with high affinity, impairs their normal functions, increase tau-hyperphosphorylation, potentiates cholinergic deficits and neuron death (Liu *et al*., 2001; Wang *et al*., 2000a and 2000b; Wang *et al*., 2003).

Dissociating Aβ from α7 by selective partial agonist attenuated these effects (Wang *et al*., 2009). Activating α7 receptors decreased Aβ products (Utsuki *et al*., 2002; Mousavi *et al*., 2009), attenuates Aβ-induced tau phosphorylation both *in vitro* and *in vivo* (Hu *et al*., 2008; Bitner *et al*., 2009) and ameliorated the cognitive deficits induced by Aβ toxicity in a mouse model (Chen *et al*., 2010). Despite controversial data showing that α7 nAChR knock-out mutation rescued cognitive decline in an APP-over expressing mouse model (Dziewczapolski *et al*., 2009), a more recent study using a mouse model crossed from APP mutant mice and α7 knockout mice showed that loss of α7 accelerated cholinergic dysfunction in basal forebrain and hippocampus at an early preplaque stage, as well as exacerbated Aβ accumulation, early stage cognitive decline and septohippocampal pathology (Hernandez *et al*., 2010).

A possible underlying mechanism might be that α7 activation induced signaling pathways regulate amyloid precursor protein (APP) metabolism via secretase activities. APP is processed by α-, β-, and γ-secretases. α-form of secreted APP (αAPPs) resulting from α-secretase cleavage is believed to be non-toxic, while the product from the collaboration of β- and γ-secretases, Aβ, is neuron toxic (Esler and Wolfe, 2001). *In vitro* studies have shown that α7 activation decreases Aβ production by suppressing γ-scretase activity, and increased αAPPs (Nie *et al*., 2010). Besides, microglia α7 activation may facilitate Aβ clearance in CNS (Takata *et al*., 2010). A recent clinical study reported that CNS Aβ clearance rate is decreased in AD patient's brain compared to elderly controls, while the Aβ production rate is not significantly differed (Mawuenyega *et al*., 2010). Therefore, microglia α7 could also be targeted to counteract the altered Aβ metabolism.

Together, α7 nAChRs have special functions in neuroprotection and cognitive improvement through activating cell viability associated cellular kinases, promoting TrkA related neuron tropic pathways and possibly preventing Aβ induced toxicity. More details from future studies will help us understand systemically about α7 receptor function in maintaining septohippocampal cholinergic phenotype and preserving hippocampal integrity at early stage of dementia.

Therapeutic Approaches Targeting α7 nAChRs

Agonist Therapy

No new AD drug has been approved by FDA since 2003. α7 receptors have been a favorable target for their special effects in memory enhancing and neuroprotection. During past decade, hundreds of compounds functioning as selective α7 agonists have been synthesized and studied in lab models. Some of them, such as 3-(2,4)-dimethoxybenzylidine anabaseine (DMXB; also known as GTS-21), have been applied to clinical research. GTS-21 (Figure 1-3) is a selective α7 receptor partial agonist (Meyer *et al*., 1998a) that has been widely studied. It has displayed promising function in improving cell viability *in vitro* and enhancing a variety of cognitive behaviors, including spatial memory in the Morris water task (Meyer *et al*., 1998a), passive and active avoidance behaviors in rats (Meyer *et al*., 1997), radial arm maze in aged rats (Arendash *et al*., 1995), delayed eye blink behavior in rabbits (Woodruff-Pak, 2003), hippocampal gating behavior in mice (Simosky *et al*., 2001), and delayed pair matching and word recall (Briggs *et al*., 1997). In contrast, the selective antagonist MLA reduces performance in radial arm maze when injected directly into the hippocampus at low concentrations (Bettany and Levin, 2001). Chronic administration of GTS-21 does not lead to significant receptor up-regulation or possess significant drug dependence

potential in contrast to nicotine (Flores *et al*., 1997). In human, Phase I clinical tests with health young male subjects indicate a positive effect of orally administrated GTS-21 on some measures of cognition without affecting autonomic and skeletal muscle systems at doses which enhance cognitive behavior (Kitagawa et al., 2003). While GTS-21 is a much weaker partial agonist on human α7 receptors than upon rat α7 receptors, its principal metabolite, 3-(4-hydroxy, 2-methoxy-benzylidene) anabaseine (4OH-GTS-21; Figure 1-3), displays good efficacy on both of them (Meyer et al., 1998a). Therefore for human application, 4OH-GTS-21 might be a better candidate. The pharmacokinetics of GTS-21 and 4OH-GTS-21 are organized in Table 2-1 and Table 2-2 (Kitagawa et al., 2003).

Besides agonist, α7 nAChR positive allosteric modulators are under intensive study (Lightfoot *et al*., 2008). Some of these drugs have succeeded in improving cognition (Timmermann *et al*., 2007; Thomsen *et al*., 2010) with low toxicity (Hu *et al*., 2009).

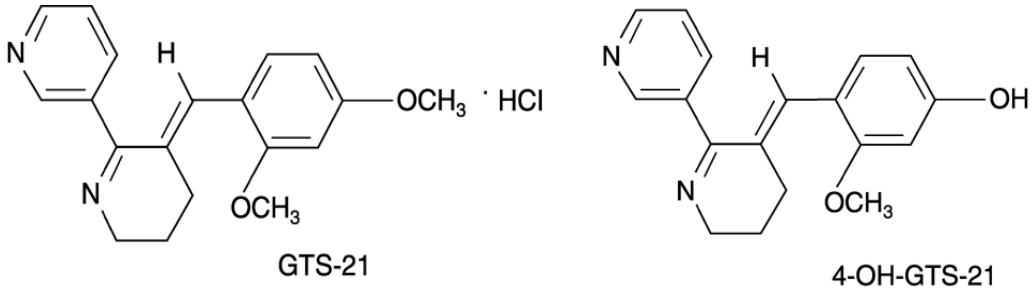

Figure 1-3: Chemical structure of GTS-21 and 4OH-GTS-21.

Gene Therapy

Although there is extensive evidence for α7 receptor mediated benefits using agonist treatment, few investigations have attempted to modify receptor function by gene delivery, despite several potential advantages of this approach.

α7 receptors display a high degree of concentration-dependent kinetics of agonist-evoked responses (Seguela *et al*., 1993; Uteshev *et al.* 2003; Papke *et al.* 2009). They desensitize very quickly; at high agonist concentrations there is little receptor function following this desensitization phase. One component of this loss of receptor function at high agonist concentrations may also be due to the receptor staying in a dysfunctional state when too many subunits are agonist-bound. Therefore, in order to obtain a long term agonist-response, the concentration must be maintained at low enough concentrations for a long term response, but not too low to elicit virtually no response. *In vivo*, particularly, this may be a difficult goal. Besides, drug treatment alone may not be sufficient due to the loss of α7 receptors in some parts of the AD brain. Increasing α7 receptor density by gene therapy provides an approach to increase receptor function that is likely either independent of drug-concentration (hence does not require higher drug doses) or perhaps even leads to more potent agonist responses (i.e. broadening the dose-response nature of the receptor). In addition, it provides a mechanism to counteract the effects of AD on receptor density. Of course, gene delivery can be combined with agonist treatment to optimize the α7 receptor responses, depending on the availability of the endogenous agonists--choline and acetylcholine.

With gene therapy, a single injection could give a long term, perhaps permanent effect that could be localized to those the brain regions affected by the disease. This is in contract to drugs that spread throughout the brain and body and may cause unwanted side effects. Gene delivery may also mediate the expression of several genes, which may be an advantage for AD, since it involves multiple pathological mechanisms.

Functional α7 gene expression involves the chaperon protein RIC-3 (Millar 2008). RIC-3 appears to act by interacting with unassembled receptor subunits within the endoplasmic reticulum (ER), thereby facilitating subunit folding and receptor assembly (Lansdell *et al*. 2005; Alexander *et al*., 2010). Heterologous expression studies performed in Xenopus oocytes have demonstrated that co-expression of C. elegans RIC-3 causes enhanced levels of functional expression of α7 receptor (Halevi *et al.* 2002), and similar results have been reported with a human homologue of RIC-3 (Halevi *et al.* 2003; Williams *et al.* 2005). In the absence of RIC-3, little or no specific binding of nicotinic radioligands is detected when the α7 subunit is expressed in mammalian cell lines, which lack endogenous RIC-3 (such as simian COS cells and some human HEK293- derived cell lines) (Millar 2008). In contrast, co-expression of RIC-3 with α7 facilitates both high levels of receptor-specific [^{125}I] α-bungarotoxin binding and the expression of functional α7 receptors (Williams *et al*., 2005). These findings support the idea that genetic modulation of RIC-3 expression could also increase α7 maturation and expression. However, to what extent RIC-3 versus α7 receptor synthesis is limiting for functional α7 receptor function in neuronal type cells (e.g., PC-12 cells) has not been well characterized, which is one of the aims of this thesis.

Specific Aims and Significance

In this study, we investigated the effects of α7 together with ric-3 gene delivery: 1) on agonist sensitivity relative to intracellular processes associated with cell survival and differentiation; 2) on TrkA receptor levels and activities.

Aim 1: Test the hypothesis that α7 and ric-3 gene delivery are both important for increasing functional α7 receptors in PC12 cells; and set up a *in vitro* model for studying underlying processes of up-regulated α7 activation.

Aim 2: Test the hypothesis that increased α7 receptor expression elevates the agonist-induced intracellular responses associated with cell viability.

Aim 3: Test the hypothesis that α7 receptor expression increases TrkA activities.

The study will help to elucidate the benefits of α7 gene delivery in terms of cytoprotection and promote the application of α7 gene therapy in Alzheimer's disease. The combination of pharmacological and genetic approaches employed in this study will reduce the likelihood that the drugs will act through unexpected, non-α7 receptor mechanisms. The long term goal of this study is to develop effective neuroprotective treatments for AD and other degenerative conditions affecting basal forebrain neurons expressing α7 nicotinic receptors.

CHAPTER 2
MATERIALS AND METHODS

Reagents

Except where noted, all chemicals used were purchased from Fisher Scientific (Hampton, NH).

Plasmid Preparations

Three plasmids were used in this study: rat α7 and algae green fluorescent protein (GFP) genes were inserted in pUF12 vector; human ric-3 gene was inserted in pCDNA3 vector, each under control of the truncated cytomegalovirus (CMV) / chicken β-actin (CBA) hybrid promoter. For plasmid preparation, a single E. coli colony was grown for 6-8 hr in 5 ml of NZY broth (Fisher Scientific, Pittsburgh, PA) containing 100 μg/ml of ampicillin (NZY/Amp) at 37°C on a shaking platform. The mixture was then inoculated into 2 L of NZY/Amp and incubated for 16~17 hr. The overnight culture was centrifuged at 4,000 g for 15 min in a Sorvall® RC-5B refrigerated super-speed centrifuge (DuPont Instruments). The pellet was resuspended in 20 ml of lysozyme buffer (10 mM Tris-HCl, 10 mM EDTA and 50 mM sucrose, pH 8.0). Lysis was initiated with 12 mg/ml lysozyme (Sigma Aldrich, St. Louis, MO) followed by NaOH/SDS solution (0.5 N NaOH and 1% SDS in water). Genomic DNA was precipitated with 3M NaAc (pH4.6-5.2) and pelleted by centrifuging at 16,000 g for 20 min. Plasmid DNA in the supernatant was precipitated with 40% PEG on ice for 10 min, pelleted at 16, 000 g for 10 min and dissolved in water. LiCl (5.5 M; 1:1, volume/volume of the solution) was added, followed by centrifugation at 16,000 g for 10 min. Plasmid DNA was precipitated from the supernatant by ice-cold isopropanol and pelleted at 16,000 g for 10 min. The pellet was dissolved in 5 M CsCl medium with ethidium bromide (0.5 mg/ml) in Optiseal Beckman tube (Beckman

Instruments, Brea, CA). Gradients were formed ultracentrifuging at 200,000 g over 19 hr at 20°C in Beckman L8-70M Ultracentrifuge. The concentrated plasmid DNA band was detected by a hand held UV lamp (366 nm). The lower band of the two bands was collected with 16 G needle (BD biosciences, San Diego, CA) and transferred to a 15 ml tube. The samples were extracted 3-4 times with equal volume isoamyl alcohol (Fisher Scientific, Pittsburgh, PA) until they are clear and then transferred to a new tube. 2.5 volume of water and the combined volume of ethanol were mixed with the sample to precipitate plasmid DNA by icing for 30 min, following with 15 min centrifuge at 5,000 g. The pellet was dissolved in TE buffer (10 mM Tris-HCl, 1 mM EDTA, PH 8.0) and then purified by 2 times phenol/chloroform extraction and 1 time chloroform extraction. The purified plasmid DNA was precipitated with absolute ethanol and NaAc (0.08 M), centrifuged at 16,000 g for 20 min, washed once with 75% ethanol, air dried and dissolved in TE. The DNA concentration was detected at 260/280 nm in a Beckman DU 650 Spectrophotometer. The DNA quality was confirmed by restriction digestion and gel electrophoresis.

Cell Culture

Rat PC12 cells (ATCC, Rockville, MD) were cultured and maintained in F12k medium (ATCC) containing 2.5% fetal bovine serum (Sigma Aldrich) and 15% horse serum (ATCC) at 37°C in a humidified atmosphere of 5% CO2. They were typically split using 0.25% Trypsin (Fisher Scientific, Pittsburgh, PA) at a 1:4 ratio every 4 days for up to 20 passages before use. The cell culture medium was removed and cells exposed to trypsin for 1~2 min and observed under microscope. The trypsin solution was removed when cell morphology became round but still attached to the culture dish. Cells were then washed from the bottom with fresh medium, completely separated by titration and

transferred into new culture dishes. Before transfection / transduction, cells were transferred to 6-well, 24-well or 96-well Costar® tissue culture treated plates (Corning Inc., Corning, NY) at approximately 70% confluence if not indicated otherwise.

Cell Gene Delivery, Differentiation and Drug Treatments

A variety of GFP expression vectors were evaluated for gene-transfer efficiency in PC12 cells: recombinant adeno associated virus (rAAV) using either serotype #2, #5, or #8, each with terminal repeats (TR) from serotype #2; calcium phosphate mediated plasmid transfection; and Lipofectamine 2000™ (Invitrogen, Carlsbad, CA) / Lipo293™ (SignaGen, Ijamsville, MD) mediated plasmid transfection. The percent of cells expressing GFP was determined by fluorescence microscopy.

For kinase assays, cells were incubated 24 hr post transfection with a specified concentration of 4OH-GTS-21 in fresh medium for 30 min, with or without a 30 min pre-treatment with 50 nM of the selective α7 nicotinic receptor antagonist methyllycaconitine (Sigma Aldrich), 50 μM ERK phosphorylation inhibitor PD 98059 (Calbiochem, La Jolla, CA) or 20 μM AKT phosphorylation inhibitor API-2 (Calbiochem).

For differentiation studies, ~40% confluenced cells were treated 24 hr after transfection with 50 ng/ml nerve growth factor (BD biosciences, San Diego, CA) for 4 days, with or without 30 min pre-treatment of MLA, PD 98059 or API-2. Nerve growth factor was added repeatedly to maintain the working concentration.

Cell Viability

Cell viability was estimated with the CyQuant™ Cell Proliferation assay kit (Molecular Probes, Invitrogen, Carlsbad, CA) according to the manufacturer's instructions. Fluorescence was measured directly on a FL600 Microplate Fluorescence

Reader (Bio-Tek Instruments, Inc, Burlington, VT) to determine the percentage of viable cells.

α7 Nicotinic Receptor Binding Assay

One day after transfection with specified plasmids, cultures were washed twice with phosphate buffered saline (PBS) and harvested in ice-cold Krebs Ringer buffer (KRH; 118 mM NaCl, 5 mM KCl, 10 mM glucose, 1 mM $MgCl_2$, 2.5 mM $CaCl_2$, 20 mM Hepes; pH 7.5). Cells were homogenized in ice-cold KRH buffer with a Polytron at setting 4 for 10 s. After two 1 ml washes with KRH at 20,000g, the membranes were incubated in 0.5 ml KRH with 50 nM [3^H] MLA (100 Ci/mmol; Tocris, Ellisville, MO), for 60 min at room temperature, plus or minus 5 mM nicotine. Tissues were washed three times with 5 ml ice-cold KRH buffer by filtration through Whatman GF/C glass microfiber paper (Brandel, Gaithersburg, MD) that was pre-incubated for 30 min with 0.5% polyethylenimine using M-24R. S Cell Harvester (Brandel Inc., Gaithersburg, MD). Liquid scintillation counting of radioactivity was conducted in a Beckman LS1800 using EcoLite (Fisher Pharmaceuticals, Hampton, NH). Nicotine-displaceable binding was calculated for each sample in triplicate in each experiment, and normalized for total protein concentrations measured with Pierce® BCA protein Assay Kit (Thermo Scientific, Rockford, IL).

Enzyme-Linked Immunosorbent Assay

Treated cells were harvested in RIPA buffer (Cell Signaling, Danvers, MA) containing protease inhibitor cocktail and phosphatase inhibitor cocktail (Thermo Scientific, Rockford, IL), sonicated and centrifuged at 4^{o}C. Supernatant was collected and frozen at -80^{o}C till use. For ERK and JNK, ELISA antibodies and standard proteins were purchased from R&D systems (Minneapolis, MN). Immulon 4HBX microplates

were coated with ERK2, p-ERK2, JNK or p-JNK capture antibody (1, 3, 3 and 2 μg/ml, respectively) overnight followed by blocking with 1% BSA in PBS/0.05% NaN_3. 100 μl cell samples or diluted standard proteins were added into the wells and incubated for 2 hr. Targeted proteins were probed by detection antibodies (0.5 μg/ml) for 2 hr and then incubated with Streptavidin-HRP (1:200) for 20min. Washes were conducted in PBS with 0.02% Tween 20. Substrate solutions (R&D Systems, Minneapolis, MN) were added for color reaction and stopped with 2 N H_2SO_4 after 20 min. AKT and p-AKT were evaluated using ELISA kits purchased from Invitrogen by following manufacture's protocol. Optical densities were determined by a microplate reader (Bio-Rad, Hercules, CA) set to 450 nm. All results were normalized for total protein concentrations and expressed as % of GFP-transfected control values.

Western Blot

Treated cells or dissected brain tissue samples were homogenized in RIPA buffer containing protease and phosphatase inhibitor cocktails and centrifuged at 4^{o}C. Supernatant was collected for protein assay or western blots. After boiling with loading buffer (Laemmli buffer containing 2% 14.2 M 2-Mercaptoethanol) for 5 min, proteins were separated on 12% Tris-HCl gels (Sigma Aldrich) and transferred to PVDF membranes (Bio-rad). The membranes were blocked by incubation in 5% skim milk in TBS buffer (0.5% Tween 20, 10 mM Tris, 50 mM NaCl, pH 8.8) at room temperature for 1 hr. All washes were conducted with TBS buffer. The membranes were incubated at 4°C overnight with the following antibodies (dilutions given in parentheses): anti-p-ERK, anti-ERK, anti-p-TrkA, anti-β actin (Cell Signaling, Danvers, MA, 1:1000), anti-TrkA (Upstate Biotechnology, New York City, NY), anti-α7 (Covance, Princeton, NJ, 1:500)

and anti-ChAT (Chemicon Inc., Billerica, MA; 1:2000). Incubation with the horseradish peroxidate-conjugated anti-mouse or anti-rabbit IgG (GE, Piscataway, NJ, 1:10000) was conducted in TBS buffer containing 5% skim milk for 45 min at room temperature. The signal was detected by the ECL detection system (PerkinElmer, Waltham, MA), according to the manufacturer's instructions, with Kodak BioMax MR film (Sigma Aldrich). The bands were quantified with ImageJ.

Caspase Assay

Cells were grown and treated in 96 well plates. Caspase activities were evaluated with an Apo-ONE® homogeneous caspase-3/7 assay kit (Promega, Madison, WI) following the manufacturer's protocol. 100 µl of Apo-ONE® were added to each well of the 96-well plate containing 100 µl of blank (culture medium), control or cells in culture. The mixture was sealed and incubated for 2 hr. Fluorescence of each well was read (excitation/emission: 485 nm / 530 nm) using Synergy 2 plate reader (BioTek Instruments Inc. Highland Park, VT) and normalized to untreated cell culture medium.

Immunofluorescence

Cells grown and transfected in 24 well plates were washed with PBS 3 times, fixed in 3% ice cold paraformaldehyde in PBS with 1 mM $MgCl_2$ at room temperature for 15 min and permeabilized with 1.0% Trition X-100 for 5 min. Non specific signals were blocked with 2% BSA for 1 hr. Either anti-α7 antibody (Sigma) or anti-p-TrkA antibody (Sigma Aldrich) was added in and incubated with cells for at least 1 hr. Both of the antibodies were 1:400 diluted in PBS with 2% BSA. Controls without primary antibody reaction were incubated in PBS with 2% BSA for the same interval. Signals were visualized by either Alexa Fluor 488 or Alexa Fluor 594 (1: 400 dilutions, Invitrogen,

Carlsbad, CA). Fluorescence pictures were taken with Axiovert 135 microscope (Zeiss, Thornwood, NY).

Virus Vector Packaging and Titration

Transfection

Plasmids were packaged into rAAV8 using the adenovirus-free method developed by Zolotukhin et al. (1999). HEK 293 cells at 70% confluence were transfected by a calcium phosphate method with pUF12-rat α7 / pUF12-GFP and rAAV8 helper plasmid pXYZ8 / rAAV5 helper plasmid pXYZ5 in an equal molar ratio. 10 cell culture dishes of 15 cm diameter were used. 1.25 ml of 2 M $CaCl_2$, 0.6 mg helper plasmid, 0.3 mg of pUF12-rat α7 or pUF12 and sterile water were mixed to the total volume of 10 ml for ten dishes. This mixture was added dropwise into equal volumes of 2X HBA while vortexing. This transfection mixture was added to 200 ml of warmed DMEM, which contained 10% FBS and 1% penicillin/streptomycin. 22 ml of this medium mixture were added to each dish. 6-hour after transfection, the mixture was removed and replaced with fresh DMEM. The cells were incubated for 3 days to reach 100% confluence and then harvested using cell scraper (Corning Inc.) and centrifuged at 4^{o}C and 3,000 g for 15 min. The cells were resuspended in AAV lysis buffer (150 mM NaCl, 50 mM Tris, pH 8.5).

Purification

The cell mix was frozen and thawed 3 times in a mixture of dry ice/ethanol (10 min freeze, 15 min thaw, vortexing every 5 min). The lysate were incubated with benzonase at 37^{o}C for 30 min to digest unpackaged DNA followed by centrifuging in 4^{o}C at 3,000 g for 30 min. The supernatant was transferred into 39 ml Optiseal tube (Beckman) with 16G syringe/needle. Pump Pro (Watson-Marlow, UK) was set up as follows: 200 µl

glass pipettes were used for intake and 100 µl glass pipettes were used for output. Pump speed was set at 37 rpm counterclockwise. The tube was rinsed with water and 15% iodixanol (IOD). The output pipette was loaded into Optiseal tubes containing samples. Pumping was started with 15% IOD (1:47 min), followed by 25% IOD (1:15 min), 40% IOD (1:47 min) and 60% IOD (1:50 min). (180 ml of 15% IOD contained 45 ml of OptiPrep (Axis-Shield Poc AS, Norway), 36 ml of 5 M NaCl, 36 ml of 5x TD (5x PBS, 5 mM MgCl 2, 12.5 mM KCl) and 63 ml water. 120 ml of 25% IOD contained 50 ml of OptiPrep, 24 ml of 5x TD, 46 ml of water and 300 µl of 0.5 % phenol red solution. 100 ml of 40% IOD solution contained 68 ml of OptiPrep, 20 ml of 5x TD and 12 ml of water; 100 ml of 60% IOD contained 100 ml of OptiPrep and 250 µl of 0.5% phenol red solution). The tubes were topped off with rAAV lysis buffer, heat-sealed and untracentrifuged at 100,000 g in Beckman L8-70M Ultracentrifuge for 2 hour at 18oC. To collect the virus, first interphase (between 60% and 40%) from bottom of tube and up to but not including second interphase was collected using 16 G syringe/needle.

Q sepharose was used for rAAV5 and rAAV8. The bottom of the Bio-Rad Econo-pac disposable chromatography column was snapped off and 5 ml of well-mixed Q sepharose (Sigma) were added into the column. The Q sepharose column was equilibrated with 20 ml of solution A (20 mM Tris/15 mM NaCl, pH 8.5), washed with 20 ml solution B (20 mM Tris/1M NaCl, pH 8.5) and again with 30 ml solution A. AAV samples was diluted with two times solution A and loaded to the column. After loading the sample, 50 ml of solution A was added to the column. The sample was eluted with 20 ml of solution C (20 mM Tris/355 mM NaCl, pH 8.5) and collected into a 50 ml conical tube. The sample was concentrated using Biomax-100K NMWL membrane

concentrator (Millipore, Billerica, MA) to 1 ml. The concentrate was then diluted with 9 ml of Ringer's solution and concentrated to 1 ml twice in order to reduce the salt concentration in virus solution. Typical final virus sample volume was approximately 300 µl. Samples was collected into siliconized tubes and stored at -20^{o}C.

Dot-Blot Assay

A dot-blot assay was used to determine the total number of genomic particles of rAAV virus (Kube and Srivastava, 1997). A 4 µl aliquot of the virus stock was treated with DNAse I (Roche, Mannheim, Germany) for 1 hour at 37^{o}C, followed by incubating with Proteinase K (Boehinger Mannheim, Germany) for another hour at 37^{o}C to obtain the encapsidated DNA. Samples were extracted with equal volume of phenol-chloroform twice and equal volume of chloroform once. The aqueous layer was transferred into a new tube and mixed with 1/10 volume of 3 M NaAc (pH 5.2) and 2.5 volumes of 100% ethanol. DNA was precipitated overnight at -80^{o}C, centrifuged at 14,000 g for 20 min, washed with 75% ethanol, air dried and dissolved in 40 µl of water.

The sample was quantified by a DNA slot blot assay using 1.7 kb EcoRI segment of pUF12 as probe and a series of dilutions of pUF12 (0.1 ng ~ 100 ng in alkaline buffer) as standard curve. For virus samples, 10 µl of 1:10 dilution and 1:1 dilution each were added into 200 µl of alkaline buffer tube. The standards and samples were boiled for 10 minutes and loaded into each well of the dot blotter. The samples were aspirated slowly with vacuum until fully soaked. The vacuum was disconnected. 400 µl alkaline buffer was added to each well and allowed to stand for 5 min, followed by vacuuming away any remaining solution. The membrane from the dot blotter was crosslinked by a UV Statalinker 1800 crosslinker (Strategene, La Jolla, CA) and placed into a small Biometra bottle, which was filled with prehybridyzation buffer (7% SDS, 0.25 M $NaHPO_4$ pH 7.2, 1

mM EDTA pH 8.0), and incubated at 65°C for 1 hr. 6 µl of biotinylated probe was diluted with 54 µl of 10 mM EDTA and denatured at 90°C for 10 min. The total 60 µl of denatured probe were added to the hybridization buffer, quickly mixed and incubated with the membrane overnight at 65 °C in Biometra oven.

A Brightstar Bio Detect kit (Ambion, TX) was used for signal detection according to the manufacture's manual. The intensities of the standard DNA bands were used to build a standard curve. The virus titers were calculated using the coefficients: 1 ng DNA = 4 x 10^{11} particles/ml. Vector stocks were ranged from 10^{12}-10^{13}genomic particles per ml.

Stereotaxic Surgery

All procedures were approved and overseen by the University of Florida Institutional Animal Use and Care Committee. B6C3F1/J wild type male mouse (~25 g, 2 months old, The Jackson Laboratory, Bar Harbor, ME) were housed and bred the in an AAALAC-accredited animal facility at the Health Science Center. Animals were warmed under a heat lamp, anesthetized with 4% isoflourane/oxygen and injected subcutaneously with carprofen (5 mg/kg) before the surgery to minimize pain and infection. rAAV8-rat α7 or rAAV8-GFP vectors (10^9 genomic particles) were injected into septum through a 27-gauge cannula connected via 26 gauge I.D. polyethylene tubing to a 10 µl syringe mounted to a CMA/100 microinjection pump at a rate of 0.15 µl /min. The injection coordinates for the left lateral septum were: +0.25 mm from Bregma; +0.35 mm from the midsaggital suture and -2.5 mm from the skull surface according to the atlas of Paxinos & Franklin (2001). The cannula was left at the injection site for 5 min and then removed slowly. The skin was sutured. Mice were warmed at 37^{o}C until recovery from anesthesia, and returned to home cages. Two weeks after injections,

mice were trained with Morris water maze tasks as described below. After behavioral evaluation, mice were deeply anesthetized with 4% isoflourane/oxygen. Half of each group was perfused with PBS; brains were excised, fixed for 48 hr in 4% paraformaldehyde and equilibrated in 30% surcrose for immunohistochemistry and immunefluorescence. The other half of them in each group were euthanized by decapitation, and the left hippocampus, right hippocampus and septum were dissected quickly, snap frozen in liquid nitrogen and stored at -80°C for biochemical procedures.

Morris Water Maze Tests

Morris water maze tests were performed to test the spatial learning and memory of mice injected with rAAV8-rat α7 or rAAV8-GFP vectors. These tests were conducted using a specially designed circular tank (75 cm interior diameter) with a white interior filled to a depth of ~34 cm with room temperature water, which was made opaque by the addition of powdered white paint. An escape platform (5.5 cm diameter), made of Plexiglas and covered with a coarse material that provided grip for climbing onto the platform, was located approximately 1.0 cm below the water surface. Various geometric high-contrast images (e.g., circles, squares, triangles) were hung above the water surface as navigational references. Mice received 8 trials daily for 2 days in order to memorize the location of the submerged platform. The mice had 60 sec to search for the platform (and were hand guided to the platform if they did not reach it during that interval). They were then allowed 30 seconds to stay on the platform. Probe test was followed with the 2-day training, in which, the platform was removed and the mice had 60 sec to search for the platform. The swim distance and percentage of time spent in each quadrant were recorded by video camera and analyzed with Image-Pro software (Media Cybernetics, Bethesda, MD).

Immunohistochemistry

Fixed forebrains blocks were cut into coronal sections (50 μm) on a sliding microtome with freezing stage. Antigen retrieval was done by incubating the sections with 50 mM sodium citrate (pH 8.5-9.0) at 80^{o}C for 30 min (Jiao et al., 1999). Antigen detection was conducted on free-floating sections by incubating the sections at 4°C in blocking solution (3% goat serum, 0.3% Triton X-100, 0.05% azide in PBS) for 1 hr at room temperature, followed by primary antibody incubation overnight at 4°C. Primary antibodies used were: anti-α7 (1:200, Covance), anti-TrkA (1:500, Upstate Biotechnology), and anti-ChAT (1:1000, Chemicon). Sections were incubated with primary antibodies diluted in blocking solution at 4°C for 3 days. Sections were then washed with PBS three times for 5 minutes each wash. Then the sections were incubated overnight at 4°C with secondary antibody (biotinylated anti-mouse IgG or biotinylated anti-rabbit IgG, 1:1000, Dako, CA) diluted in blocking solution. Sections were again washed 3 times in PBS. Next the sections were incubated for two hours at room temperature in PBS with ExtrAvidin peroxidase (HRP) conjugate (1:1000, Sigma). Washing was performed again. Development of tissue labeled with HRP was performed with a solution of 0.67 mg/mL diaminobenzidine (DAB, Sigma) / 0.003% H_2O_2/ 8 mM imidazole / 2% $NiSO_4$. The sections were mounted on Superfrost plus microscopic slides (Fisher Scientific), air dried and dehydrated by passing through water, followed by 70%, 95%, 100%, 100% ethanol (5 min each). Then they were passed through two changes of xylene, and coverslipped with Eukitt (Calibrated Instruments, Hawthorne, NY).

Some sections were used for immunofluorescence staining. After incubating with mouse anti-α7 and rabbit anti-TrkA primary antibodies, sections were washed in PBS 3

times and incubated Alex Fluo 488 labled anti-mouse IgG and Alexa Fluor 594 labled anti-rabbit IgG. Sections were washed in PBS and then mounted on Fisher Superfrost Plus slides, air-dried and coverslipped with glycerol gelatin (Sigma).

Statistical Analysis

Statistical analyses involved one-way or two-way ANOVA for main effects hypothesis testing using Prism (GraphPad software, a Jolla, CA). Post-hoc comparisons of parametric populations were made using Bonferroni's tests. Statistical analyses for mice water maze effects were conducted in SAS (SAS Institute, Cary, NC) General Linear Models procedure.

CHAPTER 3
EFFECTS OF α7 RECEPTOR GENE DELIVERY ON PROCESSES UNDERLYING CELL VIABILITY

Introduction

Cholinergic neurons are essential for normal memory-related behaviors but are dysfunctional in AD. Studies suggest that α7 nAChRs expressed on these and other neurons regulate their normal physiologic function and positively modulate their viability under apoptotic conditions. These neuroprotective functions of α7 receptor appeared to be attenuated in AD, making them suitable targets for treating this progressive memory-related disorder. Selective agonist treatments have shown success in a variety of models, however, these receptors exhibit highly dose-dependent properties. They experience fast desensitization at high agonist concentrations. An alternative approach would be increasing the receptor level by gene delivery. α7 nicotinic receptor gene delivery into mouse hippocampus by adeno-associated virus was recently shown to improve spatial memory performance (Ren *et al*., 2007b). While this improvement was likely mediated by altered receptor response to endogenous agonists, no study has attempted to evaluate the processes underlying combined effects of gene delivery with selective agonist.

Activation of α7 receptors can increase calcium accumulation both directly as well as through indirect activation of downstream L-type voltage sensitive channels, IP-3 channels, and ryanodine channels (Vijayaraghavan *et al*., 1992; Gueorguiev *et al*., 2000; Shoop *et al*., 2001; Dajas-Bailador *et al*., 2002b). Several groups including ours have demonstrated that GTS-21 and 4OH-GTS-21 α7 agonists increased intracellular calcium concentrations (Li *et al*., 2002), activated the calcium-sensitive transduction

processes such as PKA, PKC, PI3K, MAPK and JAK kinases, each is essential for α7 mediated protection against one or more apoptotic insults.

It has been well documented that extracellular signal regulated kinase 1 and 2 (ERK 1/2), member of the MAPK signaling pathway, are involved in α7 activation mediated neuroprotection (Toborek *et al*., 2007) and long term potentiation enhancement (Welsby *et al*., 2009). Data suggested that α7 nAChR agonist-triggered Ca^{2+} transients in PC12 cells induce activation of CaMKII, leading to sequential phosphorylation of MEK1/2, ERK1/2 and CREB (Nakayama *et al*., 2001; Gubbins *et al*., 2010). This pathway regulates new gene expression (Curtis and Finkbeiner, 1999) and is involved in cellular survival, synaptic plasticity and long term memory (Orban *et al*., 1999).

Another MAPK cascade member c-jun-N-terminal kinase (JNK) is more frequently involved in downstream pro-apoptosis pathways (Manning and Davis, 2003; Nishina *et al*., 2004). Knock-out mouse studies have demonstrated that removing particular JNK genes can reduce the severity in various disease scenarios, including those which are used to model neurodegenerative diseases (Bonny *et al*., 2005). There are data showing that JNK is involved in Tau and APP protein metabolism, leading to hyperphosphorylated Tau and overproduced Aβ (Reynolds *et al*., 1997; Philpott and Facci, 2008). Therefore, blocking JNK pathway may be a valuable approach for AD and other neurodegenerative disease research.

PI3K/AKT is another cellular signaling pathway responsive to α7 nAChRs activation. Nicotine induced protection in rat-cultured primary neurons was blocked by either an α7 nAChR antagonist, a PI3K inhibitor or a Src inhibitor. Levels of

phosphorylated Akt, an effector of PI3K, and anti-apoptotic protein Bcl-2 and Bcl-x were increased by nicotine administration (Shimohama *et al*., 2009). AChE inhibitor drugs used for AD treatment, e.g., donepezil and galanathamine, prevent glutamate neurotoxicity and inflammation via up-regulated AKT phosphorylation (Takada-Takatori *et al*., 2006; Shen *et al*., 2010; Tyagi *et al*., 2010) and were blocked by α7 selective antagonist MLA and JAK2 inhibitor. Therefore, it has been proposed that the α7 nAChR activation stimulates the Src family and JAK2, which activate PI3K to phosphorylate AKT and subsequently transmits the survival signal to up-regulate Bcl-2 and Bcl-x. This pathway could prevent cells from neuronal death induced by Aβ (Kihara *et al*., 2001; Shaw *et al*., 2002).

Besides ERK1/2 and AKT activation, the ability of caspase inhibitors to block neuronal cell death induced by trophic factor deprivation and other cytotoxic conditions including amyloid β exposure has provided evidence for a crucial role of caspases in apoptotic neuronal cell death (Deshmukh *et al*. 1997; Youdim *et al*. 2001; Eckert *et al*. 2003; Yuan *et al*. 2000). In addition to activating death programs, caspase activated by amyloid β can cleave tau to generate a proteolytic product and promote pathological tau filament assembly in neurons (Gamblin *et al*. 2003). Regulation of caspase activity involves MAPK / ERK1/2 and the PI3K / AKT pathways. Therefore in this study, we investigated the effects of α7 nAChR gene delivery on agonist sensitivity relative to intracellular signal processes associated with cell survival. We hypothesized that α7 receptor overexpression with the assistance of chaperone RIC-3 will increase the agonist effects on ERK phosphorylation, AKT phosphorylation and caspase activity in PC12 cells.

Results

Gene Delivery System Resulted Functional α7 Receptor Expression

Pheochromocytoma PC12 cells express α7 nAChRs and the endogenous agonists acetylcholine and choline. The signaling pathways that respond to α7 nAChR activation in these cells have been well characterized using cell lines with high intrinsic α7 receptor level (e.g., over 100 fmol/mg protein). However, the PC12 cells used in the present study was selected for its relatively low levels of endogenous functional α7 receptors expression according to ligand binding assay. This provided a more suitable model for basal forebrain cholinergic neurons in AD brain, where α7 receptor density is decreased during the disease progression.

PC12 cells are refractory to gene delivery by most vehicles, with no successful procedure reported in the literature. Therefore, a variety of gene delivery methods were evaluated initially for GFP expression efficiency in PC12 cells (Figure 3-1): rAAV, using either serotype coats #2, #5, or #8, each with terminal repeats from serotype #2); calcium phosphate, that precipitate plasmid DNA via interaction with calcium ions; and cationic lipid vectors (Lipofectamine 2000^{TM} from Invitrogen and Lipo293^{TM} from SignaGen). Among these approaches, cationic lipid vectors consistently yielded the highest transfection efficiency (15~20%) based on GFP expression, with no apparent cytotoxicity. Therefore these vectors were used for all the following *in vitro* gene delivery.

pUF-12-α7 plasmids were transfected into PC12 cells together with pcDNA-ric-3 plasmids using Lipofactamine 2000^{TM}. The functional α7 receptor density was evaluated by high affinity [^{3}H] MLA binding assay. 24 hr after transfection, the functional membrane α7 receptor level was increased by around two fold in the cells transfected

with a combination of α7 and ric-3 plasmids compared to GFP-transfected or non-transfected controls (Figure 3-2a). Transfection with the ric-3 expression vector alone, but not the α7 receptor alone, also increased [^{3}H] MLA binding (Figure 3-2a), though not to the extent observed with a combination of these vectors. None of these Lipofectamine-based vectors affected cell viability (Figure 3-2b). Besides, a 1:1 (weight/weight) ratio of α7 and ric-3 gave the highest receptor expression (Figure 3-3a). Increasing the DNA dose of this 1:1 plasmid combination to 4 µg/ml decreased total high affinity [^{3}H]MLA compared to 2 and 3 µg/ml doses (Figure 3-3b). Therefore, the PC12 cell gene delivery regimen using 1:1 (weight/weight) ratio of α7 and ric-3 with a total dose of 2 µg/ml and Lipofectamine was used for subsequent studies.

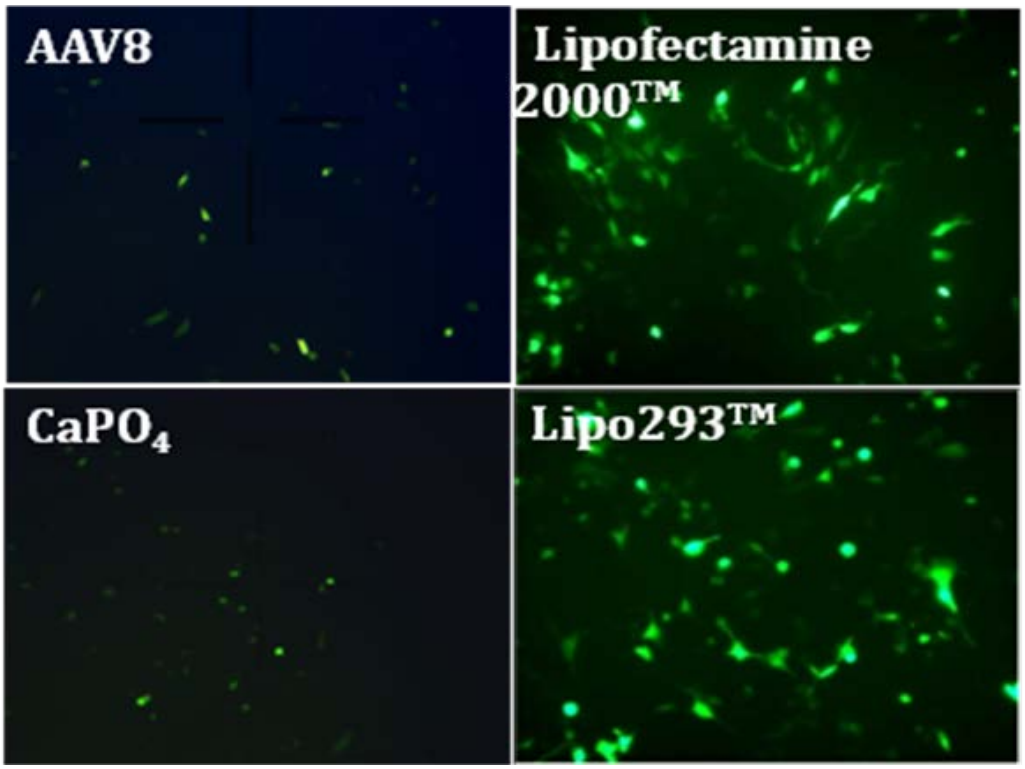

Figure 3 -1: Transfection efficiency in PC12 cells. pUF-12-GFP plasmids utilized a CBA/CMV promoter were transfected / transduced into PC12 cells (60% confluence) using: AAV8, calcium phosphate, Lipofectamine 2000™, and Lipo293™. Green fluorescence was detected by Axiovert microscope under 505nm wavelength after 24hrs of transfection.

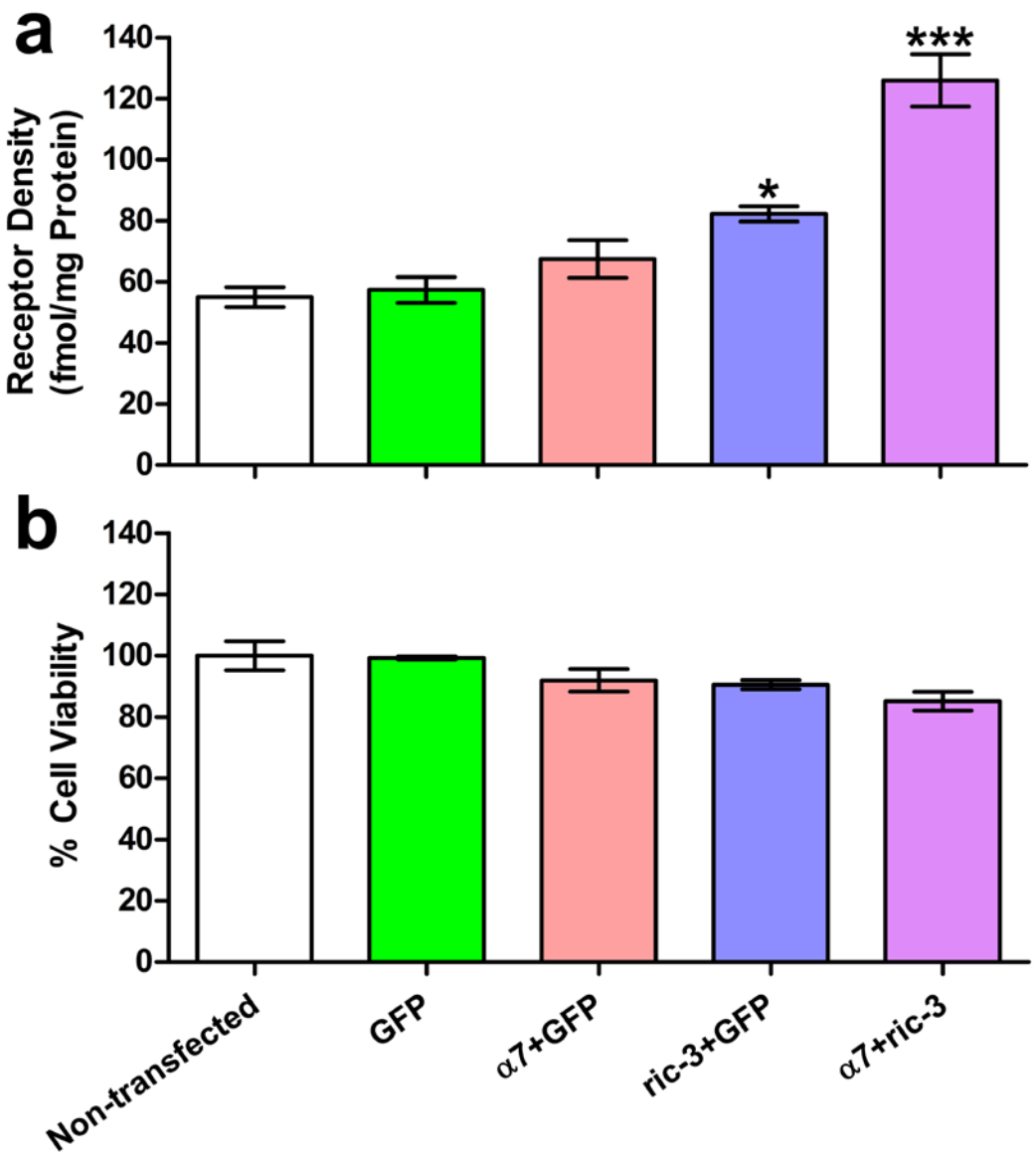

Figure 3-2: Effects of α7 and ric-3 gene delivery on α7 receptor density in PC12 cells. Functional α7 receptor levels were evaluated using high affinity [3H] MLA binding method 24 hr after transfection with 2 μg/ml specified plasmid(s). All values are means ± SEM of 2 separate experiments conducted in triplicate; mean value comparisons used one way ANOVA followed by Bonferroni's test. (a) Co-transfection with α7 and ric-3 plasmids increased high affinity, nicotine displaceable [3H] MLA binding compared to all other groups (*: $p<0.01$). Transfection with ric-3 increased binding compared to the non-transfected group (#: $p<0.05$). (b) The transfection process did not significantly affect cell viability.

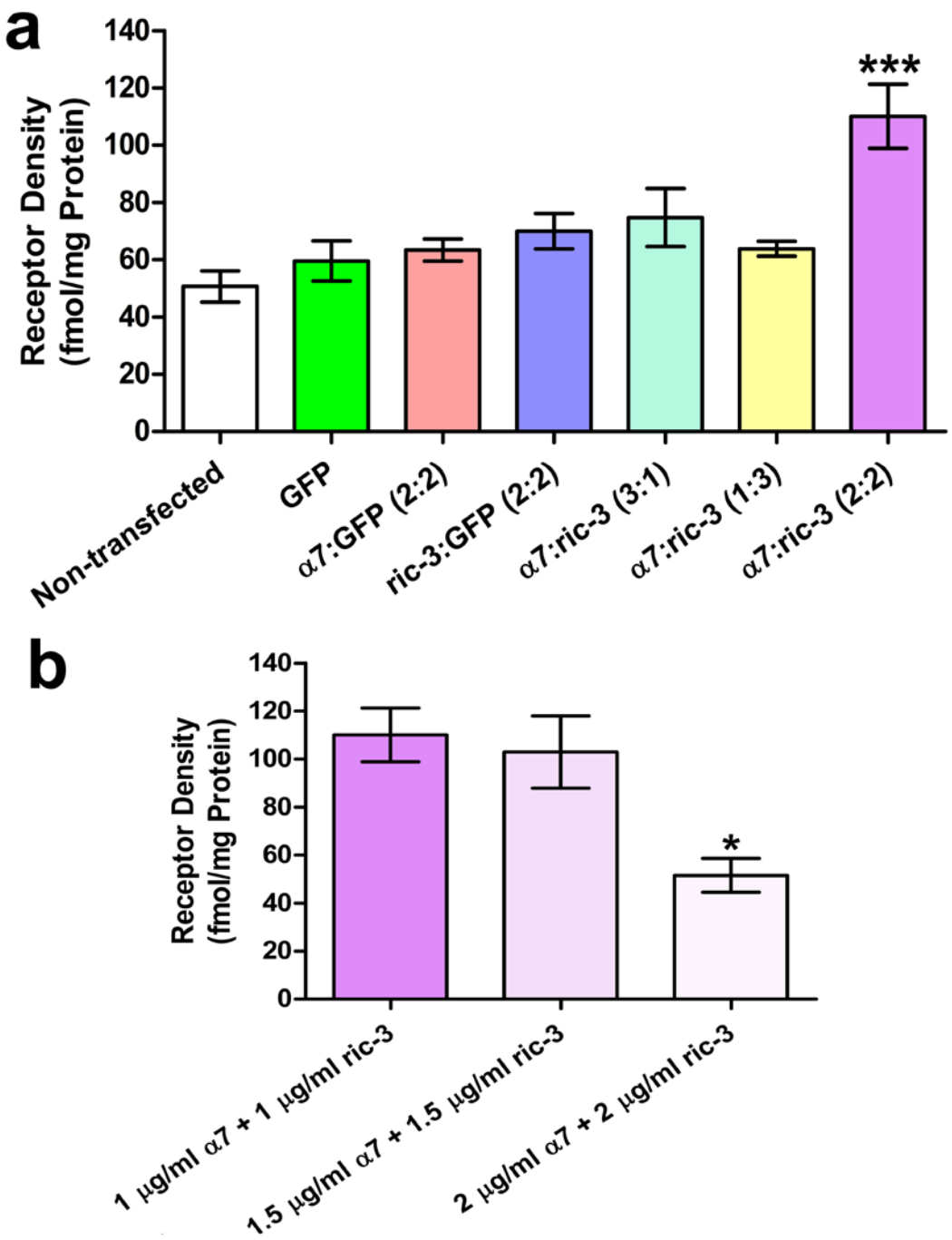

Figure 3-3: Optimization of α7 and ric-3 gene delivery ratio and dose. (a) 1:1 (weight/weight) ratio of α7 and ric-3 plasmids yielded the highest receptor expression compared to all other tested combinations. (b) A total of 4 µg/ml plasmids lowered the functional receptor expression compared to 2 or 3 µg/ml doses.

Effects of 4OH-GTS-21 on p-ERK2 and p-Akt in Transfected Cells:

α7 receptors are highly permeable to calcium (Fucile *et al*., 2003). Receptor activation by agonist can induce ERK and AKT phosphorylation via calcium influx and PI3K activation. Between the two major ERK isoforms ERK1 (p44) and ERK2 (p42), the role of ERK2 seems preeminent over that of ERK1 despite sharing the same activators and substrates (Lefloch *et al*. 2008). A pharmacology experiment was designed to investigate the response of ERK2 to α7 activation: PC12 cells were transfected with α7+ric-3 or an equal amount of GFP as control. 24 hr after transfection, the cells were treated with or without 100 nM α7 antagonist MLA for 30 min and then incubated with 1 μM, 3 μM, 10 μM or 30 μM 4OH-GTS-21 for another 30 min. The agonist concentrations chosen were broad enough to cover the range from cytoprotection to toxicity observed in previous PC12 studies (Li *et al*., 1999b). Cell samples were collected to evaluate the total protein, total ERK2 and p-ERK2 levels. ERK2 and p-ERK2 values were normalized to total protein concentrations and then to GFP transfected control without 4OH-GTS-21 or MLA treatment.

Total ERK levels were not affected by gene delivery or by a 30 min treatment with any concentration of 4OH-GTS-21 (Figure 3-4a). The p-ERK2/ERK2 ratio, an estimate of ERK2 activation, was neither attenuated by MLA pretreatment nor activated by a broad range of 4OH-GTS-21 concentrations in GFP-transfected cells (Figure 3-4b). In α7 + ric-3 transfected cells, however, 4OH-GTS-21 increased p-ERk2/ERK2 ratios in an inverted U-shaped, concentration-dependent manner compared to GFP-treated controls (Figure 3-4b). MLA sensitive, agonist-induced elevations in p-ERK2/ERK2 ratios were observed at 1-10 μM 4OH-GTS-21 concentrations (Figure 3-4c); at the 30 μM agonist

concentration, there was no activation of ERK2 phosphorylation, consistent with the rapid α7 receptor desensitization reported at this elevated 4OH-GTS-21 concentration.

Similarly, total AKT levels were not changed within 30 min of 4OH-GTS-21 treatment in any transfection group (Figure 3-5a). In the α7+ric-3 transfected group, p-AKT/AKT ratios were significantly higher than in the GFP-transfected group at the 1 μM and 3 μM 4OH-GTS-21 concentrations (Figure 3-5b). Like ERK2, AKT did not respond at the 30 μM 4OH-GTS-21 concentration. MLA pretreatment attenuated the increase in p-AKT/AKT ratios seen with 1 μM 4OH-GTS-21 in the α7 + ric-3 group (Figure 3-5c).

In order to understand the relationship between ERK and AKT activation evoked through α7 receptors, ERK phosphorylation inhibitor PD 98059 (Alessi *et al*. 1995) was preincubated with cells before agonist treatment; and p-AKT levels were evaluated afterwards. The results showed that PD 98059 blocked ERK phosphorylation (Figure 3-6a), but did not influence AKT phosphorylation either in α7 + ric-3 (Figure. 3-6b) or GFP-transfected groups (Figure 3-6c).

In contrast to the ERK and AKT systems, p-JNK/JNK ratios were not affected by either transfection with α7 + ric-3 or subsequent treatment with 4OH-GTS-21 (Figure 3-7). Total JNK levels were also unaffected by these treatments (not shown).

Effects of 4OH-GTS-21 on Caspase Activity:

In order to evaluate the effect of α7 and ric-3 gene delivery and activation on cell apoptosis, we analyzed the activity of central caspase cascade executers: caspase 3/7 (Riedl *et al*. 2004). Caspase 3/7 activities were significantly reduced after 1-10 μM 4OH-GTS-21 treatment in the α7 + ric-3 transfected groups compared to GFP-transfected controls (Figure 3-8a). This effect was potently blocked by MLA (Figure 3-8a and 3-8b).

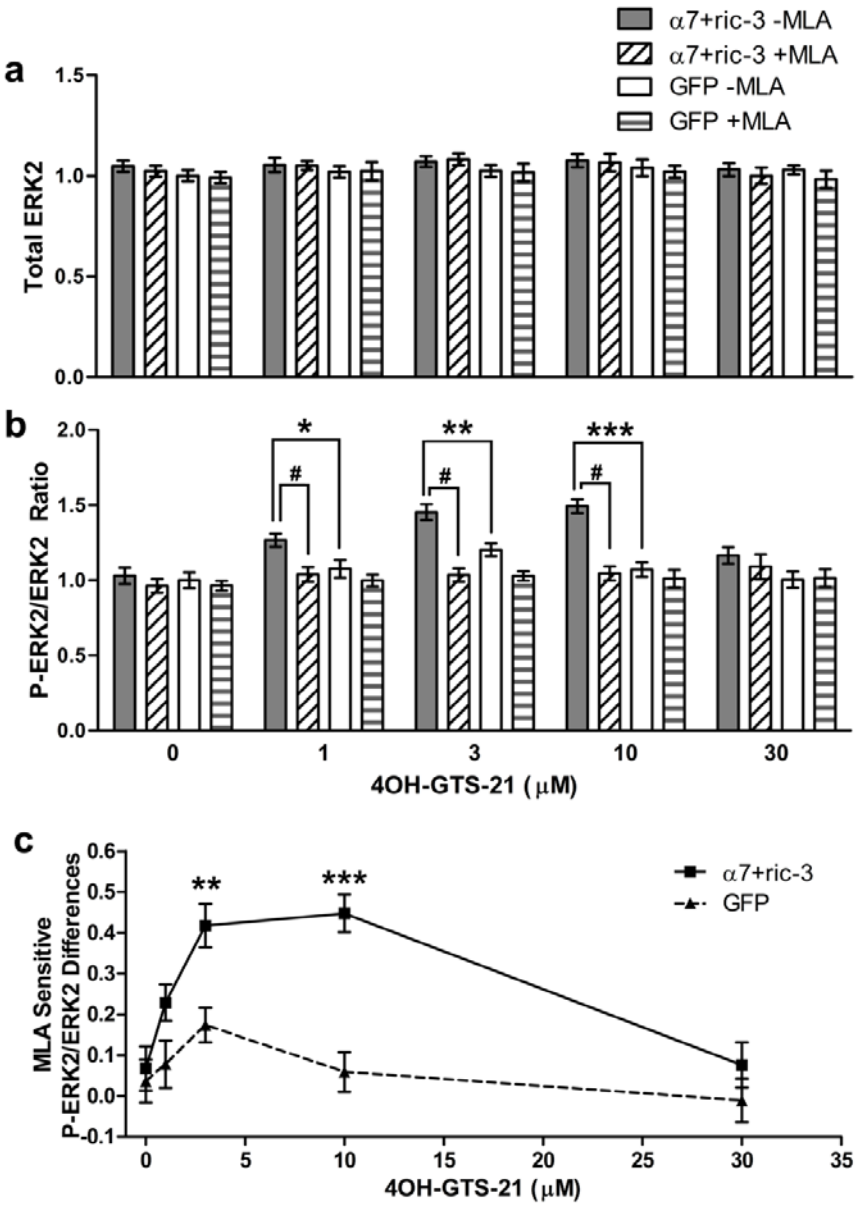

Figure 3-4: Effects of α7 overexpression on 4OH-GTS-21 induced ERK2 responses. All values are means ± SEM of 3 separate experiments conducted in duplicate; mean value comparisons used two way ANOVA followed by Bonferroni test. (*: $p<0.05$, **: $p<0.01$, ***: $p<0.001$; #: $p<0.001$) (a) Total ERK2 levels were not affected. (b) The p-ERK2/ERK2 ratios in α7 + ric-3 transfected cells were significantly higher than controls after 1-10 μM 4OH-GTS-21 treatment. The ERK2 phosphorylation induced by 4OH-GTS-21 can be totally blocked by MLA pre-treatment. (c) MLA sensitive α7 specific activity on p-ERK2/ERK2 ratios were significantly increased in α7 + ric-3 co-transfected groups compared to those in GFP transfected controls at 3 and 10 μM 4OH-GTS-21 concentrations.

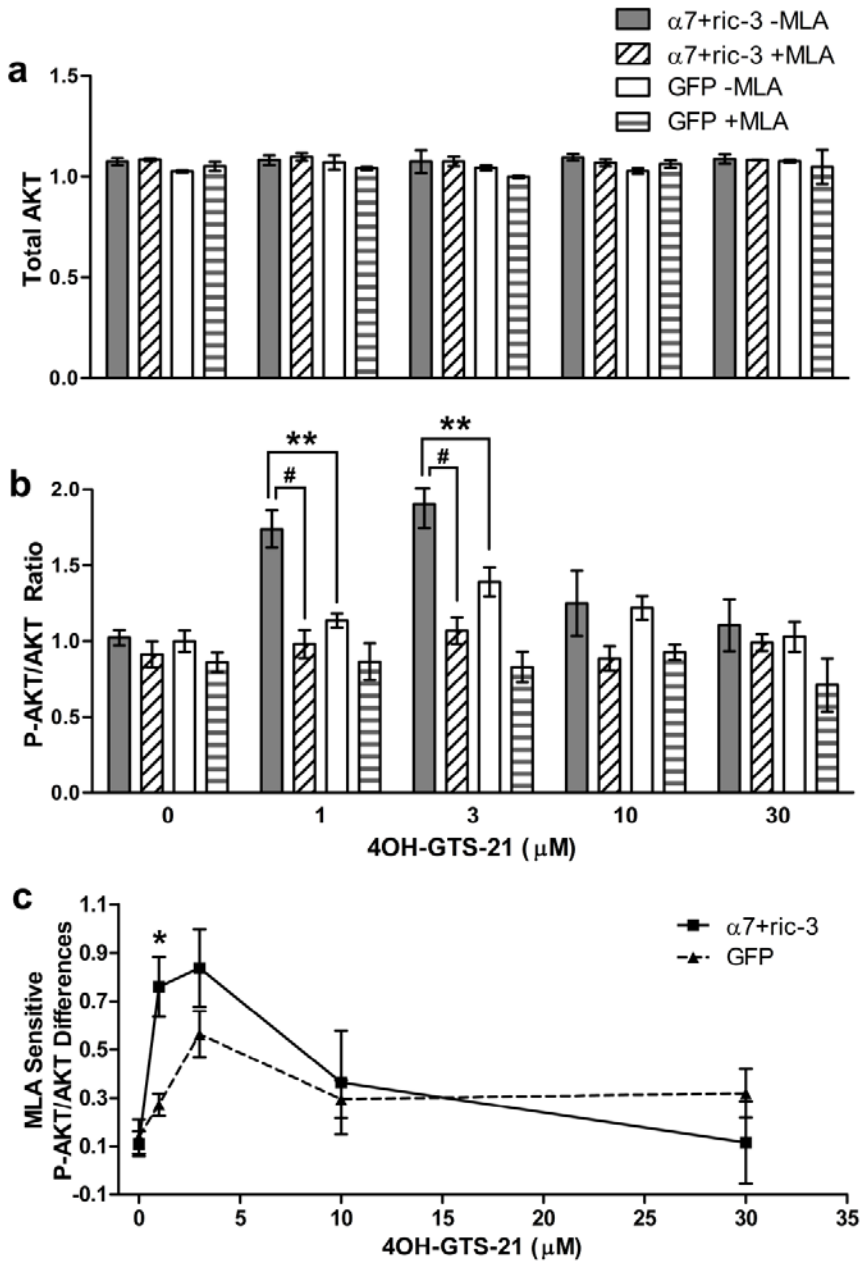

Figure 3-5: Effects of α7 overexpression on 4OH-GTS-21 induced AKT responses. All values are means ± SEM of 2 separate experiments conducted in duplicate; mean value comparisons used two way ANOVA followed by Bonferroni test. (*: $p<0.05$; **: $p<0.01$; #: $p<0.001$) (a) Total AKT levels were not affected. (b) The p-AKT/AKT ratios in α7 + ric-3 transfected cells were higher than controls at 3 -10 μM 4OH-GTS-21 concentrations. The AKT phosphorylation induced by 4OH-GTS-21 can be completely blocked by MLA pre-treatment. (c) MLA sensitive α7 specific activity on p-AKT/AKT ratios were increased in α7 + ric-3 co-transfected cells compared to GFP transfected controls at a 1 μM concentration of 4OH-GTS-21 treatment.

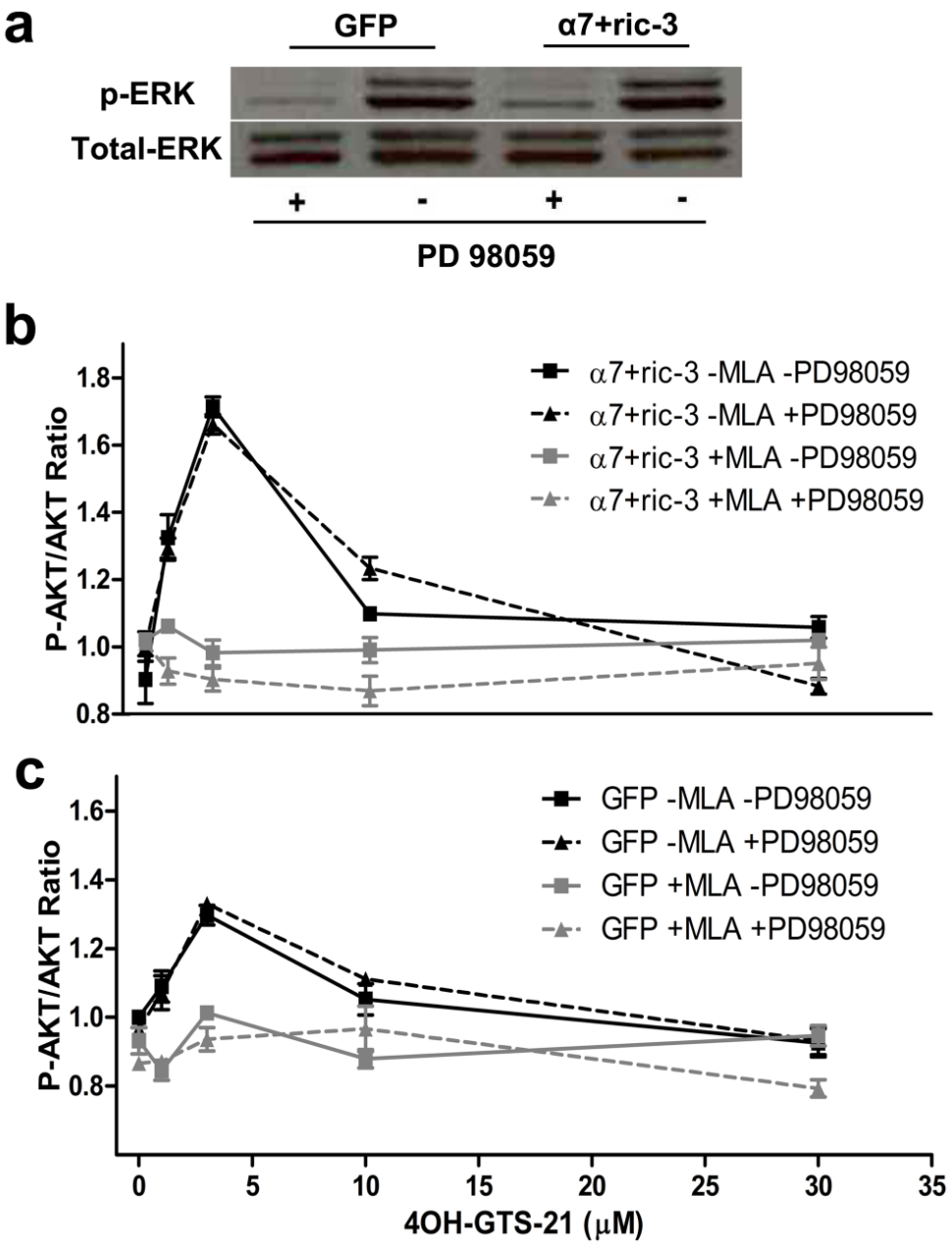

Figure 3-6: AKT phosphorylation is not affected by ERK inhibitor in the case of α7 activaton. P-AKT and AKT values were normalized to the measurements of GFP transfected control without MLA, PD98059 or 4OH-GTS-21 treatments. All values are means ± SEM of 2 separate experiments conducted in duplicate; mean value comparisons used two way ANOVA followed by Bonferroni test. (a) PD98059 potently inhibited ERK phosphorylation, but did not influence AKT phosphorylation in (b) α7 gene over-expressed cells or (c) control cells with normal α7 receptor levels.

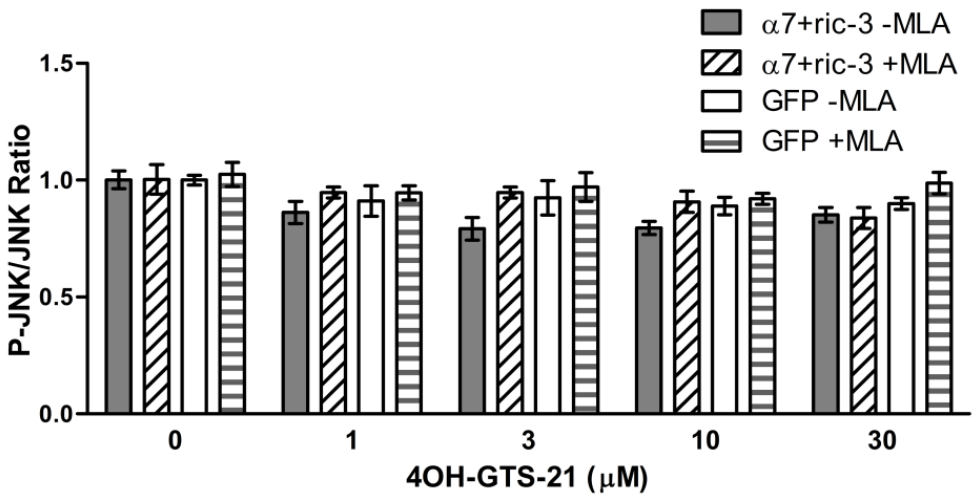

Figure 3-7: Effects of α7 overexpression and activation on JNK phosphorylation. All values are means ± SEM of 3 separate experiments conducted in duplicate; mean value comparisons used two way ANOVA followed by Bonferroni test. α7 and ric-3 gene delivery along with agonist treatment did not have a significant effect on JNK phosphrylation.

Discussion

These results show for the first time that α7 gene delivery together with ric-3 increased functional α7 receptor expression in a neuronal model and, when combined with agonist treatment, elevated ERK2 and AKT activity as well as decreased caspase3/7 activity. Although previous studies showed that α7 receptor activation through pharmacological means can promote ERK and AKT activities, this is the first demonstration that increasing the expression of α7 combined with a selective agonist can increase the activities of cell-survival related signaling pathways compared to intrinsic receptor levels alone, which is consistent with α7 receptor's cytoprotective effects.

A common problem that has been encountered with α7 subtypes is that of inefficient functional expression of recombinant receptors in artificial expression systems (Millar, 1999). α7 and ric-3 co-transfection significantly increased membrane

α7 receptor levels, consistent with the observation that RIC-3 is a chaperon protein for α7 subunit folding and assembling.

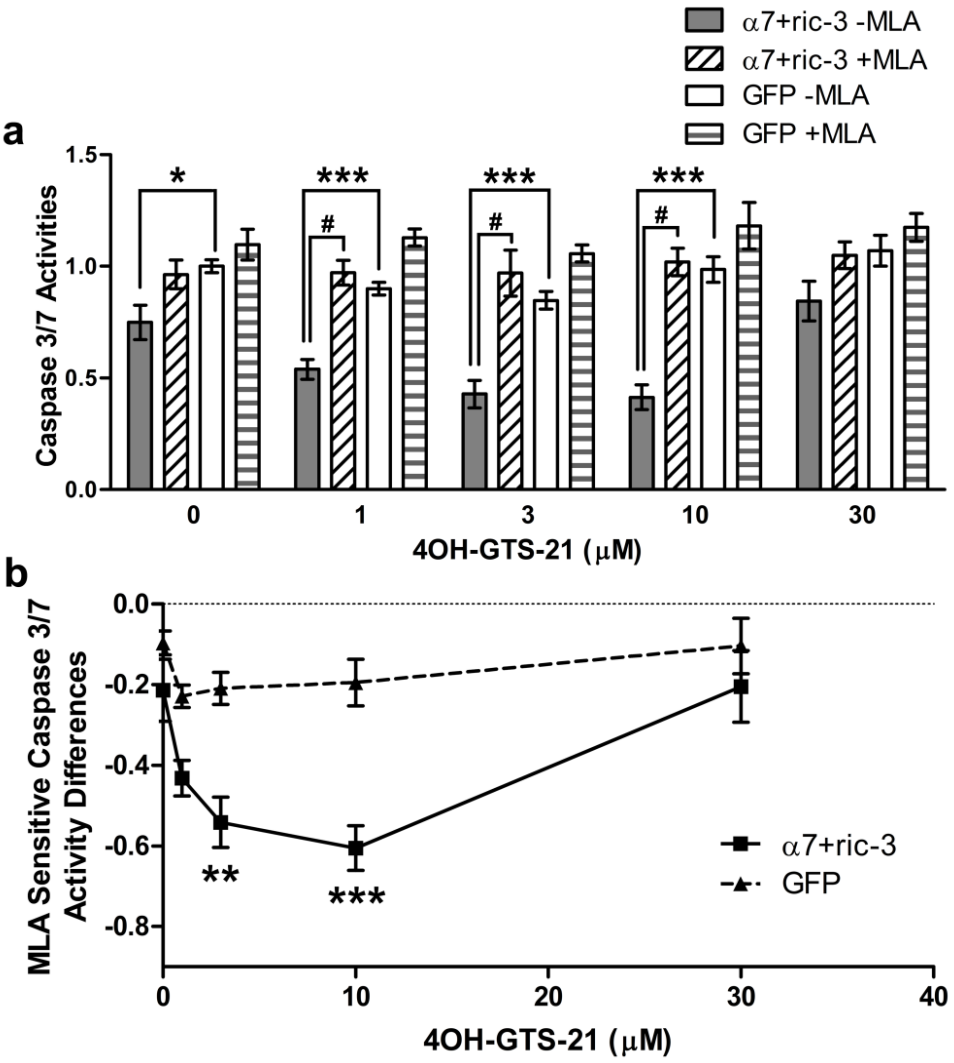

Figure 3 -8: Effects of α7 overexpression on 4OH-GTS-21 induced caspase 3/ 7 responses. Caspase 3/7 activities were assayed, normalized for protein, and expressed as the % of control cells (GFP transfected cells without 4OH-GTS-21). All values are means ± SEM of 2 experiments conducted in duplicate; mean value comparisons used two way ANOVA followed by a Bonferroni test. (a) Over-expressed α7 receptors themselves, or combined with 4 OH-GTS-21 t reatment, si gnificantly suppressed ca spase 3/ 7 activities (*: p<0.05, ***: p<0.001). This effect could be blocked by MLA (#: p<0.001); indicating an α7 specific anti-apoptotic function (**: p<0.01, ***: p<0.001, at 3 and 10 μM 4OH-GTS-21 concentration respectively) (b).

RIC-3 it was originally identified in the nematode Caenorhabditis elegans (C. elegans) as the protein encoded by the gene ric-3 (resistance to inhibitors of cholinesterase) and has subsequently been cloned and characterized from mammalian and insect species (Nguyen *et al*., 1995).It is interesting to note that Ric-3 gene delivery alone also elevated the membrane α7 receptor expression to some extent, while α7 gene delivery alone did not show a significant effect, suggesting ric-3 expression is more limiting than α7 translation for the number of functional α7 receptors in plasma membrane in this PC12 cell line. In contrast to normal aging, where both α7 mRNA and protein levels were decreased (Court *et al*. 2001), in AD α7 protein loss is observed without significant mRNA level change or even increased α7 mRNA level (Engidawork *et al*. 2001; Perry *et al*. 2001; Wevers *et al*. 2000; Hellstrom-Lindahl *et al*. 1999). These data pointed to a possibility that the α7 receptor expression deficit in AD is related with translational or post-translational problems rather than transcriptional insufficiency. Thus, RIC-3 modulation itself may be important for AD pathogenesis and a valuable target for future studies.

Selective α7 agonists have been intensively studied and broadly used for therapeutic purposes. However, α7 receptors desensitize rapidly and persistently at relatively low steady-state agonist concentrations (Seguela *et al*., 1993; Uteshev *et al*. 2003; Papke *et al*. 2009). Therefore a low agonist concentration needs to be maintained for long-term treatment. In our study, receptors still desensitize at high 4OH-GTS-21 concentrations, but the agonist efficacy at lower concentrations was increased reflecting on ERK2 and AKT phosphorylation, which play important roles in cell proliferation, differentiation and anti-apoptosis (Pettmann *et al*. 1998; Traverse *et al*. 1992; Franke *et*

al. 1997). Considering the 15~20% of plasmid transfection efficiency, the true effects might be even higher, which is quite promising for protection purposes. Although a previous study showed that α7 gene overexpression in PC12 cells alone resulted in sustained ERK phosphorylation (Utsugisawa *et al*., 2002), other studies suggested α7 induced ERK phosphorylation is a transient event (Ren *et al*., 2005; El Kouhen *et al*., 3009; Gubbins *et al*., 2010), consistant with our results. ERK phosphorylation inhibitor PB98059 did not influence AKT phosphorylation, suggesting no crosstalk between these two pathways (at least at the pathways before AKT and ERK) when induced by α7 receptor activation. Some studies showed AKT and ERK converged downstream at the level of Bcl family proteins and ribosomal s6 kinase (RSK) (Creson et al., 2009). The activation of JNK, another MAPK pathway kinase, might be necessary but not sufficient, to induce neuronal apoptosis (Manning *et al*. 2003; Yuan *et al*. 2000). In our results, JNK activity is not significantly influenced by α7 gene delivery combined with agonist treatment. However, there was a tendency for reduced JNK activation at certain 4OH-GTS-21 concentrations in the α7 and ric-3 transfected group.

Both ERK and AKT survival pathways regulate Bcl family proteins (Almeida *et al*., 2005; Shen *et al*., 2010), which have a crucial role in intracellular apoptotic signal transduction. This gene family includes both anti-apoptotic and pro-apoptotic proteins that contain one or more bcl-2 homology (BH) domains. The major anti-apoptotic members of the Bcl-2 family, Bcl-2 and Bcl-xl, are localized to the mitochondrial outer membrane and to the endoplasmic reticulum and perinuclear membrane. Overexpression of Bcl-2 attenuated the pathogenesis in a triple transgenic mice model for AD, suggesting the activation of apoptotic pathways may be an early event

contributing to the progress of AD (Rohn *et al*., 2008). Studies have shown that ERK and AKT may regulate Bcl-2 by activating CREB and enhance Bcl-2 synthesize (Creson *et al*., 2009) or by directly phosporylating Bcl-2 (Ito *et al*., 1997). Blocking ERK or AKT phosphorylation prevented the anti-apoptosis effects in neurons (Laing *et al*., 2008; Namikawa *et al*., 2000). ERK can also protect cortical neurons via inactivating Bad, the pro-apoptotic Bcl family protein, by phosphorylate it (Jin *et al*., 2002). Our studies showed Bcl-2 levels were not significantly changed after α7 and ric-3 gene delivery compared to controls. One possible reason might be that 30 min agonist treatment is not sufficient for detectable changes in Bcl-2 transcription and translation.

Bcl-2 inhibits mitochondra cytochrome C release triggered by apoptotic stimuli, thereby consequently blocking the activation of caspase cascade (Riedl and Shi, 2004). The present results showed that up-regulating α7 receptors triggered a decrease in caspase 3/7 activities. It was interesting to observe that, with no 4OH-GTS-21 present, over-expressed α7 receptors alone were sufficient to induce caspase 3/7 response compared to the GFP controls (Figure 3-8a, at 0 μM 4OH-GTS-21) but not in the case of ERK/AKT responses (Figure 3-4a and 3-4b at 0 μM 4OH-GTS-21). This suggested that over-expressed α7 receptors may regulate the caspase activity both directly and indirectly from α7 receptor mediated signaling pathways. A possible indirect pathway is that elevated α7 receptors increase the expression of nerve growth factor (Jonnala *et al*. 2002; Hernandez *et al*. 2005) which helps to down-regulate caspase activities by activating TrkA receptors. Mounting evidence suggested the involvement of caspases in the disease processes associated with AD. The activation of caspases not only triggers the apoptosis cascade, but also cleavage of APP and tau to facilitate the production of

neurotoxic Aβ and neurofibrilary tangles. Therefore, caspase inhibition may be a potential future approach for treating neurodegeneration (Rohn and Head, 2009).

In conclusion, α7 and ric-3 co-transfection increased α7 nicotinic receptor expression in PC12 cells, which, combined with selective agonist 4OH-GTS-21, increased α7 receptor mediated ERK and AKT activation as well as decreased caspase 3/7 activities. The combination of pharmacological and genetic approaches employed in this study may be useful for treating conditions such as AD which are characterized by low levels of endogenous α7 receptor expression in brain. The mechanistic studies focusing on the roles of ERK, JNK MAPKs as well as caspases are expected to reveal future targets and approaches for drug development in an AD-like milieu.

CHAPTER 4
EFFECTS OF α7 RECEPTOR GENE DELIVERY ON NEUROTROPHIN PATHWAY

Introduction

The basal forebrain cholinergic neurons are largely comprised of the nucleus basalis magnocellularis, the horizontal and vertical diagonal bands of Broca and the medial septal nucleus. Cholinergic neurons within the nucleus basalis and the septal complex provide the major source of cholinergic innervation to the cerebral cortex and hippocampus, respectively, contributing to the memory and attentional functions of those regions (Niewiadomska 2010). Cholinergic neurons are particularly vulnerable during AD, and emerging evidence shows NGF to be an essential maintenance factor for their normal function (Cuello *et al*., 2010).

NGF is one of the neurotrophic factors that stimulate axonal growth and maintain neuronal phenotype and promote neuronal survival (Siegel and Chauhan, 2000). During development, growing axons compete for limited amounts of neurotrophic factors produced by target tissues (Yuen *et al*., 1996). In adult brain, neurotrophic factors are required to maintain normal functions and specific phenotype (Sofroniew *et al*., 2001). NGF mRNA and protein are highly concentrated within basal forebrain targeted regions, such as the hippocampus and cerebral cortex (Large *et al*., 1986) and released from postsynaptic terminals. Once bound to its receptors existing on cholinergic presynatic terminals, the NGF-receptor complex is internalized and retrogradely transported from these regions to basal forebrain neuron somas (DiStefano *et al*., 1992). A wealth of data demonstrated that basal forebrain cholinergic neurons are exquisite sensitive to NGF; insufficient NGF supply may be responsible for the consistent atrophy and neuron loss seen in AD. Transection of fimbria cuts the connection between septal basal forebrain

and hippocampus, blocks NGF transportation, results in cholinergic neuron loss and mimics AD-like behavioral deficits (Lapchak 1993). NGF treatment in septum rescued cholinergic neurons that undergo degeneration following septohippocampal axotomy in rodents and primates (Hefti 1986; Williams *et al*., 1986; Kordower *et al*., 1994). Therefore, initially it was suggested that alterations in NGF synthesis within cortical production sites may be responsible for the basal forebrain cholinergic neuron death during early AD (Hefti *et al*., 1989).

However, studies with AD patients found that NGF mRNA levels in cholinergic targeted regions are unaltered, and its protein levels are even increased (Mufson *et al*., 1996). These data suggested that despite normal NGF synthesis, NGF decreasing in basal forebrain as a result of defective receptor binding and / or retrograde transport of NGF from the hippocampus / cortex to consumer neuron somas within the basal forebrain.

Basal forebrain cholinergic neurons express two types of NGF receptors: the pan-neurotrophin receptor $p75^{NTR}$ and the NGF-specific receptor tyrosine kinase TrkA (Counts and Mufson, 2005). $p75^{NTR}$ binds NGF with low affinity (Kd=nM); while TrkA binds NGF with high affinity (Kd=pM) (Lapchak 1993) and mediates the binding, internalization and retrograde transportation of target derived NGF to basal forebrain (Kaplan and Miller, 1997; Mufson *et al*., 1999). It has been found that TrkA mRNA within individual nucleus basalis neurons was significantly reduced (66%) in early AD cases relative to aged controls while $p75^{NTR}$ is not affected (Mufson *et al*., 1996; Boissiere 1997; Mufson 1997; Counts *et al*., 2004); indicating that there is a selective defect in TrkA expression in AD brain. Besides, TrkA receptor antagonist produces a depletion

of pre-exisitng cholinergic boutons (Debeir *et al*., 1999); and activation of TrkA alone prevented the degeneration of axotomized cholinergic neurons in rats (Mufson *et al*., 1996). These data suggested that signaling via TrkA receptors is a pivotal trophic event underlying the viability of these cells and reduced NGF transport may be secondary to diminished TrkA expression.

The mechanisms underlying TrkA protein reduction in cholinergic neurons in early AD are unclear. However, TrkA gene expression is under positive feedback from NGF signaling (Holtzman *et al*. 1992). Despite retrograde transportation, NGF also activates MAPK and PI3K pathway that are related to cholinergic neuron survival; results in CREB mediated transcription and new protein synthesis (Counts and Mufson, 2005). Basal forebrain cholinergic neurons exhibited rapid increases in TrkA immunostaining in 15 min of NGF application to the hippocampus (Williams *et al*., 2005), probably through the MAPK pathway. This rapid signaling pathway is diminished in aged rodents compared to young ones (Williams *et al*., 2006).

TrkA mediated NGF signaling also enhances cholinergic innervation by promoting ACh synthesis, storage and release (Lapchak 1993), which, in turn, enhances the neuronal activity and NGF synthesis in hippocampus and cortex. The impairment of this reciprocal signaling between basal forebrain cholinergic neurons and hippacampal/cortex neurons may underlie the eventual cholinergic deficits seen in the progression of AD. Therefore, as a potential therapeutic target, many studies have targeted NGF and have shown that exogenous NGF administration reversed both age-related and lesion-induced cholinergic neuronal degeneration as well as spatial memory deficits in animal models. In human, NGF gene therapy is associated with potential

risks. A Phase 1 clinical study using AAV-NGF vector with 6 subjects showed cognitive improvement in 2 subjects but revealed back pain which might due to diffused NGF at peripheral nerve system (Tuszynski *et al*., 2005).

Besides targeting NGF directly, several studies have shown that nicotine exposure selectively increased NGF levels in multiple brain regions for prolonged intervals (Garrido *et al*., 2003; Martinez-Rodriguez *et al*., 2003; Jonnala *et al*., 2002) and led to astrocytic NGF expression that was undetectable in control tissues (Martinez-Rodriguez *et al*., 2003). No increase is seen in other neurotrophins such as brain-derived neurotrophic factor (BDNF) or neurotrophin-3 (NT-3) levels (French *et al*., 1999). Also, nicotine administration increased TrkA expression *in vitro* and *in vivo* (French *et al*., 1999; Formaggio *et al*., 2010). These effects of nicotine were blocked by α7 antagonist (Jonnala *et al*., 2002; Li *et al*., 2005), suggesting the role of α7 nAChRs in modulating TrkA and NGF expression.

However, no direct evidence has shown that α7 activation will increase TrkA levels. In this study, we investigated whether α7 receptor overexpression and activation will have cellular actions that both involve TrkA receptor expression as well as mimic it. If successful, the α7 gene delivery approach will not only counteract the α7 receptor loss in basal forebrain cholinergic neurons, but also benefit the reciprocal loop of the septohippacampal pathway by elevating NGF-TrkA survival signaling. The activation of α7 and TrkA receptors transduce the message to similar cellular kinase cascades including MAPK and PI3K-AKT; which may achieve “double protection” for degenerating cholinergic neurons during AD.

Results

Effects of α7 nAChRs Overexpression on TrkA *In Vitro*

Like basal forebrain cholinergic neurons affected by AD, rat PC12 cells endogenously express both α7 and TrkA proteins and are a valuable model for studying the relationship between the two receptors. In the first report of this cell line, PC12 cell differentiation triggered NGF exposure was described, characterized by halted proliferation and extended neurite outgrowth (Greene and Tischler, 1976). The cellular signaling pathways involved in NGF mediated PC12 cell differentiation have been intensively studied; at least three independent pathways now known to contribute to this response, including ras/raf-MEK-ERK, cAMP-PKA and PI3K-AKT (Vaudry *et al*., 2002; Counts and Mufson, 2005; Yung *et al*., 2010).

In order to evaluate the effects of α7 overexpression on TrkA expression, we transfected the cells at ~40% confluence with the same doses of α7+ric-3, α7+GFP, ric-3+GFP or GFP plasmids (2 μg/ml) based on previously established gene delivery system as described in Chapter 3. 24 hr after transfection, the following antagonists was added in with fresh medium into cell culture: anti-α7, MLA; anti-ERK, PD98059 or anti-AKT, API-2 (Yang *et al*., 2004), separately or in combination, for 30 min and then removed. NGF was added to the medium repeatedly to maintain a concentration of ~50 ng/ml for 4 days, which induced neurite growth and halt proliferation. Cells were then fixed with 4% paraformaldehyde; and random pictures of each well were taken under microscope. Cells with neuron-like process(es) longer than its body length were considered as differentiated (Figure 4-1). Numbers of differentiated and total cells numbers were counted in a blinded manner. The differentiation rate of each group is summarized in Figure 4-2.

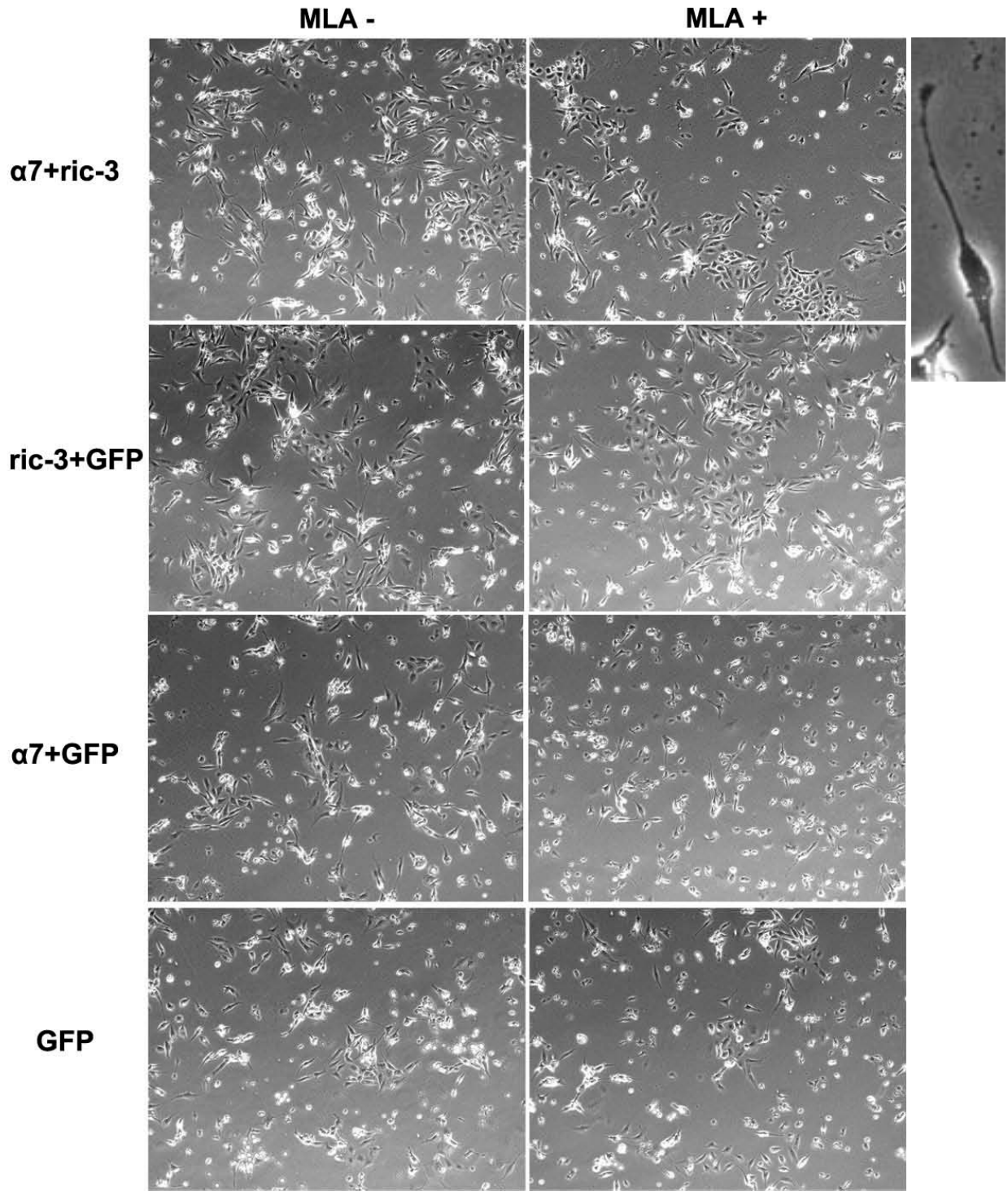

Figure 4-1: Sample pictures of PC12 differentiation. Identical treatments were repeated in triplicate culture wells. Three random pictures were then taken for each well. Enlarged panel on the right represents a cell considered differentiated (i.e., with processes longer than cell body).

In the GFP transfected control group, 4-day NGF treatment resulted in 15.62% differentiation rate, which was attenuated by MLA and PD 98059 pre-treatments (decreased 34% ($p<0.01$) and 43% ($p<0.001$), respectively) (Figure 4-2a), suggesting α7 and ERK activity is involved in NGF-induced neurite growth. The combination of MLA and PD 98059 had an additive effect on preventing differentiation (decreased 65%, $p<0.05$ compared to MLA or PD 98059 separate treatment). Ric-3 overexpression alone significantly increased differentiation (25.13%) while α7 overexpression alone did not (15.12%) compared to GFP transfected controls, consistent with the radioligand binding assay results described above showing that ric-3 transfection alone increased α7 functional expression. In α7 and ric-3 co-transfected cells, differentiation (34.04%) was significantly higher than in GFP transfected controls. Similarly, blocking α7 and ERK functions contributes additively to prevent differentiation.

AKT inhibitor API-2 prevented cellular differentiation more potently than MLA or PD 98059 (Figure 4-2b). Cells pre-treated with API-2 alone exhibited decreased differentiation rate to the same extent as those resulted from antagonist combinations. Beside its dramatic effect on cellular differentiation, API-2 also induced cell death based on the reduced total cell numbers, which was not observed in the cells treated with MLA or PD 98059.

Total TrkA levels were evaluated post-transfection and before NGF treatment. No significant differences were found among different gene delivery groups 24 hr after transfection (Figure 4-3a). However, p-TrkA immunofluorescence signals were found to be elevated after the same time interval of α7 and ric-3 co-transfection in a dose dependent manner (Figure 4-3b).

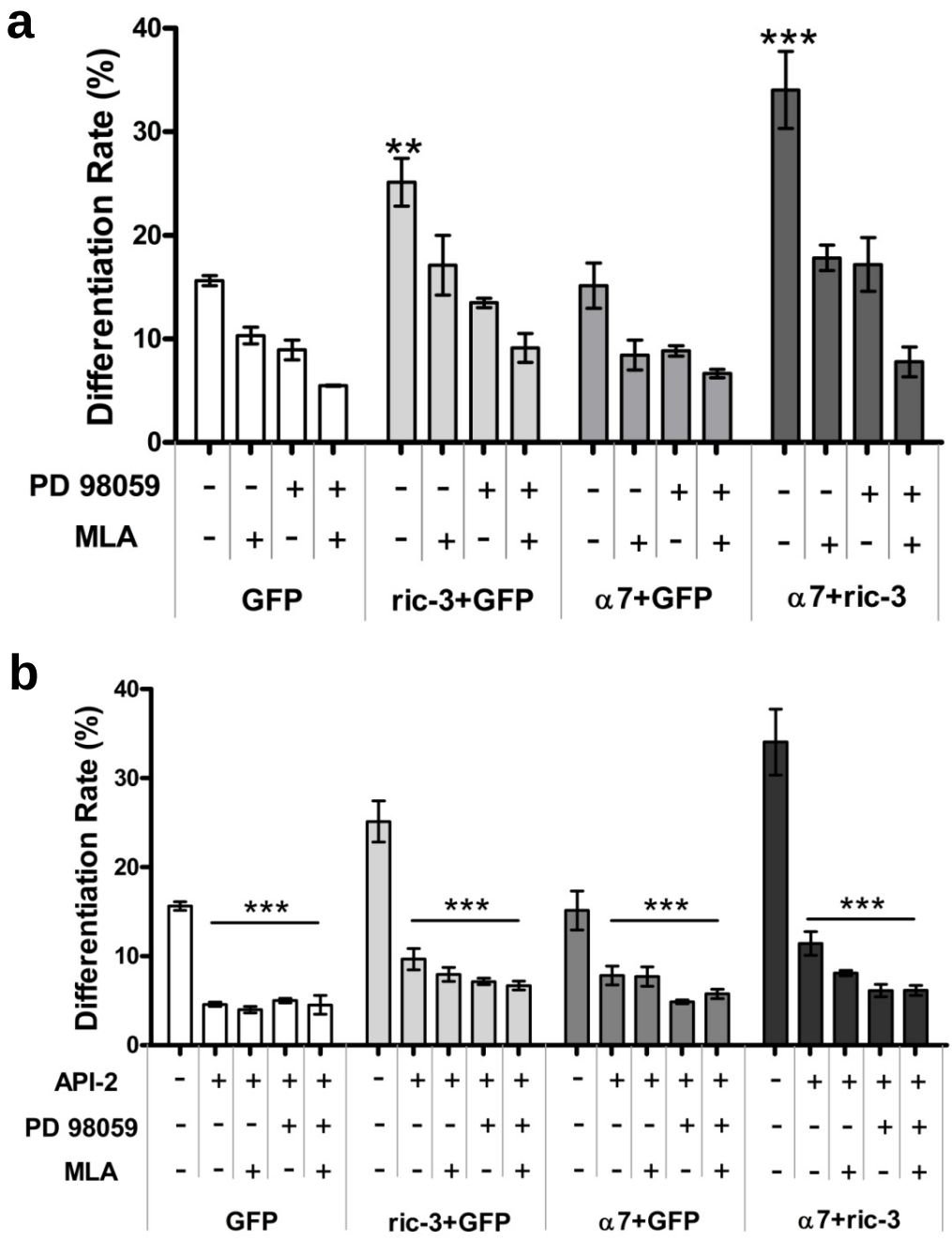

Figure 4-2: Effects of α7 and ric-3 co-transfection on NGF mediated PC12 cell differentiation. All values are means ± SEM of triplicates; mean value comparisons used two way ANOVA followed by Bonferroni test. (**: $p<0.01$; ***: $p<0.001$). (a) α7 and ric-3 co-transfection significantly increased cell differentiation rate, so as ric-3 transfection alone. PD 98059 (50 μM) and MLA (50 nM) attenuated these effects. (b) API-2 (20 μM) treatment potently prevented cell differentiation in all groups.

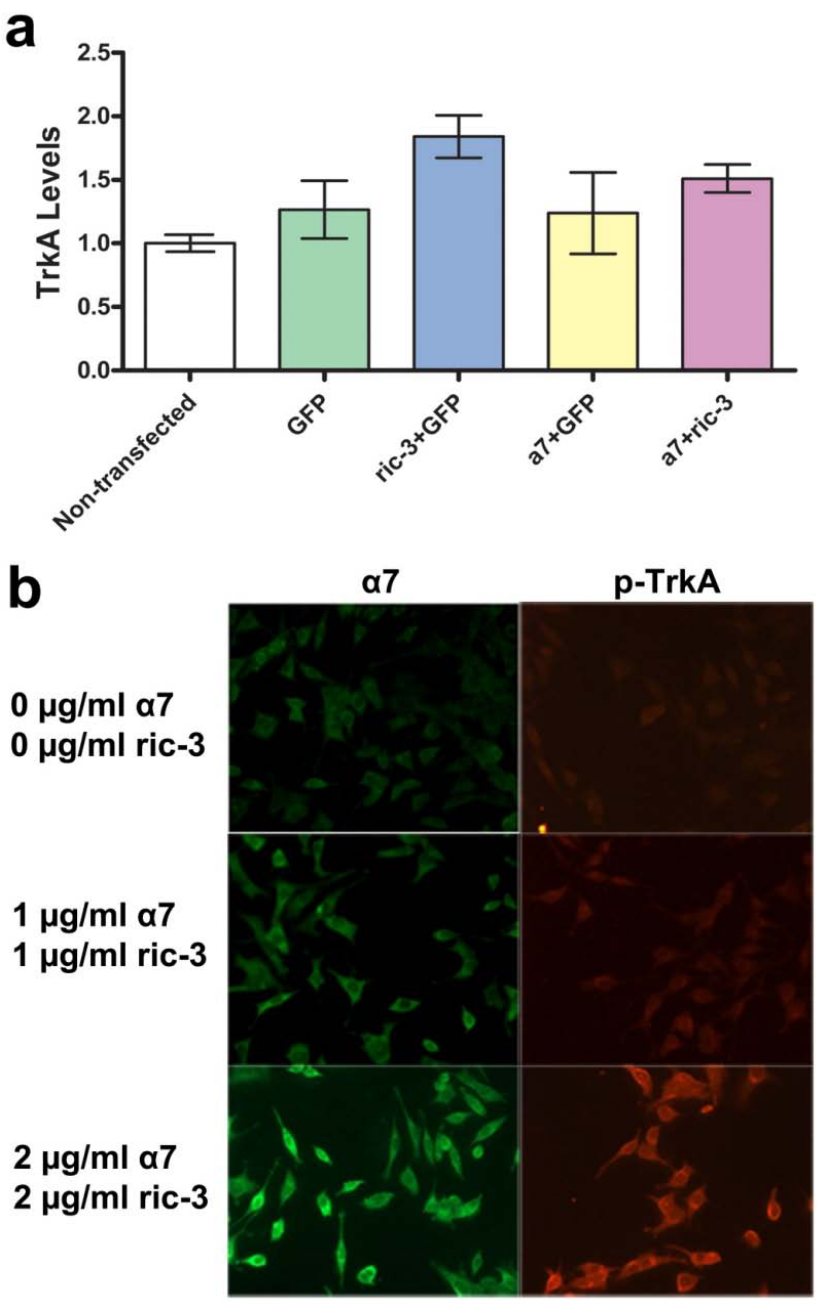

Figure 4-3: Immunoactivity of TrkA in PC12 cells after α7 and ric-3 co-transfection. (a) western blot of TrkA levels after different types of transfection. The TrkA was detected by anti-pan Trk antibody; the bands of TrkA (~135kD) were quantified by ImageJ and normalized with corresponding β-actin levels in each sample. All data were normalized to non-transfected control and expressed as mean ± SEM; N=3. (b) immunostaining for α7 and phospho-TrkA 24 hr after transfection with different α7+ric-3 doses. Secondary antibody only control (pictures not shown here) showed very low non-specific signals.

Effects of AAV8-α7 Gene Delivery on TrkA *in Vivo*

The *in vitro* study with PC12 cells suggested that α7 gene delivery can 1) increase TrkA activity 24 hr after transfection without exogenous agonist; and 2) promote PC12 cell differentiation when combined with NGF treatment. Because NGF exposure increased the expression of septal TrkA mRNA levels in aged mice, we hypothesized that *in vivo* α7 gene delivery into septum will increase TrkA expression under normal endogenous α7 agonists in young wild type mice. AAV was chosen as *in vivo* gene delivery vector since this type of virus offers the advantage of the ability to infect non-dividing cells, affording a non-pathogenic and long-term transgene expression without a substantial inflammatory response when combined with appropriate promoters. In particular, AAV with serotype 8 capsid has shown remarkable efficiency in neuron gene delivery and expression (Broekman *et al*., 2006).

Mice were injected with AAV8-GFP (10^9 genomic particles / animal), AAV8-α7-low dose (10^8 genomic particles / animal) or AAV8-α7-high dose (10^9 genomic particles / animal) into left-side septum. 18 days after injection, brain tissues were dissected and processed for western blotting. α7, TrkA and ChAT blotting densities were normalized to β-actin measurements from the same sample. All values were then normalized to the measurements of GFP controls. α7 protein levels were close to significantly increased in septum (Figure 4-4a) but greatly increased in the ipsilateral hippocampus (Figure 4-4b) in a dose dependent manner, accompanied with elevated ChAT activity at the same location (Figure 4-4b). TrkA protein levels were significantly increased in septum (Figure 4-4a) but not in the injection side hippocampus (Figure 4-4b). Neither α7 nor TrkA levels changed in right side hippocampus (Figure 4-4c).

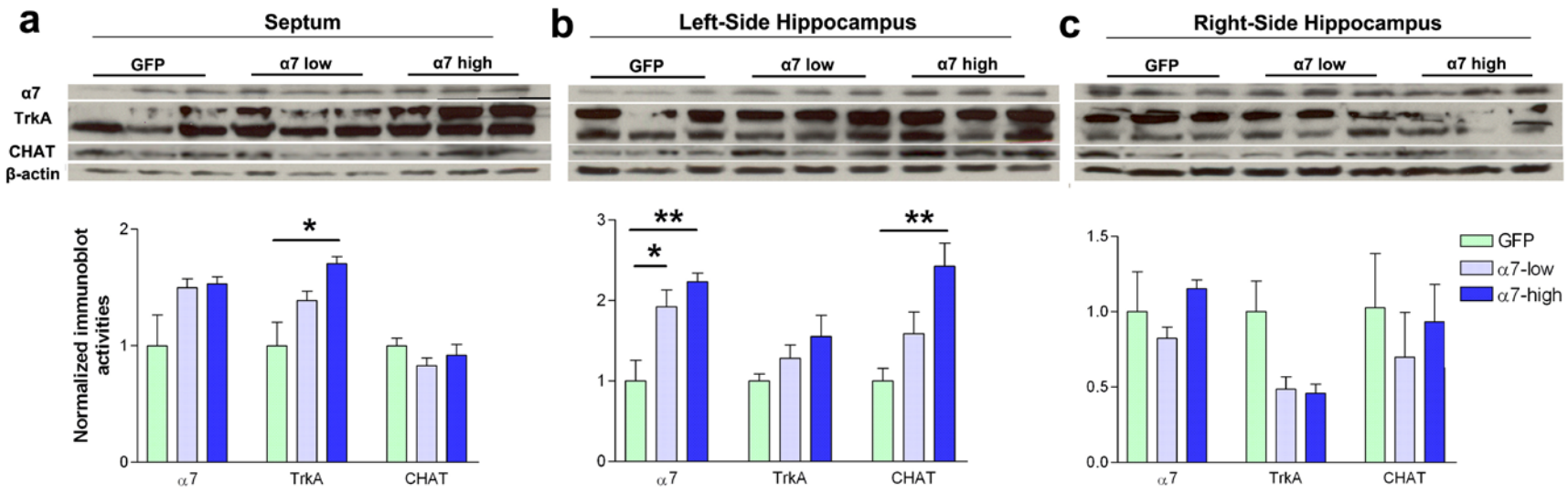

Figure 4-4: Immunoactivities of α7, TrkA and ChAT in septum, left side hippocampus and right hippocampus after α7 overexpression. Bars were expressed as means ± SEM; mean value comparisons used two way ANOVA followed by Bonferroni test. (*: $p<0.05$; **: $p<0.01$). (a) α7 levels did not change among GFP control, α7-low and α7-high groups in septum, so as ChAT activities. However, TrkA levels increased by α7 gene delivery compared to controls. (b) In left hippocampus (injection side), α7 levels were significantly elevated by gene delivery. High dose AAV8-α7 also resulted in ChAT protein elevations. TrkA levels, however, were similar among the treatment groups in this region. (c) No significant difference in α7, TrkA or ChAT expression was observed in right hippocampus (opposite to injection site).

Consistent with the results from western blots, strong TrkA immunofluorescence was observed in septum, primarily in neuron projections, where some punctuate α7 immunoreactivity was seen (Figure 4-5).

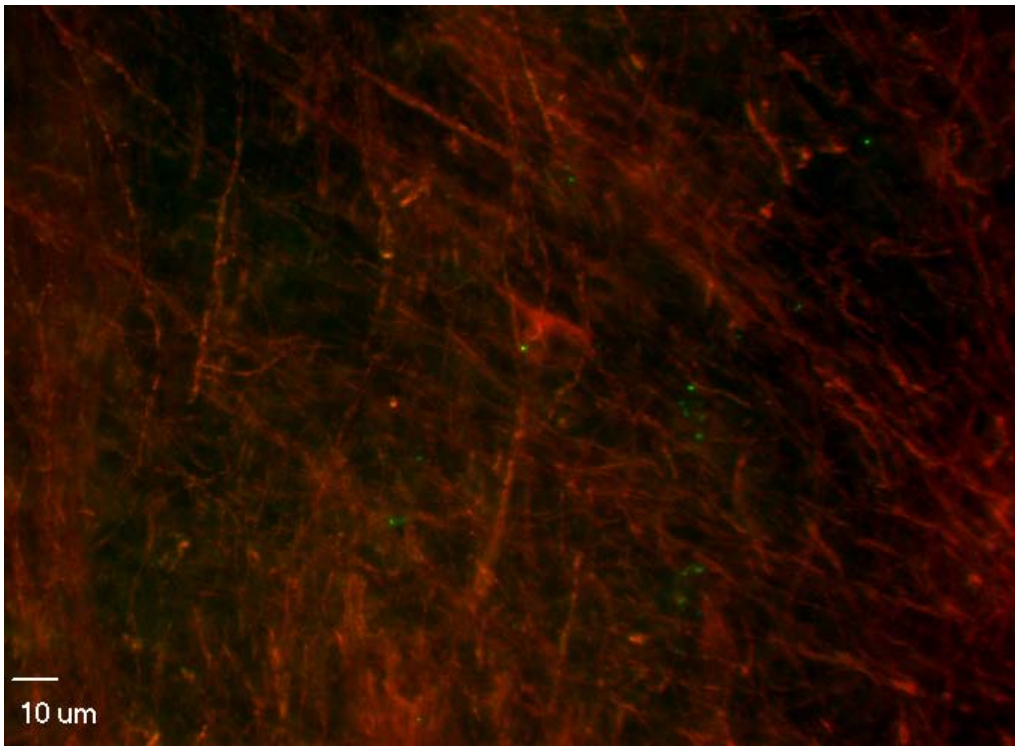

Figure 4-5: Immunofluorescence staining of TrkA and α7 protein in left septum after α7 overexpression. A coronal brain section from low dose AAV8-α7 injected mouse was incubated with mouse-anti-α7 and rabbit-anti-TrkA primary antibodies after antigen retrieval and non-specific signal blocking. Targeted signals were visualized by fluorescence labled secondary antibodies (α7: Alex Fluo 488 mouse IgG, green; TrkA: Alexa Fluor 594 rabbit IgG, red). Confocal picture was taken under spinning-disk microscopy. TrkA fluorescence was primarily seen in septal neuron axons, which project into hippocampus. A7 fluorescence could be seen at several spots, possibly in cell body.

Effects of Septal AAV8-α7 Gene Delivery on Memory Related Behavior

Memory related behavior was evaluated by Morris water maze tasks two weeks after septal gene delivery. The mice were ~12 weeks old at that time. As expected, all groups learned efficiently in the platform navigation task (Figure 4-6) since they have no cognitive deficits at this age. Probe tests were followed the navigation training, in which

the escape platform was removed from the water maze. 60 min swimming period of each mouse was recorded by video camera, and swimming tracks were captured and analyzed for times passing the platform area, percent time spent / swimming distance / swimming speed in each quadrant, etc (Figure 4-7).

The percent time spent in the target quadrant (where the platform was on training trials) (Figure 4-7 pie chart, Figure 4-8b) was not different among the treatment groups, nor were the swimming distances. The α7 low dose group showed a tendency to cross the platform region more times than GFP injected mice (p=0.07 by Student's T-test) (Figure 4-8a). They also swam faster in the opposite quadrant compared to controls (Figure 4-8c).

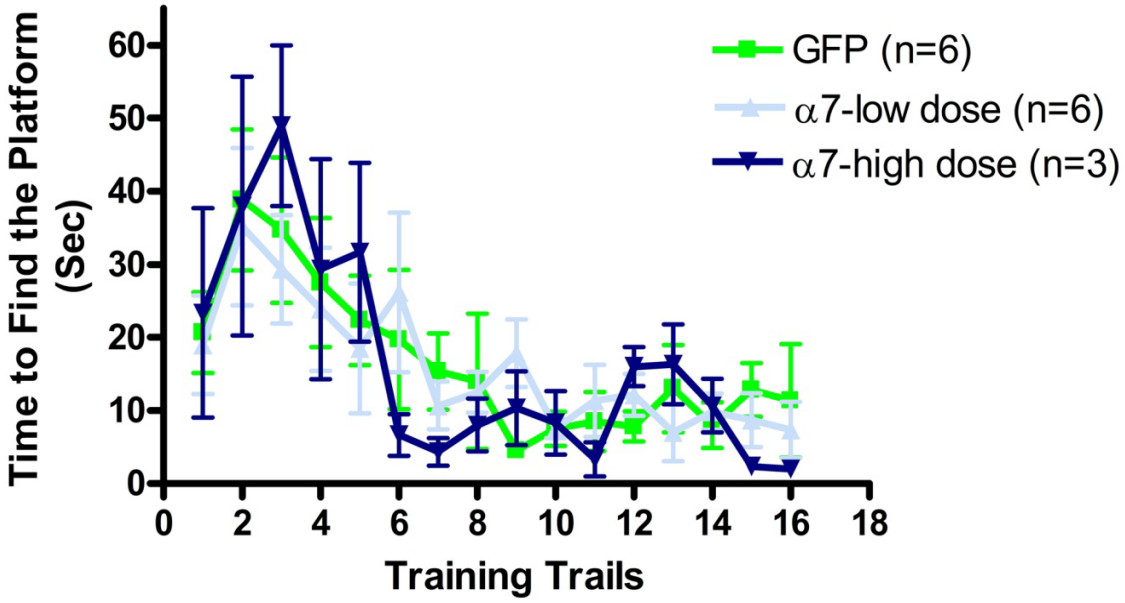

Figure 4-6: Training curves resulting from Morris water maze platform navigation task. Mice were trained for 2 days with 8 trails per day. Mice were placed into water facing the wall of the tank, each time at a different site. They were allowed to up to 60 sec to search for the escape platform, followed by 30 sec on the platform to enhance the memory. Geometric signs were hung on the tank to help navigation. Time spent to find the platform of each trial was plotted to represent a learning curve. All groups succeeded in fast locating of the platform after 2 days' training.

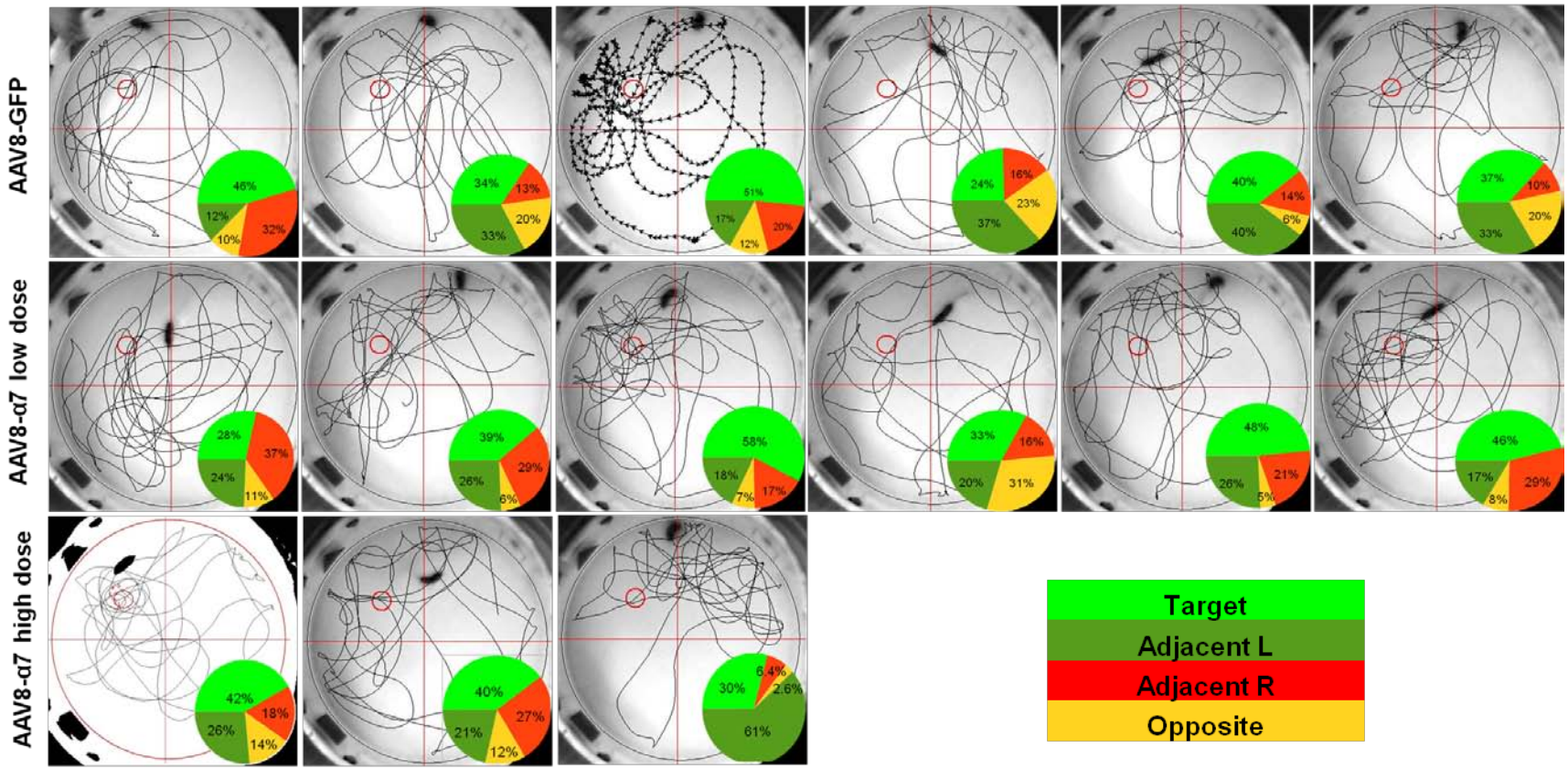

Figure 4-7: Swimming tracks of individual animal in probe test. After navigation training, the platform was removed and animals were allowed 1 min to swim, which were recorded by video camera. For analysis, water maze (black circle) was divided into four quadrants (red lines). The quadrant previously containing the escape platform (red circle) was called 'target quadrant'; the other three were called 'adjacent left', 'adjacent right' and 'opposite' quadrant, respectively. The pie chart represented the percentage of swimming time mouse spent in each quadrant.

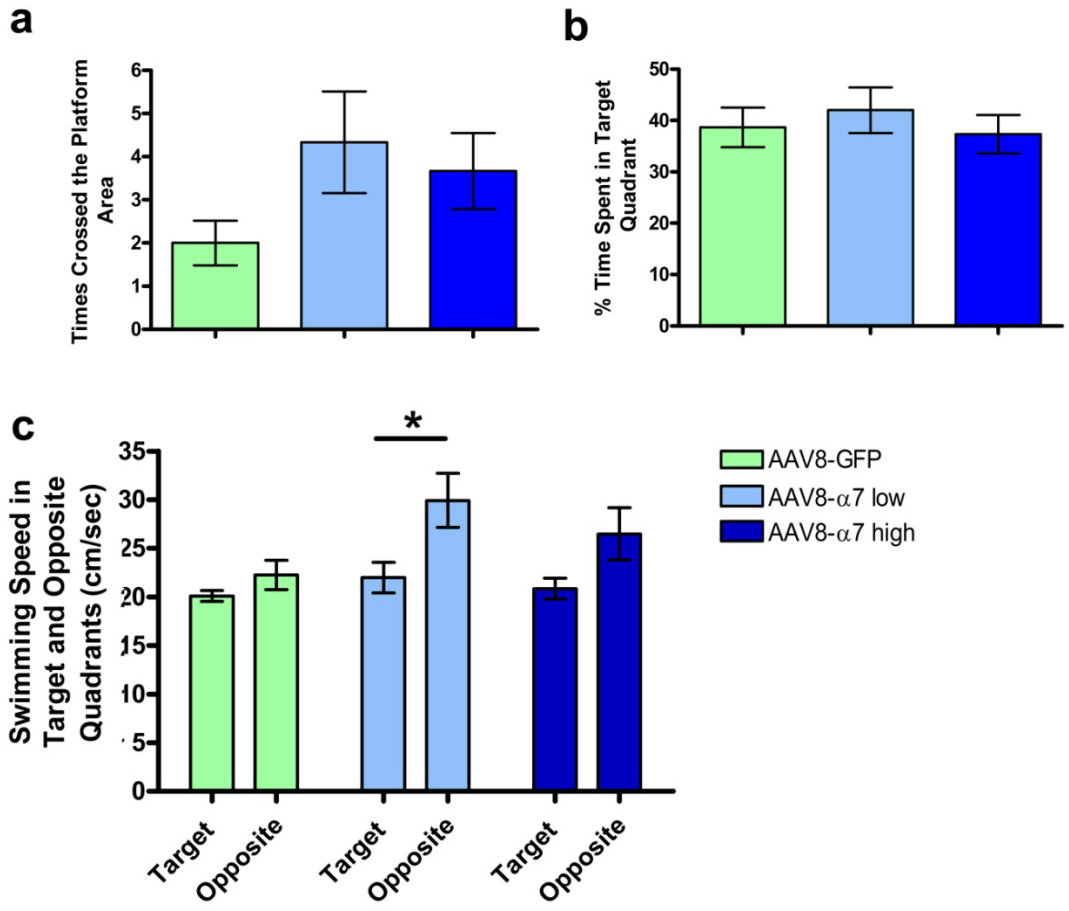

Figure 4-8: Memory related parameters resulted from probe test. (a) Average times of passing the platform area for each group. (b) Average percentage of time spent in the target quadrant. (c) Average swimming speed in target and opposite quadrants.

Discussion

Our results showed that α7 and ric-3 co-transfection increased TrkA activation mediated PC12 cell differentiation; AAV8-α7 gene delivery into mouse septum elevated TrkA protein levels in the same area and improved behavioral performance in water maze tasks. Although previous studies showed that nicotine treatment increased TrkA expression, which could be blocked by α7 antagonist, our results provided the first demonstration that, despite direct neuroprotective functions via activating cellular signaling pathways, α7 nAChRs can also modulate TrkA expression and activation.

Since the NGF-TrkA pathway tranduce differentiation and survival messages, α7 gene delivery approach may potentially result in combined protective effects from α7 nAChRs themselves as well as TrkA receptors.

NGF induces PC12 cell differentiation reflecting decreased proliferation and increased neuritic extention. Interestingly, we found that α7 and ric-3 co-transfection significantly increased the differentiation rate of the NGF treated PC12 cells, and this effect was attenuated by 30 min MLA treatment post transfection and before NGF incubation, suggesting that α7 nAChRs were partially involved in the differentiation process. Considering that the p-TrkA level but not the total TrkA protein level was elevated 24 hr post transfection, α7 possibly modulated cell differentiation via increasing NGF release, which form a complex with TrkA and induced TrkA phosphorylation. ERK inhibitor PD 98059 also attenuated PC12 cell differentiation, consistent with the fact that ERK is one of the downstream kinases responsive to NGF-induced TrkA activation. Our previous data showed that in PC12 cells the endogenous activation of up-regulated α7 nAChRs was not sufficient to induce detectable change in ERK phosphorylation (Figure 3-3 at 0 μM 4OH-GTS-21). In this study, the effects of MLA and PD 98059 were additive. These two pieces of information suggested that α7 nAChRs may be regulating PC12 cell differentiation through a non-ERK pathway(s). AKT inhibitor API-2 also decreased differentiation rate, but more effectively than either MLA or PD 98059, indicating NGF-TrkA induced differentiation is more dependent on AKT signaling pathway.

In addition, cells transfected with ric-3 or α7+ric-3 over-expressed functional α7 nAChRs (Figure 3-2a), contributing to enhanced differentiation after NGF treatment

(Figure 4-2a) and improved cell viability (Figure 4-9, ***: p<0.001 compared to GFP transfected controls with no AKT treatment). Previous study demonstrated that α7 mRNA level is up-regulated during NGF-induced PC12 cell differentiation (Takahashi, 1999). Therefore, the cytoprotective effect seen in here may result from a combination of transient α7 gene delivery, increased α7 expression during differentiation and NGF mediated cell survival. API-2, however, exhibited a negative effect on viability of these cells (Figure 4-9, ###: p<0.001 compared to cells in the same group with API-2 treatment), suggesting AKT activity is more vital for α7 mediated cytoprotection.

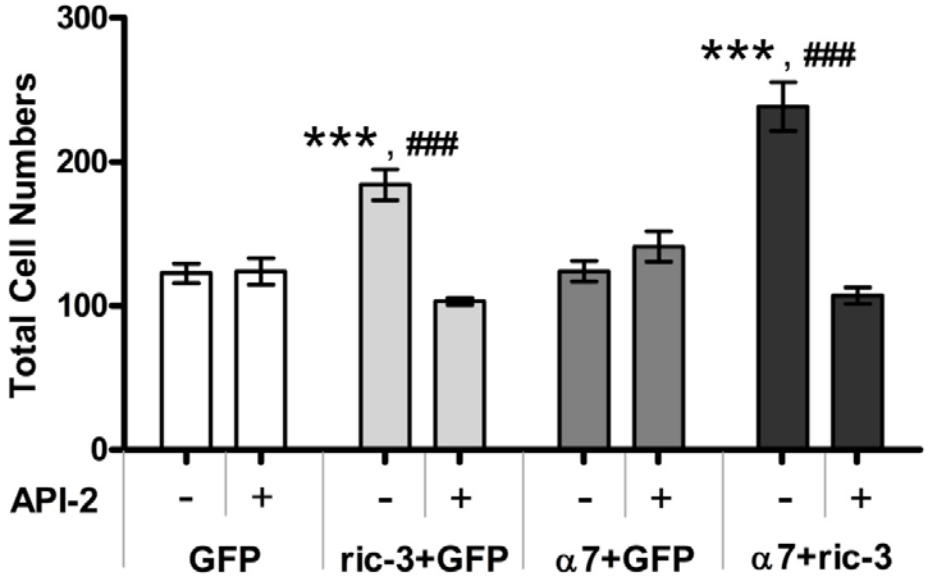

Figure 4-9: API-2 blocked cytoprotective effects seen in α7 up-regulated groups. Values were expressed as means ± SEM. Two-way ANOVA followed by Bonferroni test was used for mean value comparisons among the gene delivery groups. Student's T test was used for mean value comparisons within the same gene delivery group. Cell viabilities in ric-3 and α7+ric-3 transfected groups were significantly higher than GFP transfected controls (***: p<0.001). API-2 potently blocked this protective effect resulted from α7 overexpression (###: p<0.001).

Together, our *in vitro* study with PC12 cells demonstrated α7 nAChRs overexpression elevated TrkA phosphorylation, enhanced NGF-induced cell

differentiation and improved cell viability. The AKT signaling pathway presented pre-eminent function in conducting signals related with differentiation and survival, and can potentially be targeted in future studies.

The *in vivo* gene delivery study showed that AAV8-α7 injection into mouse left septum resulted in α7 protein increasing in left hippocampus compared to controls injected with AAV8-GFP. ChAT, which is considered to be the marker for cholinergic activity, was also elevated along with the α7 overexpression, indicating that septal cholinergic neurons projecting into hippocampus are likely responsible for at least some of the increased expression. Increased α7 nAChR expression therefore led to up-regulated TrkA protein levels in the septum, supporting our hypothesis and can be explained by the septohippocampal reciprocal loop. Two bands were observed in TrkA western blots (Figure 4-4). The bottom band represented the molecular weight of TrkA at ~140 Kd; and the top band was ~160 Kd. Interestingly, the densities of the 160 Kd bands were lower in septum (Figure 4-4a) but higher in hippocampus (Figure 4-4b and 4-4c) compared to the 140 Kd bands in the same areas. Because in hippocampus two NGF molecules (13 Kd) form dimers (26 Kd) via disulfide bridge as the active form (Wiesmann *et al*., 1999), we speculate that the 160 Kd band represented a NGF dimer-TrkA complex. In septum, endocytosed TrkA is predominantly sorted for recycling back to cell surface (Chen *et al*., 2005), which may account for why less of the higher molecular weight 'NGF-TrkA' was found.

Surprisingly, improved performance in Morris water maze tasks was observed after α7 overexpression, which is usually not easy to see in young wild type mice. Times passing the platform region were close to significantly increased in low dose AAV8-α7

injected group compared to controls, and the same mice swam faster in the opposite quadrant, which partly indicated better memory for the platform location.

In conclusion, α7 receptors were found to be involved in modulating neurotrophin pathways both *in vitro* and *in vivo*. For therapeutic application, it is possible that α7 overexpression could compensate for α7 and TrkA receptor loss early in AD, and enhance the function of the septohippocampal reciprocal loop between cholinergic and hippocampal neurons. It can also magnify the neuroprotective function by up-regulating endogenous NGF synthesis, which can avoid the adverse side effects in more systemic NGF therapy. No exogenous agonist was required in these studies, affording potential advantage in utilizing endogenous α7 agonists.

CHAPTER 6
CONCLUSION AND FUTURE DIRECTIONS

Conclusion

The cholinergic hypothesis for AD has been studied for almost 40 years. Cholinergic deterioration is one of the most consistent pathological features of all types of AD. α7 nAChRs are a favorable target for protecting the cholinergic neuron as well as improving cognitive functions in a variety of models. Although α7 selective agonists have been intensively studied and displayed promising therapeutic effects, gene therapy may provide more advantages including locally restoring the receptor loss and avoiding fast desensitization. The goal of our research is to investigate the benefits of α7 overexpression, improve our understanding in underlying neuroprotective mechanisms, and test whether α7 gene delivery could be potential approach to treat AD. Several hypotheses were involved, including: 1) up-regulated α7 receptors can increase the agonist efficacy and potency on cellular signaling pathways; 2) α7 receptors can modulate neurotrophin induced cell differentiation; and 3) AAV mediated α7 gene delivery in vivo will enhance TrkA expression.

In PC12 cells we found α7 and ric-3 co-transfection significantly increased functional α7 nAChRs, which not only elevated the responses of cellular kinases and reduced caspase 3/7 activities in response to 4OH-GTS-21, but also enhanced the cell differentiation mediated by NGF, possibly via modulating TrkA expression (Figure 6-1). All these effects were blocked by selective antagonist MLA. In mouse septum, AAV8-α7 gene delivery resulted in enhanced α7 receptor expression in the transduced side of the hippocampus and TrkA expression in septum; improved behavioral performance was observed even in young mice without cognition deficits. These effects may involve α7

activation modulated NGF synthesis, which is vital for reciprocally maintaining cholinergic functions (Figure 6-2).

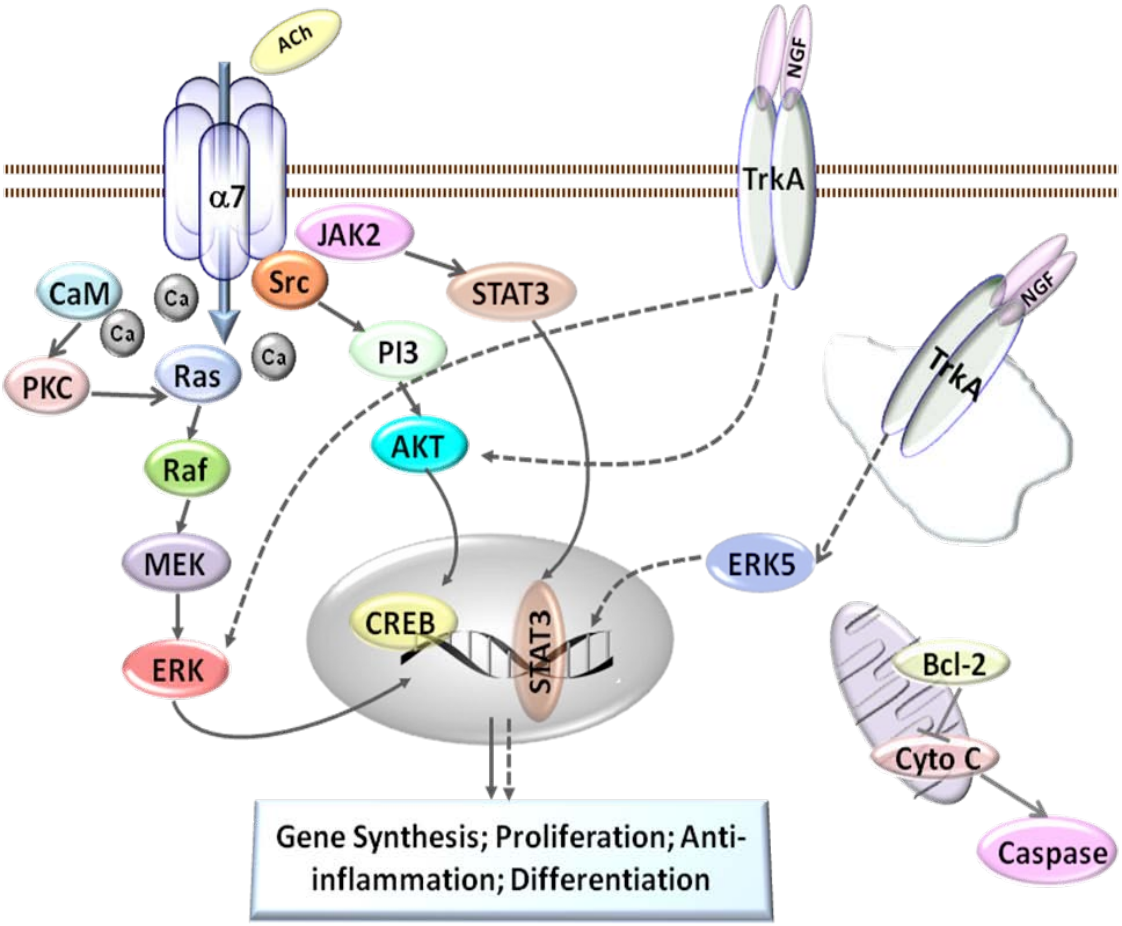

Figure 5-1: Pathways regulated by α7 and TrkA receptors in PC12 cells. Both kinds of receptors activate MAPK and PI3K/AKT pathways, which promote new gene synthesis through transcription factors like CREB. JAK2 and ERK5 are also found to be regulated by α7 and TrkA, respectively. Bcl-2 expression is increased in response to receptor activation. Bcl-2 blocks cytochrome C release from mitochondria, which induces caspase cascade. These effects regulate cell proliferation and differentiation.

Young wild type mice are a good model to investigate the effects of α7 overexpression under normal physiological conditions and endogenous neurotransmitter levels. A7 gene delivery into left side septum increased the receptor expression in left side hippocampus but not right side hippocampus, consistent with the

cholinergic projection from septum into hippocampus. For the first time, a gene therapy approach was found to increase TrkA protein levels in septum, but more NGF-binding was suggested in hippocampus, indicating the TrkA transportation and recycle under normal condition. Collectively, these results from wild type mice shed a light on the advantage of α7 overexpression in enhancing septohippocampal communication.

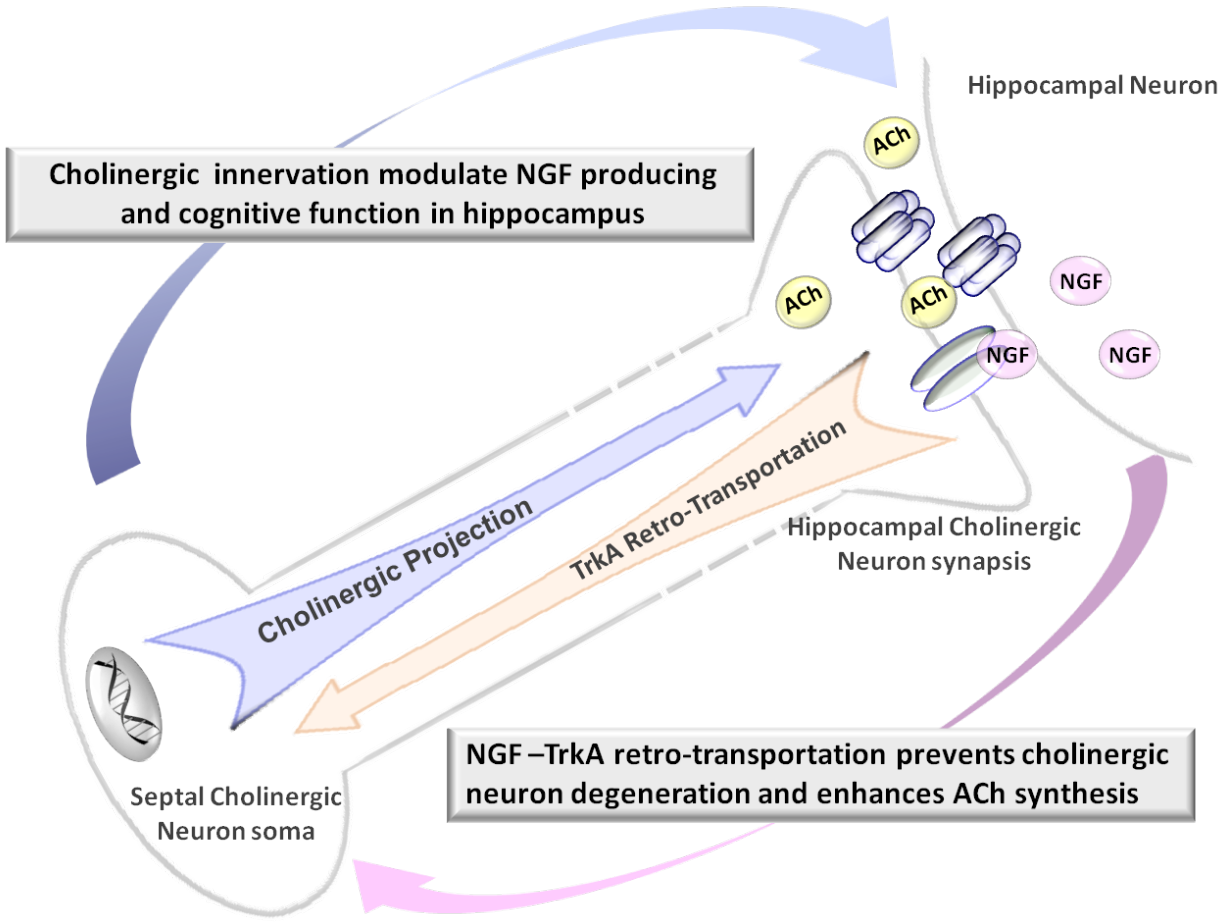

Figure 5-2: Septohippocampal reciprocal loop that may involve in α7 mediated TrkA elevation.

Future Directions

For better understanding the potential application of α7 gene therapy, aged mice or transgenic mice will be used for future studies. Aged mice have reduced α7 and TrkA expression at both mRNA and protein levels, affording a suitable model for testing the

α7 gene delivery and its effect on TrkA. Memory related behavioral deficits are more significantly observed in these mice. Proper transgenic mouse models for AD should be carefully selected according to specified purposes since there is no rodent model that recapitulates all of the symptoms and neuropathological hallmarks of AD.

In particular, NGF deficient mice exhibit cholinergic loss in the basal forebrain and neurofibrillary tangles / Aβ accumulation in the hippocampus, representing a useful model for studying the function of α7 nAChRs in modulating NGF expression as hypothesized from our research. Aβ overexpression mouse models (carry mutant APP, γ-secretase component presenilin 1 or presenilin 2) could be used for investigating the effects of α7 gene therapy on Aβ metabolism. Aβ is considered as the major toxic peptide in AD brain and the processing of its precursor protein APP has been found to be modulated by α7 nAChR activation. In turn, Aβ can competitively bind to α7 receptors and result in conflicting observations. Some groups found Aβ blocked α7 function while others found it activated α7 and induced downstream kinase phosphorylation. Previous studies in our laboratory found α7 activation by 4OH-GTS-21 protected neurons from Aβ toxicity in APP/PS1 mouse model, and α7 gene delivery into hippocampus improved special memory. Future studies that deliver α7 genes in Aβ overexpressing mouse septum will help us better characterize the correlation between α7 nAChRs and Aβ, which will benefit the application of α7 gene therapy in AD caused by abnormal Aβ accumulation. Transgenic mice carrying mutant Tau gene exhibit another major pathologic feature of AD: neurofibrillary tangles formed by hyper-phophorylated Tau. Tau is a microtubule associated protein that functioning in stabilizing cytoskeleton. AD patients have impaired septohippocampal transportation of

TrkA via cholinergic projections, implying potential deficits in normal Tau function. Therefore investigation in whether α7 overexpression affects Tau pathology in those mouse models will also be a interesting future direction. In addition, the crossed mouse models may be helpful for cocktail gene therapy, which has not been attempted yet for treating AD.

In conclusion, α7 gene delivery represents a potential approach for protecting cholinergic neurons and improving cognition. Our data characterized the effects of α7 overexpression on neuroprotective pathways including MAPK, PI3K/AKT and NGF-TrkA. Studies with specific animal models will help promote the therapeutic application of α7 gene therapy for AD as well as other α7 nAChRs involved neurodegenerative diseases.

LIST OF REFERENCES

Alessi D. R., Cuenda A., Cohen P., Dudley D. T. and Saltiel A. R. (1995) PD 098059 is a specific inhibitor of the activation of mitogen-activated protein kinase kinase *in vitro*and *in vivo*. *J. Biol. Chem.* **270**, 27489–27494.

Alexander J. K., Sagher D., Krivoshein A. V., Criado M., Jefford G. and Green W. N. (2010) Ric-3 promotes alpha7 nicotinic receptor assembly and trafficking through the ER subcompartment of dendrites. *J Neurosci.* **30**, 10112–10126.

Alkondon M., Pereira E. F. and Albuquerque E. X. (1996) Mapping the location of functional nicotinic and gamma-aminobutyric acid A receptors on hippocampal neurons. *J Pharmacol Exp Ther*. **279**, 1491–506.

Almeida R. D., Manadas B. J., Melo C. V., Gomes J. R., Mendes C. S., Grãos M. M., Carvalho R. F., Carvalho A. P. and Duarte C. B. (2005) Neuroprotection by BDNF against glutamate-induced apoptotic cell death is mediated by ERK and PI3-kinase pathways. *Cell Death Differ*. **12**, 1329–1343.

Alzheimer A. (1907) A characteristic disease of the cerebral cortex. In: Bick K., Amaducci L. and Pepeu G. The early story of Alzheimer's Diseae. *Liviana Press*, Padava Italy, pp 1–3

Arendash G.W., Sengstoch G.J., Sanberg P.R., and Kem W.R. (1995). Improved learning and memory in aged rats with chronic administration of the nicotinic receptor agonist GTS-21. *Brain Res*. **674**, 252–259.

Bartus R. T., Dean R. L. 3rd, Beer B. and Lippa A. S. (1982) The cholinergic hypothesis of geriatric memory dysfunction. *Science* **217**, 408–414.

Bettany J.H. and Levin E.D. (2001). Ventral hippocampal alpha7 nicotinic receptor blockade and chronic nicotine effects on memory performance in the radial-arm maze. *Pharmacol. Biochem. Behav*. **70**, 467–474.

Bina K. G., Guzman P., Broide R. S., Leslie F. M., Smith M. A. and O'Dowd D. K. (1995) Localization of alpha 7 nicotinic receptor subunit mRNA and alpha-bungarotoxin binding sites in developing mouse somatosensory thalamocortical system. *J. Comp. Neurol.* **363**:321–332.

Bitner R. S., Nikkel A. L., Markosyan S., Otte S., Puttfarcken P. and Gopalakrishnan M. (2009) Selective alpha7 nicotinic acetylcholine receptor activation regulates glycogen synthase kinase 3 beta and decreases tau phosphorylation *in vivo*. *Brain Res*. **1265**, 65–74.

Boissiere F., Faucheux B., Ruberg M., Agid Y. and Hirsch E. C. (1997) Decreased TrkA gene expression in cholinergic neurons of the striatum and basal forebrain of patients with Alzheimer's disease. *Exp. Neurol*. **145**, 245–252.

Bonny C., Borsello T. and Zine A. (2005) Targeting the JNK pathway as a therapeutic protective strategy for nervous system diseases. *Rev. Neurosci*. **16**, 57–67.

Bowen D. M., Sims N. R., Benton J. S., Curzon G., Davison A. N., Neary D. and Thomas D. J. (1981) Treatment of Alzheimer's disease: a cautionary note. *N. Engl. J. Med*. **305**, 1016.

Briggs C. A., Anderson, D. J., Brioni J. D., Buccafusco J. J., Buckley M. J. and AL. E. (1997) Functional characterization of the novel neuronal nicotinic acetylcholine receptor ligand GTS-21 *in vitro* and *in vivo*. *Pharmacol. Biochem. Behav*. **57**, 231–241.

Broekman M . L ., Comer L . A ., Hyman B . T. and Sena-Esteves M. (2006) A deno-associated virus vectors serotyped with AAV8 capsid are more efficient than AAV-1 or -2 serotypes for widespread gene delivery to the neonatal mouse brain. Neuroscience 138, 501–510.

Broide R. S. and Leslie F. M. (1999) The alpha7 nicotinic acetylcholine receptor in neuronal plasticity. *Mol Neurobiol*. **20**, 1–16.

Castro N. G. and Albuquerque E. X. (1993) Brief-Lifetime, fast-inactivating ion channels account for the r-bungarotoxin-sensitive nicotinic response in hippocampal neurons. *Neurosci. Lett*. **164**, 137–140.

Changeux J. P., Kasai M. and Lee C. Y. (1970) Use of a snake venom toxin to characterize the cholinergic receptor protein. *Proc. Natl. Acad. Sci. U S A*. **67**, 1241–1247.

Chen L., Wang H., Zhang Z., Li Z., He D., Sokabe M. and Chen L. (2001) DMXB (GTS-21) ameliorates the cognitive deficits in beta amyloid(25-35(-)) injected mice through preventing the dysfunction of alpha7 nicotinic receptor. *J. Neurosci. Res.* **88**, 1784–1794.

Chen Z. Y., Ieraci A., Tanowitz M. and Lee F. S. (2005) A novel endocytic recycling signal distinguishes biological responses of Trk neurotrophin receptors. *Mol. Biol. Cell* **16**, 5761–5772.

Clarke P. B., Schwartz R. D., Paul S. M., Pert C. B. and Pert A. (1985) Nicotinic binding in rat brain: autoradiographic comparison of [3H]acetylcholine, [3H]nicotine, and [125I]-alpha-bungarotoxin. *J. Neurosci*. **5**, 1307–1315.

Cooper E., Couturier S. and Ballivet M. (1991) Pentameric structure and subunit stoichiometry of a neuronal nicotinic acetylcholine receptor. *Nature* **350**, 235–238.

Cooper J. D., Salehi A., Delcroix J. D., Howe C. L., Belichenko P. V., Chua-Couzens J. Kilbridge J. F., Carlson E. J., Epstein C. J. and Mobley W. C. (2001) Failed retrograde transport of NGF in a mouse model of Down's syndrome: reversal of cholinergic neurodegenerative phenotypes following NGF infusion. *Proc. Natl. Acad. Sci. USA* **98**, 10439–10444.

Counts S. E., Nadeem M., Wuu J., Ginsberg S. D., Saragovi H. U. and Mufson E. J. (2004) Reduction of cortical TrkA but not p75(NTR) protein in early-stage Alzheimer's disease. *Ann. Neurol*. **56**, 520–531.

Counts S. E. and Mufson E. J. (2005) The role of nerve growth factor receptors in cholinergic basal forebrain degeneration in prodromal Alzheimer disease. J Neuropathol. *Exp. Neurol*. **64**, 263–272.

Court J., Martin-Ruiz C., Piggott M., Spurden D., Griffiths M. and Perry E. (2001) Nicotinic receptor abnormalities in Alzheimer's disease. *Biol. Psychiatry.* **49**, 175–184.

Couturier S., Bertrand D., Matter J. M., Hernandez M. C., Bertrand S., Millar N., Valera S., Barkas T. and Ballivet M. (1990) A neuronal nicotinic acetylcholine receptor subunit (alpha 7) is developmentally regulated and forms a homo-oligomeric channel blocked by alpha-BTX. *Neuron* **5**, 847–856.

Coyle J. T., Price D. L. and DeLong M. R. (1983) Alzheimer's disease: a disorder of cortical cholinergic innervation. *Science* **219**, 1184–1190.

Creson T. K., Yuan P., Manji H. K. and Chen G. (2009) Evidence for involvement of ERK, PI3K, and RSK in induction of Bcl-2 by valproate. *J. Mol. Neurosci*. **37**, 123–134.

Cuello A. C., Bruno M. A. and Bell K. F. (2007) NGF-cholinergic dependency in brain aging, MCI and Alzheimer's disease. *Curr. Alzheimer Res.* **4**, 351–358.

Cuello A. C., Bruno M. A., Allard S., Leon W. and Iulita M. F. (2010) Cholinergic involvement in Alzheimer's disease. A link with NGF maturation and degradation. *J. Mol. Neurosci*. **40**, 230–235.

Curtis J. and Finkbeiner S. (1999) Sending Signals from the Synapse to the Nucleus: Possible Roles for CaMK, Ras/ERK, and SAPK Pathways in the Regulation of synaptic Plasticity and Neuronal Growth. *J. Neurosci*. Res. **58**, 88–95.

Dajas-Bailador F. A., Soliakov L. and Wonnacott S. (2002a) Nicotine activates the extracellular signal regulated kinase 1/2 via the alpha7 nicotinic acetylcholine receptor and protein kinase A, in SH-SY5Y cells and hippocampal neurones. *J. Neurochem.* **80**, 520–530.

Dajas-Bailador F., Mogg A. J. and Wonnacott S. (2002b) Intracellular Ca^{2+} channels evoked by stimulation of nicotinic acetylcholine receptors in SH-SY5Y cells: contribution of voltage-operated Ca^{2+} channels and Ca^{2+} stores. *J. Neurochem*. **81**, 606–619.

Davies P. (1979) Neurotransmitter-related enzymes in senile dementia of the Alzheimer type. *Brain Res*. **171**, 319–327.

Debeir T., Saragovi H. U. and Cuello A. C. (1999) A nerve growth factor mimetic TrkA antagonist causes withdrawal of cortical cholinergic boutons in the adult rat. *Proc. Natl. Acad. Sci. U S A* **96**, 4067–4072.

Deshmukh M. and Johnson E. M. Jr. (1997) Programmed cell death in neurons: focus on the pathway of nerve growth factor deprivation-induced death of sympathetic neurons. *Mol. Pharmacol.* **51**, 897–906.

DiStefano P. S., Friedman B., Radziejewski C., Alexander C., Boland P., Schick C. M., Lindsay R. M. and Wiegand S. J. (1992) The neurotrophins BDNF, NT-3, and NGF display distinct patterns of retrograde axonal transport in peripheral and central neurons. *Neuron* **8**, 983–993.

Dominguez del Toro E., Juiz J. M., Peng X., Lindstrom J. and Criado M. (1994) Immunocytochemical localization of the alpha 7 subunit of the nicotinic acetylcholine receptor in the rat central nervous system. *J. Comp. Neurol*. **349**, 325–342.

Dubus P., Faucheux B., Boissiere F., Groppi A., Vital C., Vital A., Agid Y., Hirsch E. C. and Merlio J. P. (2000) Expression of Trk isoforms in brain regions and in the striatum of patients with Alzheimer's disease. *Exp. Neurol*. **165**, 285–294.

Dziewczapolski G., Glogowski C. M., Masliah E. and Heinemann S. F. (2009) Deletion of the α 7 nicotinic acetylcholine receptor gene improves cognitive deficits and synaptic pathology in a mouse model of Alzheimer's disease. *J Neurosci*. **29**, 8805–8815.

Eckert A., Marques C. A., Keil U., Schüssel K. and Müller W. E. (2003) Increased apoptotic cell death in sporadic and genetic Alzheimer's disease. *Ann. N. Y. Acad. Sci.* **1010**, 604–609.

Egea J., Rosa A. O., Sobrado M., Gandía L., López M. G. and García A. G. (2007) Neuroprotection afforded by nicotine against oxygen and glucose deprivation in hippocampal slices is lost in alpha7 nicotinic receptor knockout mice. *Neuroscience.* **145**, 866–72.

El Kouhen R., Hu M., Anderson D. J., Li J. and Gopalakrishnan M. (2009) Pharmacology of alpha7 nicotinic acetylcholine receptor mediated extracellular signal-regulated kinase signalling in PC12 cells. *Br. J. Pharmacol*. **156**, 638–648.

Engidawork E., Gulesserian T., Balic N., Cairns N. and Lubec G. (2001) Changes in nicotinic acetylcholine receptor subunits expression in brain of patients with Down syndrome and Alzheimer's disease. *J. Neural. Transm.* **Suppl. 61**, 211–222.

Esler W. P. and Wolfe M. S. (2001) A portrait of Alzheimer secretases--new features and familiar faces. *Science* **293**, 1449–1454.

Fischer W., Wictorin K., Björklund A., Williams L. R., Varon S. and Gage FH. (1987) Amelioration of cholinergic neuron atrophy and spatial memory impairment in aged rats by nerve growth factor. *Nature* **329**, 65–68.

Flores C. M., Davila-Garcia I., Ulrich Y. M., Kellar K. J. (1997) Differential regulation of neuronal nicotinic receptor binding sites following chronic nicotine administration. *J. Neurosci.* **69**, 2216–2219.

Formaggio E., Fazzini F., Dalfini A. C., Di Chio M., Cantù C., Decimo I., Fiorini Z., Fumagalli G. and Chiamulera C. (2010) Nicotine increases the expression of neurotrophin receptor tyrosine kinase receptor A in basal forebrain cholinergic neurons. *Neuroscience* **166**, 580–589.

Franke T. F., Kaplan D. R. and Cantley L. C. (1997) PI3K downstream AKTion blocks apoptosis. *Cell* **88**, 435–437.

French S. J., Humby T., Horner C. H., Sofroniew M. V. and Rattray M. (1999) Hippocampal neurotrophic and trk receptor mRNA levels are altered by local administration of nicotine, carbachyol and pilocarpine. *Brain Res. Mo. Brain Res*. **67**, 124–136.

Fucile S., Renzi M., Lax P. and Eusebi F. (2003) Fractional Ca(2+) current through human neuronal alpha7 nicotinic acetylcholine receptors. *Cell Calcium*. **34**, 205–209.

Gamblin T. C., Chen F., Zambrano A. *et al.* (2003) Caspase cleavage of tau: linking amyloid and neurofibrillary tangles in Alzheimer's disease. *Proc. Natl. Acad. Sci.* **100**, 10032–10037.

Garrido R., King-Pospisil K., Son K. W., Hennig B. and Toborek M. (2003) Nicotine upregulates nerve growth factor expression and prevents apoptosis of cultured spinal cord neurons. *Neurosci. Res*. **47**, 349–355.

Gotti C. and Clementi F. (2004) Neuronal nicotinic receptors: from structure to pathology. *Prog Neurobiol*. **74**, 363–396.

Gubbins E. J., Gopalakrishnan M. and Li J. (2010) Alpha7 nAChR-mediated activation of MAP kinase pathways in PC12 cells. *Brain Res*. **1328**, 1–11.

Gueorguiev V. D., Zeman R. J., Meyer E. M. and Sabban E. L. (2000) Involvement of alpha7 nicotinic acetylcholine receptors in activation of tyrosine hydroxylase and dopamine beta-hydroxylase gene expression in PC12 cells. *J. Neurochem*. **75**, 1997–2005.

Halevi S., McKay J., Palfreyman M., Yassin L., Eshel M. and Jorgensen E. (2002) The C. elegans ric-3 gene is required for maturation of nicotinic acetylcholine receptors. *EMBO J.* **21**, 1012–1020

Halevi S., Yassin L., Eshel M., Sala F., Sala S., Criado M. and Treinin M. (2003) Conservation within the RIC-3 gene family: effectors of mammalian nicotinic acetylcholine receptor expression. *J. Biol. Chem.* **278**, 34411–34417.

Hardy J. and Selkoe D. J. (2002) The amyloid hypothesis of Alzheimer's disease: progress and problems on the road to therapeutics. *Science* **297**, 353–356.

Hefti F. (1986) Nerve growth factor promotes survival of septal cholinergic neurons after fimbrial transections. *J. Neurosci*. **6**, 2155–2162.

Hefti F., Hartikka J. and Knusel B. (1989) Function of neurotrophic factors in the adult and aging brain and their possible use in the treatment of neurodegenerative diseases. *Neurobiol. Aging*. **10**, 515–533.

Hellström–Lindahl E., Mousavi M., Zhang X., Ravid R. and Nordberg A. (1999) Regional distribution of nicotinic receptor subunit mRNAs in human brain: comparison between Alzheimer and normal brain. *Brain Res. Mol. Brain Res.* **66**, 94–103.

Hernandez C. M. and Terry A. V. Jr. (2005) Repeated nicotine exposure in rats: effects on memory function, cholinergic markers and nerve growth factor. *Neuroscience*. **130**, 997–1012.

Hernandez C. M., Kayed R., Zheng H., Sweatt J. D. and Dineley K. T. (2010) Loss of alpha7 nicotinic receptors enhances beta-amyloid oligomer accumulation, exacerbating early-stage cognitive decline and septohippocampal pathology in a mouse model of Alzheimer's disease. *J. Neurosci*. **30**, 2442–2453.

Holladay M. W., Dart M. J. and Lynch J. K. (1997) Neuronal nicotinic acetylcholine receptors as targets for drug discovery. *J. Med. Chem*. **40**, 4169–4194.

Holtzman D. M ., Li Y. , Parada L. F ., Kinsman S. , Chen C. K ., Valletta J. S ., Zhou J., Long J. B ., Mobley W. C . (1992) p140trk mRNA m arks NGF-responsive forebrain neurons: evidence that trk gene expression is induced by NGF. *Neuron* **9**, 465–478.

Hu M., Waring J. F., Gopalakrishnan M. and Li J. (2008) Role of GSK-3beta activation and alpha7 nAChRs in Abeta(1-42)-induced tau phosphorylation in PC12 cells. *J. Neurochem*. **106**, 1371–1377.

Hu M ., G opalakrishnan M . an d Li J. (2009) P ositive al losteric modulation o f al pha7 neuronal nicotinic acetylcholine receptors: lack of cytotoxicity in PC12 cells and rat primary cortical neurons. *Br. J. Pharmacol*. **158**, 1857–1864.

Ito T., Deng X., Carr B. and May W. S. (1997) Bcl-2 phosphorylation required for anti-apoptosis function. *J. Biol. Chem*. **272**, 11671–11673.

Jiao Y., Sun Z., Lee T., Fusco F. R., Kimble T. D., Meade C. A., Cuthbertson S. and Reiner A. (1999) A simple and sensitive antigen retrieval method for free-floating and slide-mounted tissue sections. J. Neurosci. Methods 93, 149–162.

Jin K., Mao X. O., Zhu Y. and Greenberg D. A. (2002) MEK and ERK protect hypoxic cortical neurons via phosphorylation of Bad. *J. Neurochem*. **80**, 119–125.

Jones S., Sudweeks S. and Yakel J. L. (1999) Nicotinic receptors in the brain: correlating physiology with function. *Trends Neurosci*. **22**, 555–561.

Jonnala R.R., Terry A.V. Jr. and Buccafusco J.J. (2002) Nicotine increases the expression of high affinity nerve growth factor receptors *in vitro* and *in vivo*. *Life Sci*. **70**, 1543–1554.

Kaplan D. R. and Miller F. D. (1997) Signal transduction by the neurotrophin receptors. *Curr. Opin. Cell Biol*. **9**, 213–221.

Karlin A. and Akabas M. H. (1995) Toward a structural basis for the function of nicotinic acetylcholine receptors and their cousins. *Neuron* **15**, 1231–1244.

Kerwin J. M., Morris C. M., Perry R. H. and Perry E. K. (1992) Hippocampal nerve growth factor receptor immunoreactivity in patients with Alzheimer's and Parkinson's disease. *Neurosci. Lett*. **143**, 101–104.

Kihara T., Shimohama S., Sawada H., Honda K., Nakamizo T., Shibasaki H., Kume T. and Akaike A. (2001) Alpha7 Nicotinic receptor transduces signals to phosphatidylinositol 3-kinase to block amyloid-induced neurotoxicity. *J. Biol. Chem.* **276**, 541–546.

Kitagawa H., Takenouchi T., Azuma R., Wesnes K. A., Kramer W. G., Clody D. E. and Burnett A. L. (2003). Safety, pharmacokinetics, and effects on cognitive function of multiple doses of GTS-21 in healthy, male volunteers. *Neuropsychopharmacology* **28**, 542–551.

Kordower J. H., Winn S. R., Liu Y. T., Mufson E. J., Sladek J.R. Jr, Hammang J. P., Baetge E. E. and Emerich D. F. (1994) The aged monkey basal forebrain: rescue and sprouting of axotomized basal forebrain neurons after grafts of encapsulated cells secreting human nerve growth factor. *Proc. Natl. Acad. Sci. USA* **91**, 10898–10902.

Kube D. M. and Srivastava A. (1997) Quantitative DNA slot blot analysis: inhibition of DNA binding to membranes by magnesium ions. *Nucleic. Acids Res*. **25**, 3375–3376.

Laing J. M., Golembewski E. K., Wales S. Q., Liu J., Jafri M. S., Yarowsky P. J. and Aurelian L. (2008) Growth-compromised HSV-2 vector Delta RR protects from N-methyl-D-aspartate-induced neuronal degeneration through redundant activation of the MEK/ERK and PI3-K/Akt survival pathways, either one of which overrides apoptotic cascades. *J. Neurosci. Res*. **86**, 378–391.

Lansdell S. J., Gee V. J., Harkness P. C., Doward A. I., Baker E. R. and Gibb A. J. (2005) RIC-3 enhances functional expression of multiple nicotinic acetylcholine receptor subtypes in mammalian cells. *Mol. Pharmacol.* **68**, 1431–1438.

Lapchak P. A. (1993) Nerve growth factor pharmacology: application to the treatment of cholinergic neurodegeneration in Alzheimer's disease. *Exp. Neurol*. **124**, 16–20.

Large T. H., Bodary S. C., Clegg D. O., Weskamp G., Otten U. and Reichardt L. F. (1986) Nerve growth factor gene expression in the developing rat brain. *Science* **234**, 352–355.

Lefloch R., Pouysségur J. and Lenormand P. (2008) Single and Combined Silencing of ERK1 and ERK2 Reveals Their Positive Contribution to Growth Signaling Depending on Their Expression Levels. *Mol. Cell Biol.* **28**, 511–527.

Li X. D., Arias E., Jonnala R. R., Mruthinti S. and Buccafusco J. J. (2005) Effect of amyloid peptides on the increase in TrkA receptor expression induced by nicotine *in vitro* and *in vivo*. *J. Mol. Neurosci*. **27**, 325–336.

Li Y., King M. A., Grimes J., Smith N., De Fiebre C. M. and Meyer E.M. (1999a). Alpha7 nicotinic receptor mediated protection against ethanol-induced cytotoxicity in PC12 cells. *Brain Res*. **816**, 225–228.

Li Y ., P apke R . L ., Martin E . J. , H e Y . J., M illard W. J. an d Meyer E . M . (1999b) Characterization o f t he ne uroprotective an d t oxic effects of al pha7 nicotinic receptor activation in PC12 cells. *Brain Res*. **830**, 218–225.

Li Y., Meyer E. M., Walker D. W., Millard W. J., He Y. J. and King M. A. (2002). Alpha7 nicotinic receptor activation inhibits ethanol-induced mitochondrial dysfunction, cytochrome c release and neurotoxicity in primary rat hippocampal neuronal cultures. *J. Neurochem*. **81**, 853–858.

Lightfoot A . P ., Kew J. N. and Skidmore J. (2008) A lpha7 nicotinic acetylcholine receptor agonists and positive allosteric modulators. *Prog. Med. Chem*. **46**, 131–171.

Liu Q. S., Kawai H. and Berg D. K. (2001) Beta-Amyloid peptide blocks the response of α7-containing nicotinic receptors on hippocampal neurons. *Proc. Natl. Acad. Sci. U S A* **48**, 4734–4739.

MacDermott A. B., Role L. W. (1999) and Siegelbaum SA. Presynaptic ionotropic receptors and the control of transmitter release. *Annu. Rev. Neurosci*. **22**, 443–485.

Manning A. M. and Davis R. J. (2003) Targeting JNK for therapeutic benefit: from junk to gold? *Nat. Rev. Drug Discov*. **2**, 554–565.

Marks M. J., Stitzel J. A., Romm E., Wehner J. M. and Collins AC. (1986) Nicotinic binding sites in rat and mouse brain: comparison of acetylcholine, nicotine, and alpha-bungarotoxin. *Mol. Pharmacol*. **30**, 427–436.

Marrero M. B., Papke R. L., Bhatti B. S., Shaw S. and Bencherif M. (2004) The neuroprotective effect of 2-(3-pyridyl)-1-azabicyclo[3.2.2]nonane (TC-1698), a novel alpha7 ligand, is prevented through angiotensin II activation of a tyrosine phosphatase. *J. Pharmacol*. Exp. Ther. **309**, 16–27.

Marrero M. B. and Bencherif M. (2008) Convergence of alpha 7 nicotinic acetylcholine receptor-activated pathways for anti-apoptosis and anti-inflammation: central role for JAK2 activation of STAT3 and NF-kappaB. *Brain Res*. **1256**, 1–7.

Martinez–Rodriguez R., Toledano A., Alvarez M. I., Turegano L., Colman O., Roses P., Gomez de Segura I. and De Miguel E. (2003) Chronic nicotine administration increases NGF-like immunoreactivity in frontoparietal cerebral cortex. *J. Neurosci. Res.* **173**, 708–716.

Mattson M. P. (2004) Pathways towards and away from Alzheimer's disease. *Nature* **430**, 631–639.

Mawuenyega K. G., Sigurdson W., Ovod V., Munsell L., Kasten T., Morris J. C., Yarasheski K. E. and Bateman RJ. (2010) Decreased clearance of CNS beta-amyloid in Alzheimer's disease. *Science* **330**, 1774.

Messi M. L., Renganathan M., Grigorenko E. and Delbono O. (1997) Activation of alpha7 nicotinic acetylcholine receptor promotes survival of spinal cord motoneurons. *FEBS Lett*. **411**, 32–38.

Mesulam M. M. and Van Hoesen G. W. (1976) Acetylcholinesterase-rich projections from the basal forebrain of the rhesus monkey to neocortex. *Brain Res*. **109**, 152–157.

Meyer E. M., Tay E. T., Papke R. L., Meyers C., Huang G. and De Fiebre C. (1997). 3-[2,4-Dimethoxybenzylidene] anabaseine (DMXB) selectively activates rat alpha7 receptors and improvees memory-related behaviors in a mecamylamine-sensitive manner. *Brain Res*. **768**, 49–56.

Meyer E. M., Kuryatov A., Gerzanich V., Lindstrom J., Papke R. L. (1998a) Analysis of 3-(4-hydroxy, 2-Methoxybenzylidene)anabaseine selectivity and activity at human and rat alpha-7 nicotinic receptors. *J. Pharmacol. Exp. Ther*. **287**, 918–925.

Meyer E. M., Meyers C. and King M. A. (1998b) The selective alpha7 nicotinic receptor agonist DMXB protects against neocortical neuron loss after nucleus basalis lesions. *Brain Res*. **786**, 152–154.

Millar N. S. (1999) Heterologous expression of mammalian and insect neuronal nicotinic acetylcholine receptors in cultured cell lines. *Biochem. Soc. Trans*. **27**, 944–950.

Millar N. S. (2008) RIC-3: a nicotinic acetylcholine receptor chaperone. *Br. J. Pharmacol.* **153**, S177–183.

Molinuevo J. L., Lladó A. and Rami L. (2005) Memantine: targeting glutamate excitotoxicity in Alzheimer's disease and other dementias. *Am. J. Alzheimers Dis. Other Demen*. **20**, 77–85.

Mousavi M. and Hellström-Lindahl E. (2008) Nicotinic receptor agonists and antagonists increase sAPPalpha secretion and decrease Abeta levels *in vitro*. *Neurochem. Int*. **54**, 237–244.

Mufson E. J., Li J. M., Sobreviela T. and Kordower J. H. (1996) Decreased trkA gene expression within basal forebrain neurons in Alzheimer's disease. *Neuroreport*. **8**, 25–29.

Mufson E. J., Lavine N., Jaffar S., Kordower J. H., Quirion R. and Saragovi H. U. (1997) Reduction in p140-TrkA receptor protein within the nucleus basalis and cortex in Alzheimer's disease. *Exp. Neurol*. **146**, 91–103.

Mufson E. J., Kroin J. S., Sendera T. J. and Sobreviela T. (1999) Distribution and retrograde transport of trophic factors in the central nervous system: functional implications for the treatment of neurodegenerative diseases. *Prog. Neurobiol*. **57**, 451–484.

Nakayama H., Numakawa T., Ikeuchi T. and Hatanaka H. (2001) Nicotine-induced phosphorylation of extracellular signal-regulated protein kinase and CREB in PC12h cells. *J. Neurochem*. **79**, 489–98.

Namikawa K., Honma M., Abe K., Takeda M., Mansur K., Obata T., Miwa A., Okado H. and Kiyama H. (2000) Akt/protein kinase B prevents injury-induced motoneuron death and accelerates axonal regeneration. *J. Neurosci*. **20**, 2875–2886.

Nguyen M., Alfonso A., Johnson C. D. and Rand J. B. (140) Caenorhabditis elegans mutants resistant to inhibitors of acetylcholinesterase. *Genetics* **140**, 527–535.

Nie H. Z., Shi S., Lukas R. J., Zhao W. J., Sun Y. N. and Yin M. (2010) Activation of α7 nicotinic receptor affects APP processing by regulating secretase activity in SH-EP1-α7 nAChR-hAPP695 cells. *Brain Res*. **1356**, 112–120.

Niewiadomska G., Mietelska-Porowska A. and Mazurkiewicz M. (2010) The cholinergic system, nerve growth factor and the cytoskeleton. *Behav. Brain Res*. [Epub ahead of print]

Nishina H., Wada T. and Katada T. (2004) Physiological Roles of SAPK/JNK Signaling Pathway. *J. Biochem*. **136**, 123–126.

Orban P. C., Chapman P. F. and Brambilla. (1999) Is the Ras-MAPK signaling pathway necessary for long-term memory formation? *Trends Neurosci*. **22**, 38–44.

Orr-Urtreger A., Göldner F. M., Saeki M., Lorenzo I., Goldberg L., De Biasi M., Dani J. A., Patrick J. W. and Beaudet AL. (1997) Mice deficient in the alpha7 neuronal nicotinic acetylcholine receptor lack alpha-bungarotoxin binding sites and hippocampal fast nicotinic currents. *J. Neurosci*. **17**, 9165–9171.

Papke R. L., Kem W. R., Soti F., López-Hernández G. Y. and Horenstein N. A. (2009) Activation and desensitization of nicotinic Alpha7-type acetylcholine receptors by benzylidene anabaseines and nicotine. *J. Pharmacol. Exp. Ther.* **329**, 791–807.

Paxinos G. and Franklin K. B. J. (2001) The Mouse Brain in Stereotaxic Coordinates. Second Edition, *Academic Press*, San Diego.

Perry E. K., Morris C. M., Court J. A., Cheng A., Fairbairn A. F., McKeith I. G., Irving D., Brown A. and Perry R. H. (1995) Alteration in nicotine binding sites in Parkinson's disease, Lewy body dementia and Alzheimer's disease: possible index of early neuropathology. *Neuroscience* **64**, 85–95.

Perry E. K., Martin-Ruiz C. M. and Court J. A. (2001) Nicotinic receptor subtypes in human brain related to aging and dementia. *Alcohol.* **24**, 63–68.

Pettmann B. and Henderson C. E. (1998) Neuronal cell death. *Neuron*. **20**, 633–647.

Philpott K. L. and Facci L. (2008) MAP kinase pathways in neuronal cell death. CNS Neurol. Disord. *Drug Targets*. **7**, 83–97.

Ren K., Puig V., Papke R. L., Itoh Y., Hughes J. A. and Meyer E. M. (2005) Multiple calcium channels and kinases mediate a7 nicotinic receptor neuroprotection in PC12 cells. *J. Neurochem*. **94**, 926–933.

Ren K., King M. A., Liu J., Siemann J., Altman M., Meyers C., Hughes J. A. and Meyer E. M. (2007a) The alpha7 nicotinic receptor agonist 4OH-GTS-21 protects axotomized septohippocampal cholinergic neurons in wild type but not amyloid-overexpressing transgenic mice. *Neuroscience* **148**, 230–237.

Ren K., Thinschmidt J., Liu J., Ai L., Papke R. L., King M. A., Hughes J. A. and Meyer E. M. (2007b) α7 Nicotinic receptor gene delivery into mouse hippocampal neurons leads to functional receptor expression, improved spatial memory-related performance, and tau hyperphosphorylation. *Neuroscience* **145**, 314–322.

Reynolds C. H., Utton M. A., Gibb G. M., Yates A. and Anderton B. H. (1997) Stress-activated protein kinase/c-Jun N-terminal kinase phosphorylates Tau protein. *J. Neurochem.* **68**, 1736–1744.

Riedl S. J. and Shi Y. (2004) Molecular mechanisms of caspase regulation during apoptosis. *Nat. Rev. Mol. Cell Biol*. **5**, 897–907.

Rohn T. T., Vyas V., Hernandez-Estrada T., Nichol K. E., Christie L. A. and Head E. (2008) Lack of pathology in a triple transgenic mouse model of Alzheimer's disease after overexpression of the anti-apoptotic protein Bcl-2. *J. Neurosci*. **28**, 3051–3059.

Rohn T. T. and Head E. (2009) Caspases as therapeutic targets in Alzheimer's disease: is it time to "cut" to the chase? *Int. J. Clin. Exp. Pathol*. **2**, 108–118.

Role L. W. and Berg D. K. (1996) Nicotinic receptors in the development and modulation of CNS synapses. *Neuron* **16**, 1077–1085.

Rosa A. O., Egea J., Gandía L., López M. G. and García A. G. (2006) Neuroprotection by nicotine in hippocampal slices subjected to oxygen-glucose deprivation: involvement of the alpha7 nAChR subtype. *J. Mol. Neurosci*. **30**, 61–62.

Salehi A., Delcroix J. D. and Swaab D. F. (2004) Alzheimer's disease and NGF signaling, *J. Neural. Transm*. **111**, 323–345.

Sargent P. B. (1993) The diversity of neuronal nicotinic acetylcholine receptors. *Annu. Rev. Neurosci.***16**, 403–443.

Schoepfer R., Conroy W. G., Whiting P., Gore M. and Lindstrom J. (1990) Brain alpha-bungarotoxin binding protein cDNAs and MAbs reveal subtypes of this branch of the ligand-gated ion channel gene superfamily. *Neuron* **5**, 35–48.

Scott S. A., Mufson E. J., Weingartner J. A., Skau K. A. and Crutcher K. A. (1995) Nerve growth factor in Alzheimer's disease: increased levels throughout the brain coupled with declines in nucleus basalis. *J. Neurosci*. **15**, 6213–6221.

Séguéla P., Wadiche J., Dineley-Miller K., Dani J. A. and Patrick J. W. (1993) Molecular cloning, functional properties, and distribution of rat brain alpha 7: a nicotinic cation channel highly permeable to calcium. *J. Neurosci*. **13**, 596–604.

Shaw S., Bencherif M. and Marrero M. B. (2002) Janus kinase 2, an early target of alpha 7 nicotinic acetylcholine receptor-mediated neuroprotection against Abeta-(1-42) amyloid. *J. Biol. Chem*. **277**, 44920–44924.

Shen H., Kihara T., Hongo H., Wu X., Kem W. R., Shimohama S., Akaike A., Niidome T. and Sugimoto H. (2010) Neuroprotection by donepezil against glutamate excitotoxicity involves stimulation of alpha7 nicotinic receptors and internalization of NMDA receptors. *Br. J. Pharmacol*. **161**, 127–139.

Shen J., Wu Y., Xu J. Y., Zhang J., Sinclair S. H., Yanoff M., Xu G., Li W. and Xu G. T. (2010) ERK- and Akt-dependent neuroprotection by erythropoietin (EPO) against glyoxal-AGEs via modulation of Bcl-xL, Bax, and BAD. *Invest. Ophthalmol. Vis. Sci.* **51**, 35–46.

Shimohama S., Greenwald D. L., Shafron D. H., Akaika A., Maeda T., Kaneko S., Kimura J., Simpkins C. E., Day A. L. and Meyer EM. (1998) Nicotinic alpha 7 receptors protect against glutamate neurotoxicity and neuronal ischemic damage. *Brain Res*. **779**, 359–363.

Shimohama S. (2009) Nicotinic receptor-mediated neuroprotection in neurodegenerative disease models. *Biol. Pharm. Bull*. **32**, 332–336.

Shoop R. R., Chang K. T., Ellisman M. H. and Berg D. K. (2001) Synaptically driven calcium transients via nicotinic receptors on somatic spiness. *J. Neurosci*. **21**, 771–781.

Siegel G . J. and Chauhan N B. (2000) Neurotrophic factors in A lzheimer's and Parkinson's disease brain. Brain Res. *Brain Res. Rev.* **33**, 199–227.

Simosky J. K., Stevens K. E. and Kem W. R. and Freedman R. (2001). Intragastric DMXB-A, an alpha7 nicotinic agonist, improves deficient sensory inhibition in DBA/2 mice. *Biol. Psychiatry*. **50**, 493–500.

Sofroniew M. V., Howe C. L. and Mobley W. C. (2001) Nerve growth factor signaling, neuroprotection, and neural repair. *Annu. Rev. Neurosci*. **24**, 1217–1281.

Takada-Takatori Y., Kume T., Sugimoto M., Katsuki H., Sugimoto H. and Akaike A. (2006) Acetylcholinesterase inhibitors used in treatment of Alzheimer's disease prevent glutamate neurotoxicity via nicotinic acetylcholine receptors and phosphatidylinositol 3-kinase cascade. *Neuropharmacology* **51**, 474–86.

Takahashi T., Yamashita H., Nakamura S., Ishiguro H., Nagatsu T. and Kawakami H. (1999) Effects of nerve growth factor and nicotine on the expression of nicotinic acetylcholine receptor subunits in PC12 cells. *Neurosci. Res*. **35**, 175–181.

Takata K., Kitamura Y., Saeki M., Terada M., Kagitani S., Kitamura R., Fujikawa Y., Maelicke A., Tomimoto H., Taniguchi T. and Shimohama S. (2010) Galantamine-induced amyloid-{beta} clearance mediated via stimulation of microglial nicotinic acetylcholine receptors. *J. Biol. Chem*. **285**, 40180–40191.

Terry A. V. Jr and Buccafusco J. J. (2003) The cholinergic hypothesis of age and Alzheimer's disease-related cognitive deficits: recent challenges and their implications for novel drug development. *J. Pharmacol. Exp. Ther*. **306**, 821–827.

Thomsen M. S., Hansen H. H., Timmerman D. B. and Mikkelsen J. D. (2010) Cognitive improvement by activation o f al pha7 nicotinic acetylcholine receptors: f rom animal models to human pathophysiology. *Curr. Pharm. Des*. **16**, 323–343.

Timmermann D. B., Grønlien J. H., Kohlhaas K. L., Nielsen E. Ø., Dam E., Jørgensen T. D., Ahring P. K. , Peters D., Holst D. , Christensen J. K ., Malysz J. , Briggs C. A., Gopalakrishnan M . an d Olsen G . M . (2007) A n a llosteric m odulator of t he alpha7 ni cotinic acetylcholine r eceptor poss essing co gnition-enhancing properties *in vivo*. *J. Pharmacol. Exp. Ther*. **323**, 294–307.

Toborek M., Son K. W., Pudelko A., King-Pospisil K., Wylegala E. and Malecki A. (2007) ERK 1/2 signaling pathway is involved in nicotine-mediated neuroprotection in spinal cord neurons. *J. Cell. Biochem*. **100**, 279–292.

Traverse S., Gomez N., Paterson H., Marshall C. and Cohen P. (1992) Sustained activation of the mitogen-activated protein (MAP) kinase cascade may be required for differentiation of PC12 cells. Comparison of the effects of nerve growth factor and epidermal growth factor. *J. Biochem.* **288**, 351–355

Tuszynski M . H ., Thal L. , Pay M ., Salmon D . P., U H. S ., Bakay R ., Patel P ., Blesch A., Vahlsing H. L., Ho G., Tong G., Potkin S. G., Fallon J., Hansen L., Mufson E. J., Kordower J. H., Gall C. and Conner J. (2005) A phase 1 clinical trial of nerve growth factor gene therapy for Alzheimer disease. *Nat. Med*. **11**, 551–555.

Tyagi E., Agrawal R., Nath C. and Shukla R. (2010) Cholinergic protection via alpha7 nicotinic acetylcholine receptors and PI3K-Akt pathway in LPS-induced neuroinflammation. *Neurochem. Int*. **56**, 135–142.

Uteshev V. V., Meyer E. M. and Papke R. L. (2003) Regulation of neuronal function by choline and 4O H-GTS-21 through al pha 7 nicotinic r eceptors. *J. Neurophysiol.* **89**, 1797–1806.

Utsugisawa K., Nagane Y., Obara D. and Tohgi H. (2002) Over-expression of alpha7 nicotinic acetylcholine receptor induces sustained ERK phosphorylation and N-cadherin expression in PC12 cells. *Brain Res. Mol. Brain Res*. **106**, 88–93.

Utsuki T., Shoaib M., Holloway H., Ingram D., Wallace W., Haroutunian V., Sambamurti K., Lahiri D. and Greig N. (2002). Nicotine lowers the secretion of the Alzheimer's amyloid beta-protein precursor that contains amyloid beta-peptide in rat. *J. Alzheimers Dis*. **4**, 405–415.

Vijayaraghavan S., Pugh P. C., Zhang Z.W., Rathouz M. M. and Berg D.K. (1992) Nicotinic receptors that bind alpha-bungarotoxin on neuerons raise intracellular free Ca^{2+}. *Neuron* **8**, 353–362.

Wang H. Y., Lee D. H., D'Andrea M. R., Peterson P. A., Shank R. P. and Reitz A. B. (2000a) β-Amyloid1-42 binds to α7 nicotinic acetylcholine receptor with high affinity: implications for Alzheimer's disease pathology. *J. Biol. Chem*. **275**, 5626–5632.

Wang H. Y., Lee D. H., Davis C. B. and Shank R. P. (2000b) Amyloid peptide Aβ1-42 binds selectively and with pico-molar affinity to α7 nicotinic acetylcholine receptors. *J. Neurochem*. **75**, 1155–1161.

Wang H. Y., Li W., Benedetti N. J. and Lee D. H. (2003) α7 Nicotinic acetylcholine receptors alphpa7 nicotinic acetylcholine receptors mediate β-amyloid peptides-induced tau protein phosphorylation. *J. Biol. Chem*. **278**, 31547–31553.

Wang H. Y., Stucky A., Liu J., Shen C., Trocme-Thibierge C. and Morain P. (2009) Dissociating beta-amyloid from α 7 nicotinic acetylcholine receptor by a novel therapeutic agent, S 24795, normalizes α 7 nicotinic acetylcholine and NMDA receptor function in Alzheimer's disease brain. *J. Neurosci*. **29**, 10961–10973.

Welsby P. J., Rowan M. J. and Anwyl R. (2009) Intracellular mechanisms underlying the nicotinic enhancement of LTP in the rat dentate gyrus. *Eur. J. Neurosci*. **29**, 65–75.

Wenk H., Bigl V. and Meyer U. (1980) Cholinergic projections from magnocellular nuclei of the basal forebrain to cortical areas in rats. *Brain Res*. **2**, 295–316.

Wenk G. L. (2003) Neuropathologic changes in Alzheimer's disease. J. Clin. Psychiatry **64 Suppl 9**, 7–10.

Wevers A., Burghaus L. , Moser N ., Witter B ., Steinlein O . K., Schütz U ., Achnitz B., Krempel U ., Nowacki S ., Pilz K ., Stoodt J. , Lindstrom J. , De V os R. A., Jansen Steur E . N . and Schröder H . (2000) E xpression o f ni cotinic acetylcholine r eceptors in A lzheimer's disease: postmortem i nvestigations and experimental approaches. *Behav. Brain Res.* **113**, 207–215.

Whitehouse P. J., Struble R. G., Clark A. W. and Price D. L. (1982) Alzheimer disease: plaques, tangles, and the basal forebrain. *Ann. Neurol*. **12**, 494.

Wiesmann C., Ultsch M. H., Bass S. H. and de. Vos. A. M. (1999) Crystal structure of nerve growth factor in complex with the ligand-binding domain of the TrkA receptor. *Nature* **401**, 184–188.

Williams L. R. , Varon S ., Peterson G. M ., Wictorin K ., Fischer W ., Bjorklund A . and Gage F. H. (1986) Continuous infusion of nerve growth factor prevents basal forebrain neuronal death after fimbria fornix transection. *Proc. Natl. Acad. Sci. U S A* **83**, 9231–9235.

Williams M. E., Burton B., Urrutia A., Shcherbatko A., Chavez-Noriega L. E., Cohen C. J. and Aiyar J. (2005) R ic-3 promotes functional expression of t he ni cotinic acetylcholine receptor α7 subunit in mammalian cells. *J. Biol. Chem.* **280**, 1257–1263.

Woodruff-Pak, D.S. (2003). Mecamylamine reversal by nicotine and by a partial alpha7 nicotinic acetylcholine receptor agonist (GTS-21) in rabbits tested with delay eyeblink classical conditioning. *Behav. Brain Res*. **143**, 159–167.

Yang L., Dan H. C., Sun M., Liu Q., Sun X. M., Feldman R. I., Hamilton A. D., Polokoff M., Nicosia S. V., Herlyn M., Sebti S. M. and Cheng J. Q. (2004) Akt/protein kinase B signaling inhibitor-2, a selective small molecule inhibitor of Akt signaling with antitumor activity in cancer cells overexpressing Akt. *Cancer Res*. **64**, 4394–4399.

Youdim M. B. and Weinstock M. (2001) Molecular basis of neuroprotective activities of rasagiline and the anti-Alzheimer drug TV3326 [(N-propargyl-(3R)aminoindan-5-YL)-ethyl methyl carbamate]. *Cell Mol. Neurobiol.* **21**, 555–573.

Yuan J. Y. and Yankner B. A. (2000) Apoptosis in the nervous system. *Nature* **407**, 802–809.

Yuen E. C., Howe C. L., Li Y., Holtzman D. M. and Mobley W. C. (1996) Nerve growth factor and the neurotrophic factor hypothesis. *Brain Dev*. **18**, 362–368.

Zolotukhin S., Byrne B. J., Mason E., Zolotukhin I., Potter M., Chesnut K., Summerford C., Samulski R. J. and Muzyczka N. (1999) Recombinant adeno-associated virus purification using novel methods improves infectious titer and yield. *Gene Ther*. **6**, 973–985.

BIOGRAPHICAL SKETCH

Yan Ren was born in Huzhou, China in November 1984, to Qiaozhen Pu and Bao'er Ren. Starting at an early age, Yan was immersed in different interests and hobbies. Her favorite activities at that time were painting, reading and gardening. After high school, Yan matriculated at Fudan University for her undergraduate study, majoring in life sciences. Yan started with her first research project when she was a sophomore, studying gene mutation related with carcinogenesis. It was in Fudan University that she met and fell love with Lin Zhang, who became her husband later. In summer 2006, Yan received her Bachelor of Science degree in life sciences and was accepted into Graduate Program of Genetics and Genomic of University of Florida, Gainesville. In 2007, Yan joined the laboratory of Jeffrey A. Hughes in the Department of Pharmaceutics, and pursued her doctoral research in Alzheimer disease under supervision of Dr. Jeffrey A. Hughes and Dr. Edwin M. Meyer. In 2009, Yan continued her research project under supervision of Dr. Sihong Song after Dr. Jeffrey A. Hughes leaving the University of Florida for Roche. Outside of lab, Yan was interested in cooking, traveling and studying Chinese traditional medicine. She received her Ph.D. from the University of Florida in the spring of 2011. In the future, Yan hopes to pursue a career in pharmaceutical research, as well as caring for her family.